Dissertation

submitted to the

Combined Faculty of Natural Sciences and Mathematics

of the Ruperto Carola University Heidelberg, Germany

for the degree of

Doctor of Natural Sciences

Presented by

M.Sc. Ambra Villani

Born in: Milan, Italy

Oral examination: 14.12.2018

In vivo analysis of neuronal clearance by microglia uncovers a new compartment in the phagocytic pathway

Referees: Dr. Alexander Aulehla

Prof. Dr. Ulrike Müller

TABLE OF CONTENTS

ABSTRACT

Clearance of apoptotic cells by professional, tissue resident macrophages is crucial during development, maintenance of tissue homeostasis and disease. Phagocytic cells can engulf and process several dying cells with high efficiency while still maintaining their dynamic behaviour and morphology. Effective intracellular processing of ingested cells is likely to be crucial for the phagocyte to function, but the underlying cellular mechanisms are poorly understood. Here, we investigate this by focusing on microglia, the tissue resident macrophages of the Central Nervous System (CNS). In particular, we take advantage of the optical transparency of the zebrafish embryo and apply a combination of genetic, chemical and imaging approaches to study phagocytosis of neurons *in vivo*.

In this study we focus on *bubblebrain* (*blb*), a zebrafish mutant that has bloated microglia. The cell body of *blb* microglia is occupied by a single large vesicle that grows progressively. By comparing wild type and *blb* embryos we discovered that efficient processing of engulfed neurons depends on the shrinkage and packaging of phagosomes into the gastrosome, a unique cellular compartment with distinct ultra-structural and molecular features. Moreover, we show that the *blb* phenotype is caused by lack of Slc37a2, a putative glucose-6-phosphate transporter localized on phagosomes. Loss of Slc37a2 prevents phagosomal shrinkage, and this in turn results in the expansion of the gastrosome and in the dramatic bloating of the cell. Interestingly, we show that gastrosomal defects impact on microglial activities and affect the ability of these cells to engulf neurons and to migrate towards brain injuries. Thus, this work provides experimental evidence for the existence of the gastrosome, a critical new component of the phagocytic pathway that allows easy manipulation of key microglial activities *in vivo*.

ZUSAMMENFASSUNG

Die Beseitigung apoptotischer Zellen durch professionelle, Gewebe-ansässige Makrophagen ist von entscheidender Bedeutung bei Entwicklungsprozessen, während der Aufrechterhaltung der Gewebehomöostase und der Ausprägung von Krankheiten. Phagozytische Zellen können mehrere sterbende Zellen mit hoher Effizienz aufnehmen und prozessieren, während sie ihr dynamisches Verhalten und ihre Morphologie beibehalten. Eine effektive intrazelluläre Verarbeitung aufgenommener Zellen ist vermutlich entscheidend für die Funktion der Phagozyten, wobei die zugrundeliegenden zellulären Mechanismen kaum verstanden sind. In dieser Arbeit untersuchen wir dies, indem wir uns auf Mikroglia konzentrieren, die Gewebe-ansässigen Makrophagen des zentralen Nervensystems (ZNS). Insbesondere nutzen wir die optische Transparenz des Zebrafisch-Embryos und wenden eine Kombination aus genetischen, chemischen und bildgebenden Verfahren an, um die Phagozytose von Neuronen *in vivo* zu untersuchen.

In dieser Studie charakterisieren wir *bubblebrain* (*blb*), eine Zebrafisch-Mutante mit aufgeblähten Mikroglia. Der Zellkörper von *blb*-Mikroglia ist von einem einzigen großen Vesikel besetzt, das progressiv wächst. Durch den Vergleich von Wildtyp- und *blb*-Embryonen haben wir entdeckt, dass die effiziente Verarbeitung aufgenommener Neuronen von der Verkleinerung und Verpackung der Phagosomen in das Gastrosom abhängt, einem einzigartigen Zellkompartiment mit ausgeprägten ultrastrukturellen und molekularen Merkmalen. Darüber hinaus zeigen wir, dass der *blb*-Phänotyp durch das Fehlen von Slc37a2, einem mutmaßlichen Glucose-6-Phosphat-Transporter, der auf Phagosomen lokalisiert ist, verursacht wird. Der Verlust von Slc37a2 verhindert die Verkleinerung des Phagosoms, was wiederum zur Expansion des Gastrosoms und zum dramatischen Aufblähen der Zelle führt. Interessanterweise können wir zeigen, dass gastrosomale Defekte Auswirkungen auf die Mikrogliaaktivität haben und die Fähigkeit dieser Zellen beeinflussen, Neuronen zu phagozytieren und zu Hirnläsionen zu migrieren. Somit liefert diese Arbeit einen experimentellen Beweis für die Existenz des Gastrosoms, einer entscheidenden neuen Komponente bei der Phagozytose, die eine einfache *in vivo* Manipulation von Schlüsselaktivitäten der Mikroglia erlaubt.

LIST OF ABBREVIATIONS

AD: Alzheimer's Disease
ADP: Adenosine DiPhosphate
ALPS: Autoimmune LymphoProliferative Syndrome
ALS: Amylotrophyc Lateral Sclerosis
AO: Acridine Orange
APP: Amyloid Precursors Protein
AR: Adrenergic Receptor
ATP: Adenosine TriPhosphate
attB: ATTachment site Bacterium
attL: ATTachment site left
attP: ATTachment site Phage
attR: ATTachment site right
BAI1: Brain specific Angiogenesis Inhibitor 1
Blb: BubbLeBrain
cAMP: Ayclic Adenosine MonoPhosphate
ChR2: ChannelRhodopsin 2
CLEM: Correlative Light Electron Microscopy
CNS: Central Nervous System
COPD: Chronic Obstructive Pulmonary Disease
CPT: Camptothecin
CRISPR: Clustered Regularly Interspaced Short Palindromic Repeats
DC: Dendritic Cell
DMEM: Dulbecco's Modified Eagle's Medium
DMSO: DiMethyl SulfOxide
DNA: DeoxyriboNucleic Acid
Dpf: Days Post Fertilization
DREADDs: Designer Receptors Exclusively Activated by Designer Drugs
DSB: Double Strand Break
EM: Electron Microscopy
ENU: N-Ethyl-N-nitrosoUrea
FBS: Fetal Bovine Serum
fMLP: N-formyl peptides
G2A: G protein coupled receptor 132
G6P: Glucose-6-Phosphate
G6PT: Glucose-6-Phosphate Transporter
GPCR: G protein-coupled receptors
HB: Hind Brain
HDR: Homology Directed Repair
HOPS: HOmotypic fusion and vacuole Protein Sorting
Hpf: Hours Post Fertilization
ICAM3: IntraCellular Adhesion Molecule 3
ILV: Intra Luminal Vesicle

KI: Knock In
KO: Knock Out
Lamp1/2: Lysosome-Associated Membrane Protein 1 and 2
LB: Latex Beads
LPC: Lysophosphatidylcholine
LSD: Lysosomal Storage Disorder
MGF-E8: Milk fat Globule-EGF factor 8
MOs: Morpholinos
mRNA: messenger RNA
NHEJ: Non-Homologous End Joining
NIRB: Near InfraRed Branding
NLS: Nuclear Localization Sequence
NMDA: N-Methyl-D-Aspartate
NR: Neutral Red
OT: Optic Tectum
PAF: Platelet Activating Factor
PCD: Programmed Cell Death
PCR: Polymerase Chain Reaction
PD: Parkinson's Disease
PFA: ParaFormAldehyde
PS: PhosphatidylSerine
PtdIns(3)P: PhosphaTidylINoSitol 3-Phosphate
PTU: N-PhenylThioUrea
RASSLs: Receptors Activated Solely by Synthetic Ligands
S1P: Sphingosin-1-phosphate
sgRNAs: Single Guide RNAs
SLC: SoLute Carrier
SPIM: Single Plan Illumination Microscopy
SSR: Site-Specific Recombinase
TALENs: Transcription Activator-Like Effector Nucleases
tFTs: Tandem Fluorescent protein Timers
TGN: Trans Golgi Network
TIM4: T-cell Immunoglobulin Mucin receptor 4
TM: Trans Membrane
TRAIL: TNF-Related Apoptosis-Inducing Ligand
UAS: Upstream Activation Sequence
UDP: Uridine DiPhosphate
UTP: Uridine TriPhosphate
vRh: Vertebrate Rhodopsin
WB: Western Blot
WGA: Wheat Germ Agglutin
YS: Yolk Sac
ZFNs: Zinc Finger Nucleases
Z-VAD-fmk: Carbobenzoxy-valyl-alanyl-aspartyl-[O-methyl]-fluoromethylketone

LIST OF FIGURES

To Kamil, my husband
Who offered unconditional love, tolerance and inspiration throughout my study

“Ho perso un po’ la vista, molto l’udito.
Alle conferenze non vedo le proiezioni e non sento bene.
Ma penso più adesso di quando avevo vent’anni.
Il corpo faccia quello che vuole. Io non sono il corpo: io sono la mente.”

Rita Levi Montalcini

1 INTRODUCTION

You make decisions, take actions, affect the world, receive feedback from the world, incorporate into yourself, then the updated "you" makes more decisions, and so forth, round and round (from "I am a strange loop", Douglas Hofstadter).

Every day, depending on the circumstances, we take actions that affect not only ourselves, but also people around us. In a similar way, cells of our body constantly interact with the environment and feedback on themselves and their surroundings to maintain homeostasis. Moreover, cells often serve multiple functions, being involved in complicated intracellular networks and feedback loops. Cells have different methods to communicate with each other, interact and work together performing essential processes necessary for survival and both multicellular and unicellular organisms heavily rely on cell-cell communication. Biologists have always been fascinated by these processes and the aim is to understand the mechanisms in place to coordinate these events at the cellular and tissue scale.

A great model to study these mechanisms is the immune system, our line of defence against infectious organisms and other invaders. This is divided into two branches, the so-called adaptive immune system and the innate one; several cell types in each group work together and feed back to each other to maintain the homeostasis of the organism. The immune system, not only defends us from external pathogens, but also ensures the health of the organism by removing aged and damaged cells. By engulfing unwanted material, cells of our immune system, such as macrophages, eliminate potential harmful and infectious agents from our body. This process is highly regulated and improper uptake or digestion of the engulfed material can lead to severe cellular disfunctions that will inevitably reflect on the functioning of the whole tissue leading to a disease state.

A great model to study this delicate equilibrium and sophisticated machinery is the removal and digestion of apoptotic cells, a fundamental process in development, homeostasis and disease.

1.1 APOPTOSIS

Apoptosis (from Greek apóptōsis, "falling off") is a sequence of well-defined and highly conserved molecular mechanisms also known as programmed cell death (PCD). First defined in 1972 (Kerr et al., 1972), apoptosis is an active process characterized by distinct morphological features and is considered a vital component of various processes including embryonic development, immunity and cell turnover (Cole and Ross, 2001; Elmore, 2007; Meier et al., 2000; Oppenheim, 1991; Yamashita, 2003). While during necrosis the integrity of the cell membranes is immediately lost leading to cell swelling with consequent content spilling and inflammation, during apoptosis, the cytoplasmic membranes and organelles remain intact. Already in the early process of PCD, as a result of the condensation of chromatin and organelles, the dying cell is subjected to shrinkage and then to blebbing. This process leads to the formation of the so called "apoptotic bodies", a morphological hallmark of PCD which consist of cytoplasm with tightly packed organelles with or without a nuclear fragment. The mechanisms of apoptosis are highly complex, involving an energy-dependent cascade of molecular events. The intracellular machinery and the morphological changes associated with PCD are shared among different cell types and evolutionary conserved across species. Apoptosis ends with the final act of cellular disposal in which phagocytic cells engulf cellular corpses and associated debris. Importantly, apoptotic cells actively participate in the initial phases of this process by altering their morphology, displaying important modifications to their membranes and exposing specific signals that are important for recognition and uptake.

1.1.1 PHYSIOLOGIC APOPTOSIS

The process of apoptosis is as important as its counterpart, mitosis. Indeed, PCD has an opposite but complementary role to cell proliferation in the regulation of all cell populations. To maintain homeostasis in the adult human body, around 10 billion cells are estimated to undergo apoptosis daily (Renehan et al., 2001). Obviously, this number can significantly increase during development, aging or diseases.

Apoptosis is necessary, for example, to get rid of pathogen-invaded cells and it is a vital component of wound healing. As shown by Greenhalgh, in fact, thanks to PCD inflammatory cells are removed and the granulation tissue that forms during the healing process can evolve into scar tissue (Greenhalgh, 1998). Dysregulated apoptosis during this process can lead to

pathologic conditions characterized by excessive scarring and fibrosis. Moreover, PCD also plays a central role in remodelling tissue during adulthood (Lund et al., 1996; Tilly et al., 1991) and it is an essential mechanism to control cell number especially in tissue with high turnover rate. Apoptosis is also needed to eliminate auto-aggressive immune cells during maturation in the central lymphoid organs (Osborne, 1996; Rathmell and Thompson, 2002). Furthermore, as an organism grows older, some cells begin to deteriorate at a faster rate and are eliminated without an inflammatory response thanks to PCD.

It is clear that apoptosis has to be tightly regulated since too much or too little cell death may lead to pathological conditions.

1.1.1.1 Developmental apoptosis

Being a mechanism by which unwanted cells are eliminated, apoptosis has a tremendous relevance during embryogenesis. Our understanding of apoptosis actually transpired from the investigation of Caenorhabditis elegans development (Ellis and Horvitz, 1986; Horvitz, 1999; Sulston et al., 1983). In this animal, Sulston and colleagues showed that out of 1090 somatic cells, exactly 131 cells undergo cell death at particular points during the developmental process (Sulston et al., 1983). Hence the definition of "programmed cell death", which involves the genetically determined elimination of cells. Genetic screens in C. elegans have been very effective in identifying key molecular players of apoptosis (Ellis and Horvitz, 1986; Knapp et al., 1986; Raff et al., 1993). In particular, while loss of function of ced-3,4 and eng-1 genes abolish apoptosis, ced-9 mutants are characterized by excessive apoptosis (Lettre and Hengartner, 2006). Remarkably, those mechanism are incredibly conserved across species, from nematodes to mammals (Lord and Gunawardena, 2012).

Indeed, all developing organisms produce excess cells that are subsequently removed via apoptosis as a step of normal development. In this context, three different categories have been established (Glücksmann, 1951). "Phylogenic apoptosis" is the elimination of embryonic cells or structures characteristic of an evolutionary ancestor and that are no longer needed in the adult. In addition, this category includes the elimination of structures that are needed only transiently during development such as the tadpole's tale. "Morphogenic apoptosis" instead, by removing unwanted cells, sculpts tissues and occurs mainly in areas of folding, cavitation or fusion of tissues. Here, a typical example is digit separation by the removal of interdigital cells (Chen and Zhao, 1998). Finally, "histogenetic apoptosis" is the removal of cells following tissue

remodelling or maturation, such as the loss of neurons typical of brain development. This in the central nervous system (CNS), is perhaps one of the most striking roles for apoptosis. Here, neurons are first produced in large excess and successively many of them undergo PCD (Knapp et al., 1986; Raff et al., 1993). It has been shown that neurons have to compete for a limited amount of target-derived neurotrophic factors, which they receive by forming functional synaptic connections with their targets. As a consequence, neurons that fail to connect are eliminated by apoptosis (Cowan et al., 1984; Elliott and Shadbolt, 1998; Oppenheim, 1991). In this sense, a classic example is the development of sympathetic neurons and oligodendrocytes that depend on nerve growth factor and platelet-factor, respectively (Barres et al., 1992; Levi-Montalcini, 2005).

1.1.2 PATHOLOGIC APOPTOSIS

Inappropriate apoptosis (either too much or too little) is an important factor in many human conditions including many types of cancer, autoimmune disorders, neurodegenerative diseases and ischemic damage. In cancer normal mechanisms of cell cycle regulation are compromised and suppression of apoptosis during carcinogenesis is thought to play a central role in the progression of some cancers (Kerr et al., 1994). Moreover, tumour cells can acquire resistance to apoptosis by expression of anti-apoptotic proteins (Miyashita and Reed, 1995) or by alteration of various cell signalling pathways. In addition to cancer, not enough apoptosis can result in diseases such as autoimmune lymphoproliferative syndrome (ALPS) (Worth et al., 2006). In general, insufficient apoptosis of auto-aggressive B or T cells results in multiple autoimmune diseases. On the other hand, excessive apoptosis can be a feature of neurodegenerative disease and ischemia-associated injury. For example, the Alzheimer's disease (AD) is a neurodegenerative condition caused by mutations in amyloid precursors protein (APP) and presenilins. These mutations cause the deposition of amyloid beta in extracellular deposits known as plaques. Those are thought to be neurotoxic and also to induce apoptosis by causing oxidative stress or by triggering death ligand expression in neurons and glia (Ethell and Buhler, 2003).

1.2 IMPORTANCE OF APOPTOTIC CELL CLEARANCE

Today, we know that the final step of apoptosis is the clearance of apoptotic cells, a process known as efferocytosis. Efficient efferocytosis contributes to sculpting organs, eliminate abnormal, non-functional or harmful cells and maintain homeostasis. Remarkably, even in tissues where cellular turnover is high - such as lung, intestine, thymus and bone marrow - uncleared apoptotic cells are rarely seen because of the impressive efficiency in apoptotic cell clearance (De Paepe et al., 2004; Elliott and Ravichandran, 2010; 2016; Elliott et al., 2009; Lee et al., 2016). Efferocytosis is an evolutionary conserved process, and early studies in C. elegans suggested that apoptotic cells are recognized and cleared even before they are fully dead (Hoeppner et al., 2001; Reddien et al., 2001). The engulfment of apoptotic cells, in fact, is performed by both professional phagocytes (such as macrophages and dendritic cells) and by non-professional phagocytes (such as epithelial cells, fibroblast and endothelial cells) while the plasma membrane integrity of the dying cell is still preserved. Metazoa have multiple mechanisms in place to handle cell clearance, often depending on the tissue and apoptotic cell type (Gregory, 2009), underlying the importance of this process to maintain immune tolerance and tissue homeostasis. Indeed, failure in clearing apoptotic cells causes the loss of membrane integrity over time, and the progress to secondary necrosis which can induce tissue inflammation due to the release of cellular contents or the exposure of otherwise sequestered intracellular molecules (Poon et al., 2014). This may provide the immunogenic impetus for the onset of some autoimmune disorders in humans, including rheumatoid arthritis and systemic lupus erythematosus (Gaipl et al., 2004).

While the phagocytic machinery is highly conserved regardless the nature of the engulfed target, what distinguish the phagocytosis of apoptotic cells from the phagocytosis of most bacteria or necrotic cells is the lack of pro-inflammatory immune response. Indeed, Henson and Bratton (Henson and Bratton, 2013) provided early evidence that clearance of apoptotic cells by macrophages gives rise to anti-inflammatory effects. In response to efferocytosis, macrophages secrete cytokines, arachidonate metabolites as well as a range of pro-resolving mediators which have been shown to reduce LPS-induced inflammation both *in vitro* and *in vivo* (Henson and Bratton, 2013). Moreover, Weavers and colleagues recently showed that phagocytosis of apoptotic cells is able to prime macrophages for future inflammatory response

by creating a sort of molecular memory usually attributed to adaptive immunity (Weavers et al., 2016).

Hence, it is clear that professional phagocytes such as macrophages, are not simple "garbage collectors" responsible for clearing the tissue from unwanted material, but rather scavengers coordinating and integrating cellular and tissue responses to different stimuli. As described in more details in the following chapter, during phagocytosis signal exchange between the phagocyte and its target is key to ensure efficient clearance. The mechanism of phagocytosis is itself a central regulator of how a cell responds to tissue changes, and contributes to tissue homeostasis.

1.3 PHAGOCYTOSIS: A MULTI-STEP PROCESS

The first observation and description of phagocytosis dates back to 1883, when Elie Metchnikoff described in the starfish-larvae the presence of amoeba-like cells (which he named phagocytes, from Greek words meaning "devouring cells") able to engulf foreign bodies such as bacteria (Gordon, 2008). Today, we still use the same terminology to describe the regulated uptake of large particulate material (such as bacteria or apoptotic cells) into cytosolic membrane-bound vesicles named phagosomes. Evolutionary conservation of this process from the starfish-larvae to mammals shows that this is an essential biological process which ensures both self-defence and homeostasis of the organism.

Work from many groups has shown that phagocytosis is a multi-step process that can be divided in four major steps: attraction of the phagocyte to the target, formation of the phagosome, maturation and finally resolution (Figure 1.1); each of these steps involves multiple reactions that require extraordinary spatial and temporal coordination (Levin et al., 2016).

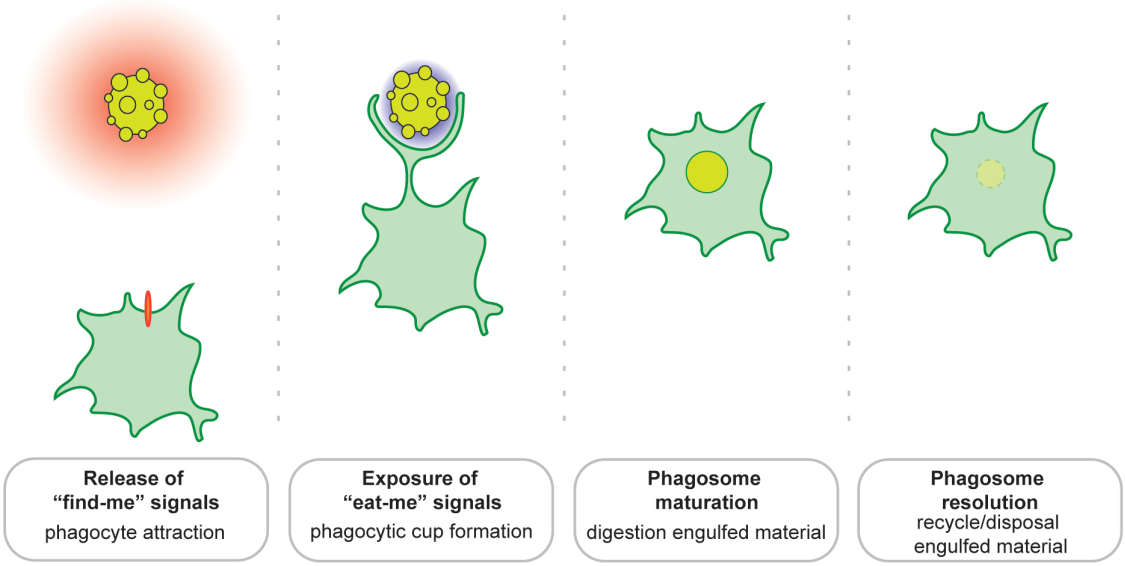

Figure 1.1. The steps of efficient apoptotic cell clearance.

First, "find-me" signals released by the apoptotic cell are recognized by their cognate receptor on the surface of the phagocyte. This interaction triggers the phagocyte to migrate to the location of the apoptotic cell. Second, the phagocyte recognizes exposed "eat-me" signals exposed on the surface of the apoptotic cells via their phagocytic receptors. This induce the formation of a phagocytic cup around the target. As a subsequent step, the newly formed phagosome will undergo a series of fusion and fission events with other organelles of the phagocytic and endocytic pathways, a process known as "phagosome maturation". Here the engulfed material is digested by the phagocyte. The last event, known as "phagosome resolution" is the less understood step of phagocytosis. Presumably, here the digested material gets recycled or disposed by the phagocyte.

Phagocytosis is initiated by engagement of the phagocyte surface receptors that recognize specific ligands exposed or released by the target. Phagocytic receptors initiate a signalling cascade that induces important cytoskeletal modifications which lead to the formation of pseudopod-like structures that surround the target. The newly formed phagosome undergoes a series of fusion and fission events with other cytosolic organelles to ensure degradation of the engulfed material. Finally, the phagocyte must digest and either dispose or recycle the phagosomal content.

Since the first observation of phagocytosis in 1883 (Gordon, 2008), our knowledge has grown exponentially, but many aspects of this process remain unknown. Although receptor-ligand pairs (especially involved in the recognition of the target) might vary depending on the target, the phagocytic machinery is highly conserved and there is a considerable overlap with the endocytic process. In the next paragraphs, I will describe in details the different steps involved in phagocytosis by focusing in particular on the engulfment and processing of apoptotic cells.

1.3.1 "FIND-ME": ATTRACTION OF THE PHAGOCYTE TOWARDS THE TARGET

The first and most obvious requirement for efficient apoptotic cell clearance is bringing the phagocyte in close proximity to its target. In some cases, this can happen passively, as for aged red blood cells which are brought in contact with spleen macrophages thanks to the vascular flow (Kohyama et al., 2012). In other circumstances, for example for pathogen engulfment or efferocytosis by non-professional phagocytes, the interaction with the target can be mediated by simple adjacency (Bray, 2001). However, more frequently, phagocytes must actively survey their environment and migrate towards the target and this is mediated by a signal exchange between the two cells. During efferocytosis, for example, it has been shown that apoptotic cells release so called "find-me" signals that stimulate long-range attraction, promoting the recruitment of the phagocyte to the site of death (Casano and Peri, 2015; Kettenmann et al., 2011; Serhan, 2014). To date, several find-me signals released by dying cells have been reported (Figure 1.2). These include Lysophosphatidylcholine (LPC), Sphingosin-1-phosphate (S1P), fractalkine (CX3CL1) and nucleotides such as ATP and UTP (Elliott et al., 2009; Gude et al., 2008; Lauber et al., 2003; Truman et al., 2008).

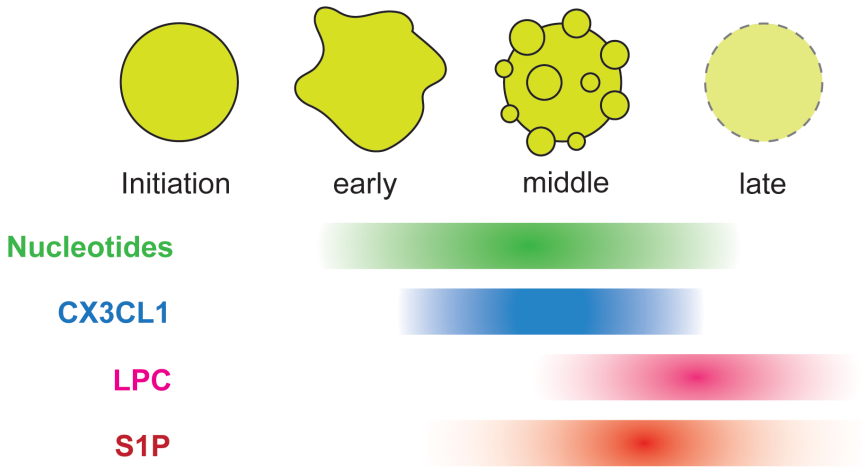

Figure 1.2. Apoptotic stages and release of find-me signals.

Generalized key features of apoptotic cells at different stages after induction of apoptosis. Blebbing, the typical morphological change of apoptosis, occurs between early and middle stages. The formation of apoptotic bodies is accompanied by the release of the so-called "find-me" signals (nucleotides, CX3CL1, LPC and S1P), necessary for the recruitment of phagocytes.

By testing the ability of the cell culture supernatant from apoptotic cells to trigger macrophages chemotaxis, Lauber and colleagues were the first to identify LPC as a find-me signal. They suggested that this is released by apoptotic cells via the caspase-3-dependent activation of phospholipase A2 (Lauber et al., 2003). The binding of LPC to G2A (G protein coupled receptor 132) triggers chemotaxis of macrophages (Peter et al., 2008). However, recently it has been argued that this model is unlikely to work *in vivo* as the concentration of LPC required to induce chemotaxis (20-30 μM) is rather high and might never be reached physiologically (Hochreiter-Hufford and Ravichandran, 2012; Nagata et al., 2010).

S1P is another lipid that is suggested to act as a find-me signal as it is able to induce phagocyte migration (Gude et al., 2008). However, only few reports have focused on the role of S1P in the context of cell death removal and no S1P receptor has yet been shown to mediate chemotaxis (Rosen and Goetzl, 2005).

Fractalkine is the only chemokine shown to be acting as a "find-me" signal (Truman et al., 2008). It is a membrane-associated protein and, upon induction of apoptosis, the extracellular domain is actively cleaved and released in the extracellular medium by neurons and apoptotic B cells. The released peptide binds its receptor CX3CR1 and induces microglia and macrophages chemotaxis.

Finally, secretion of nucleotides and binding to purinergic receptors has also been suggested to mediate phagocyte attraction towards apoptotic cells. The chemotactic nature of ATP and UTP has been largely described (Davalos et al., 2005; Honda et al., 2001; Sieger et al., 2012), however direct proof of their implication in efferocytosis *in vivo* is still limited. The Ravichandran group demonstrated that depletion of extracellular nucleotides by apyrase treatment or deletion of the purinergic receptor P2Y2 cause a delay in the clearance of apoptotic cells by macrophages in the murine thymus (Elliott et al., 2009). Similarly, UDP released by dying hippocampal neurons stimulates phagocytic clearance by microglia (Koizumi et al., 2007). Subsequent studies showed that release of nucleotides is mediated by pannexin channels, which open during apoptosis via caspase-dependent cleavage of their C-terminal tail (Chekeni et al., 2010). Nonetheless, since extracellular nucleotides are unstable and promptly degraded by nucleotidase, they have been suggested to be short-range chemoattractant for tissue resident macrophages rather than long-distance signals (Ravichandran, 2010).

Hence, "find-me" signals can vary significantly and it is still unclear whether they function in an additive or synergistic manner and if different signals could be released at different stages of apoptosis and have alternative functions such as enhancing the phagocytic machinery or the ability to digest the ingested cargo.

1.3.2 "EAT-ME": FORMATION OF THE PHAGOSOME

Phagocytes recognize their prey using receptors that specifically bind to ligands exposed on the surface of the target. During efferocytosis, in particular, apoptotic cells expose the so called "eat-me" signals which allow the phagocyte to sense damage and selectively recognize and remove the dying cells from the living-healthy tissue (Casano and Peri, 2015; Kettenmann et al., 2011; Medina and Ravichandran, 2016). Upon binding, the phagocytic receptors are activated to transmit an intracellular signalling which leads to the rearrangement of the actin cytoskeleton. This results in the formation of a phagocytic cup around the target to allow its engulfment.

To date, numerous eat-me signals have been identified including binding of complement C1q to the apoptotic cell (Ravichandran and Lorenz, 2007), expression of intracellular adhesion molecule 3 (ICAM3) (Devitt et al., 1998) and exposure of intracellular proteins such as calreticulin and annexin I (Arur et al., 2003; Gardai et al., 2005). However, the first and best characterized eat-me signal is the membrane phospholipid phosphatidylserine (PS). PS is

normally confined to the inner leaflet of the plasma membrane but it is exposed to the outer leaflet after induction of apoptosis (Fadok et al., 1998a). The exposure of PS as an "eat-me" signal is found not only in mammals but also in Drosophila, C. Elegans and Zebrafish (Darland-Ransom et al., 2008; Fadok et al., 1992; Hong, 2004; Segawa and Nagata, 2015). Extracellularly exposed PS is recognized by multiple membrane receptors such as T-cell immunoglobulin mucin receptor 4 (TIM4), brain specific angiogenesis inhibitor 1 (BAI1), stabilin-2 (Miyanishi et al., 2007; Park et al., 2007a; 2007b; Rodriguez-Manzanet et al., 2010) and bridging molecules, such as milk fat globule-EGF factor 8 (MGF-E8) and Gas6, that recognize PS and then engage phagocytosis cell surface receptors for engulfment (Ishimoto et al., 2000; Zizzo et al., 2012). More recently, live imaging in zebrafish has allowed to uncover the dynamics of apoptotic neuronal cell clearance by microglia. During brain clearance microglia, the resident macrophages of the brain, engulf single apoptotic neurons by extending highly dynamic branches with large phagocytic cups at their distal tips. Two PS-receptors, BAI1 and TIM4, are required for this process. In particular, while BAI1 has a role in forming the phagocytic cup around the target, TIM4 helps stabilizing this structure by polymerizing F-actin around the phagocytic cup (Mazaheri et al., 2014).

In addition to detecting "eat-me" signals expressed on the apoptotic cells, phagocytes can further distinguish between live and dead target thanks to the exposure of so called "don't-eat-me" signals resent on the surface of living healthy cells. Those include adhesion-related proteins CD47 and CD31. CD47 is expressed on different types of cells and can interact with the inhibitory receptor SIRP1α on phagocytes to restrain the engagement of the phagocytic machinery (Willingham et al., 2012). Similarly, CD31 on viable cells can interact with CD31 on phagocytes to provide a spatially confined repulsion signal to prevent engulfment (Brown et al., 2002). The precise mechanism of action of such "don't eat-me" signals is not yet fully understood, however their exposure has been studied in different contexts. For example, it has been shown that exposure of CD47 is a specific mechanism adopted by cancer cells to escape phagocytosis (Barkal et al., 2018; Brightwell et al., 2016).

1.3.3 DIGESTION: PHAGOSOME MATURATION

Following internalization, the newly formed phagosome undergoes a drastic transformation via a series of fusion and fission events with cytosolic organelles such as endosomes and lysosomes. During this step, known as "maturation", gradual phagosomal acidification

generates a hostile and degradative environment that causes the digestion of the phagocytic cargo. This process has been studied extensively both *in vivo* and *in vitro* and many key molecular markers have been identified. By analogy with the endosomal compartments, phagosomal maturation can be divided into substages: early, late and the phagolysosomal stage (Figure 1.3).

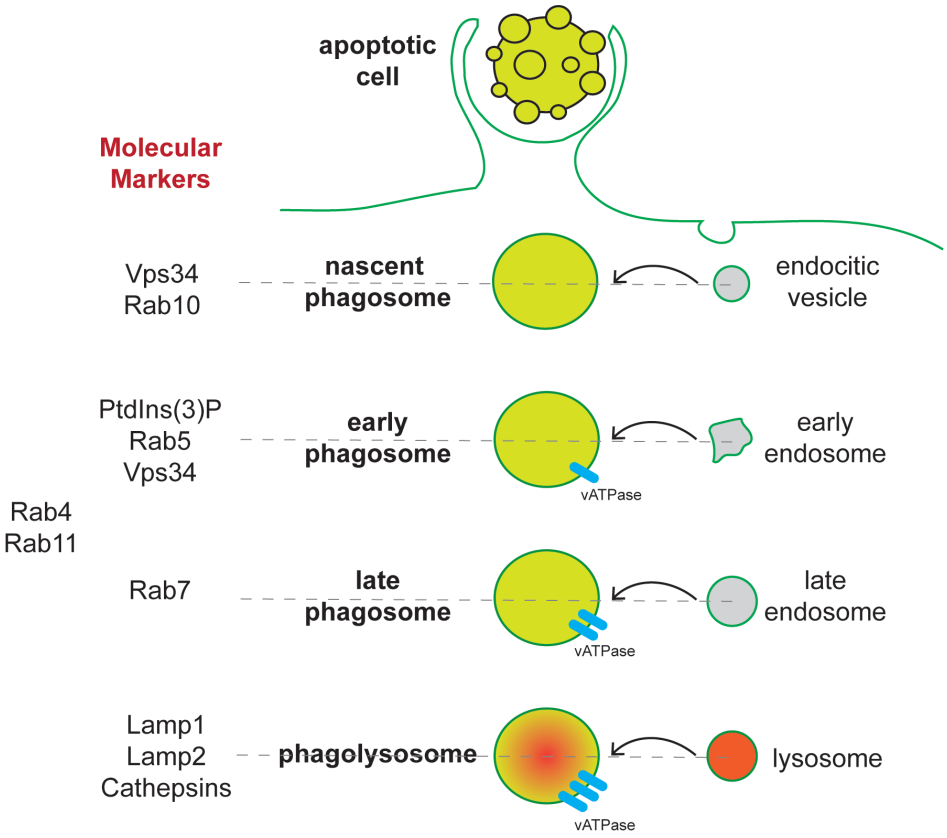

Figure 1.3. Phagosomal maturation: events and molecular markers.

The lumen of nascent phagosomes strongly resembles the extracellular environment. Multiple molecules, such as PtdIns(3)P, Rab5, Rab7 and Lamp1/2, are produced/recruited on the surface of phagosomes at different stages, driving the stepwise phagosome maturation process. During phagosome maturation, nascent phagosomes sequentially fuse with early endosomes, late endosomes and lysosomes forming early phagosomes, late phagosomes and phagolysosomes respectively, and gradually acquiring the membrane and luminal properties of these organelles. The phagosomal lumen at every maturation step is also progressively acidified thanks to the acquisition of additional copies of the proton pump vATPase.

1.3.3.1 The early phagosome

First, the GTPase Dynamin is recruited to the apoptotic cell-phagocyte interface where it interacts with the kinase Vps34. This interaction leads to the recruitment to the surface of the phagosome of Rab5, a small GTPase broadly considered as an early marker of phagocytosis (Roberts et al., 2000; Vieira et al., 2003). Active Rab5 promotes membrane fusion events and

Vps34 itself is one of its effectors; accordingly, Fratti and colleagues showed that inhibition of Vps34 arrests phagosomal maturation (Fratti et al., 2001). The product of Rab5 and Vps34 activity is PtdIns3P, the characteristic phosphoinositide of the early phagosome (Vieira et al., 2001). While the cargo is targeted for degradation, several components are thought to be recycled especially during degradation of apoptotic cells. Although the mechanisms involved in these processes are still largely unknown, the Rab GTPases Rab4, Rab10 and Rab11 have been implicated in recycling and phagosome maturation (Cardoso et al., 2010; Cox et al., 2000; Damiani et al., 2004).

1.3.3.2 The late phagosome

The early phagosome then fuses with late endosomes, thereby becoming a late phagosome. This is characterized by a more acidic pH due to the acquisition of additional copies of the proton pump vATPase. A crucial step during the early-to-late phagosome transition is the switch from Rab5 to Rab7 on the phagosome's membrane, which is therefore considered a molecular marker for this stage of maturation (Harrison et al., 2003; Kinchen et al., 2008; Nordmann et al., 2010; Plemel et al., 2011). At the Rab7 positive stage, the Homotypic fusion and vacuole Protein Sorting (HOPS) complex is recruited to the phagosome, leading to Rab7 activation and, ultimately, fusion of the phagosome with the lysosomal network (Kinchen et al., 2008).

1.3.3.3 The phagolysosome

The phagolysosome is the final degradative compartment. It is generated via the fusion of late phagosomes with lysosomes. Live imaging in zebrafish has shown that phagolysosome are the most prevalent vesicular compartments in the phagocytic microglia and that the a1 subunit of the v0-ATPase complex is essential for the heterotypic fusion between phagosomes and lysosomes. In particular, its absence leads to failure in phagolysosome formation with a consequent accumulation of "undigested" material (Peri and Nüsslein-Volhard, 2008). Moreover, Kimberle Shen and colleagues showed that RagA and Lamtor4, two components of the Rag-Ragulator complex, are essential regulator of lysosomes in microglia. Indeed, RagA deficiency causes and expansion of lysosomal compartments in microglia leading to inefficient digestion of apoptotic neuronal debris (Shen et al., 2016).

The phagolysosome is enriched in lysosome-associated membrane proteins 1 and 2 (Lamp1 and Lamp2), which are considered molecular markers of this stage. Phagolysosomes are highly acidic, oxidative and contain lytic enzymes (Harrison et al., 2003; Kinchen et al., 2008; Meehan et al., 2016). Finally, cargo digestion relies on the activity of several catalytic enzymes such as Cathepsins that function at acidic pH (Flannagan et al., 2012; Harrison et al., 2003; Kinchen et al., 2008).

1.3.4 RESOLUTION: HOW DOES PHAGOCYTOSIS END?

A fascinating but poorly studied step of phagocytosis is how phagosomes get reabsorbed or resolved. When a phagocyte ingests a prey, it is likely to double its protein, carbohydrate and lipid content, yet professional phagocytes manage to rapidly engulf multiple targets. In general, the phagolysosome can catabolize its content via the activity of a diverse arsenal of hydrolytic enzymes. However, the products of this breakdown must be processed to allow the phagocyte to return to homeostasis. Park and colleagues showed that the mitochondrial membrane protein UCP2 positively regulate the engulfment capacity of phagocytes. In fact, while overexpression of UCP2 enhances efferocytosis *in vitro*, loss of its expression reduced the phagocytic activity both *in vitro* and *in vivo* (Park et al., 2011). DNAse II is a lysosomal enzyme responsible for degrading ingested nucleic acids, and lack of this enzyme leads to accumulation of short DNA strands in abnormal storage structures (Kawane et al., 2001; 2003; Mukae et al., 2002). Proteins are degraded into polypeptides and further into amino acids that can serve as nutrients for the phagocytes. To this aim, Cathepsins (which are divided into serine, cysteine and aspartate proteases) are activated at specific maturation stages in lysosomes thanks to the acidic pH (Flannagan et al., 2012; Kinchen and Ravichandran, 2008). Among the different macromolecules, lipids serve several important functions within a cell and are therefore strictly regulated. Interestingly, few studies show that apoptotic-derived cholesterol becomes part of the cholesterol pool of the phagocyte which handle the additional lipid load by increasing their basal efflux mechanism via ABCA1 (Gerbod-Giannone et al., 2006; Kiss et al., 2006).

Although we have some insights about the mechanisms responsible for the degradation of different macromolecules deriving from the engulfed target, our understanding of phagosomal resolution is still very limited. Different lines of evidence point to the existence of post-lysosomal compartments, however -to date- we lack a clear understanding of this final stage.

1.3.5 THE IMPACT OF PHAGOCYTOSIS

Efficient engulfment by motile phagocytes require the execution of two distinct but connected cellular functions: migration toward the target and its subsequent phagocytosis. Those are both energy intensive processes which involve large-scale reorganization of the phagocyte cytoskeleton and overlapping signalling pathways. To date, it is unclear how major cellular events are integrated. Recent studies suggest that events downstream from internalization significantly influence the phagocytic capacity of a cell to engulf additional targets (Krieser et al., 2002; Park et al., 2011; Schrijvers, 2005; Wu et al., 2000). Moreover, it has been shown that blocking digestion or degradation can lead to a variety of cellular and tissue disfunctions that are known as Lysosomal Storage Disorders (LSDs) (Berg et al., 2016; Peri and Nüsslein-Volhard, 2008; Samie and Xu, 2014). Oram and colleagues also showed that impairments in cholesterol efflux are linked to dyslipidemia and atherosclerosis (Oram and Heinecke, 2005). There is evidence for positive and negative feedback loops that operate downstream of phagocytosis. Indeed, after efferocytosis, phagocytes may undergo functional changes and decrease the production of pro-inflammatory cytokines and increase secretion of anti-inflammatory ones (Fadok et al., 1998b).

Although the relevance of the final stage of phagocytosis is becoming more and more clear, the notion that phagosomes need to undergo resolution has not been given enough attention. Consequently, the molecular and tissue implications of resolution are still unexplored.

1.4 TISSUE RESIDENT MACROPHAGES

More than a century ago, Elie Metchnikoff described for the first time the process of phagocytosis and its main player: the phagocyte. A phagocyte is any cell capable of engulfment, for instance, some amoebae behave like macrophage in vertebrates, which suggest that the capability to phagocytose appeared early during evolution.

To date, it has become clear that animals have several distinct populations of phagocytes which are responsible for the homeostatic removal of cellular corpses, debris and pathogens. Classically, phagocytes have been categorized as professional and non-professional depending on how effective they are at phagocytosis. The main difference between the two categories, is that the professional phagocytes display specific receptors able to recognize their targets, therefore being highly efficient in clearing the tissue from unwanted material.

Mononuclear phagocytes include circulating monocytes in the bloodstream as well as dendritic cells and macrophages. In particular, macrophages are the resident phagocytic cells in lymphoid tissues (lymph nodes, spleen) and nonlymphoid tissues, such as liver (Kupfer cells), lung (alveolar macrophages), kidney (kidney macrophages), skin (Langherans cells) and brain (microglia). At these sites, macrophages perform diverse roles in health and disease. They contribute to the steady-state tissue homeostasis via the clearance of apoptotic cells and the release of growth factors, but also upon infection they activate and engulf pathogens and produce pro-inflammatory cytokines (Davies et al., 2013).

Several elegant studies suggest that embryonic yolk sac (YS) derived stem cells colonize most tissues and contribute to the resident macrophage pool (Gomez Perdiguero et al., 2014; Hoeffel et al., 2015). Although they share a common myeloid origin, tissue resident macrophages are characterized by distinct morphologies and functions. Interestingly, genes commonly found in all macrophages are differentially expressed within distinct populations, indicating that specific profiles are likely to result from the crosstalk between the cell ontogeny and the local environment (Gosselin et al., 2014; 2017; Heinz et al., 2010; Lavin et al., 2014). Moreover, cellular heterogeneity is not only observed among different subsets of resident macrophages, but also within the same population. This is, for example, the case of microglia, whose distribution and morphology within the brain is not uniform (Lawson et al., 1990). Also, their expression of surface receptors, as well as cytokines and trophic factors, is highly

heterogeneous both at mRNA and protein levels, reflecting a certain variety in housekeeping functions and responsiveness to stimuli (Hanisch, 2013).

Thus, tissue resident macrophages are both extremely heterogeneous as they fulfil specific functions depending on the tissue they reside in, and highly plastic, able to adapt to different conditions and new environments (Gosselin et al., 2014; Lavin et al., 2014) and to react to multiple stimuli.

1.5 MICROGLIA: THE RESIDENT MACROPHAGES OF THE BRAIN

Microglia are the tissue resident macrophages which orchestrate innate immune responses in the vertebrate CNS. Interestingly, in the brain, microglia fulfil both immune-related and glial-functions by playing crucial roles during development, homeostasis and disease.

The discovery of microglia dates back in the late 19th century. It was first Santiago Ramón Cajal who defined the existence in the brain of a "third element" distinct from astrocytes and neurons, but it was only Pío del Río-Hortega, in 1919, to introduce the term that we use today and to describe in detail both microglia and oligodendrocytes (Sierra et al., 2016). In the same year, Río-Hortega published a series of four papers in which he identified these new glial cells, highly ramified and with a small soma (hence the name "microglia") which he characterized morphologically and functionally under physiological and pathological conditions. The author extensively studied microglia during both development and adulthood and across several different vertebrate species and it is astonishing how, in spite of the limited techniques available at that time, most of his hypothesis remain still true today.

1.5.1 MICROGLIA ARE HIGHLY DYNAMIC AND PLASTIC CELLS

In his first 1919 work, Río-Hortega described the protocol he developed to specifically stain microglia. He found that microglial cells were present in all regions of the brain even though in different densities, and he described those as cell with a reduced soma and long, thin processes which form complex protrusions. He also showed that microglia were able to undergo a hypertrophic transformation and acquire multiple shapes and elongated forms (Sierra et al., 2016). After being neglected for more than 50 years, this cell population is now again subject of much attention. Classically, microglia have been divided in two subtypes: "resting" microglia, distinguished by ramified and highly branched morphology, and "activated" microglia, characterized by an amoeboid shape classical of pathological conditions. While it is true that microglia are highly dynamic and can acquire different morphologies, it is also clear that these descriptions are misleading oversimplifications. Live imaging in both mice and zebrafish embryos showed the very active nature of the so called "resting" microglia. These cells form a highly dynamic and non-overlapping network in the brain with their branched morphology, constantly scanning the surrounding tissue (Nimmerjahn et al., 2005; Peri and Nüsslein-Volhard, 2008). Using live imaging in the intact mouse brain, branched microglia have been

shown to be highly active and to rapidly respond to different stimuli (Nimmerjahn et al., 2005). Transgenic lines in zebrafish further show that microglia continuously engulf neurons with their long processes and transport them back towards the cell body (Peri and Nüsslein-Volhard, 2008). The term "resting" has been in fact substituted with "surveying" as suggested by Hanisch and Kettemann (Hanisch and Kettenmann, 2007).

Microglia are not only very dynamic, but also exceptionally plastic. For example, works conducted in mice showed that brain macrophages have unique gene expression profiles during different phases of development to the extent that it has been proposed to divide microglia in three different groups: early (E10.4-14), pre-microglia [E14-postnatal day (P) 9], and adult microglia (P28 on) (Bennett et al., 2016; Matcovitch-Natan et al., 2016). While some genes which are considered canonical microglial markers (e.g. P2Y12) are expressed already very early during development, other are expressed only in adult microglia (e.g. MafB, Tmem119) (Bennett et al., 2016; Matcovitch-Natan et al., 2016). Recently, many groups got interested in studying the transcription profile of microglia with the aim of determining what defines microglia and how do they vary across time, space and individuals. What is clear from these studies is that the transcriptomic profile of those cells varies not only between different developmental stages, but also age, sex, brain regions and even gut microbiota (Grabert et al., 2016; Matcovitch-Natan et al., 2016; Ransohoff and Khoury, 2016). Microglial functional roles are shaped by complex regulatory networks in their local milieu: many factors are released in discrete brain regions to drive specific microglia functions (Arnò et al., 1AD; Lelli et al., 2013; Mosher et al., 2012; Schafer et al., 2012; Wang et al., 2012). Interestingly, microglia gene expression is dramatically altered by removing microglia from their physiological environment to culture them (Bohlen et al., 2017) showing the importance of working with those cells *in vivo*, in intact systems.

Nowadays, it is clear that microglia are highly dynamic and plastic cells, continuously in contact with their local environment, able to exchange information with it and within each other and to react to different signals.

1.5.2 MICROGLIA ONTOLOGY

In his third publication, Río-Hortega addressed the origin of microglia and he presented arguments in support of their mesodermal origin. Once again, he was right, and after much unnecessary discussion, today it is clear that microglia are, in fact, of mesodermal origin and

derive from early yolk sac macrophages that colonize the brain during embryogenesis. Also, the hematopoietic embryonic origin of microglial cells is conserved across vertebrate species (Ginhoux et al., 2013). For example, it has been shown that absence of pU.1, the myeloid transcription factor, leads to complete depletion of microglia both in mouse and fish (Beers et al., 2006; Peri and Nüsslein-Volhard, 2008). As a further prove for the hematopoietic origin of microglia, deletion of the macrophage specific receptor CSF-1R leads to the complete absence of microglia in mouse (Erblich et al., 2011; Ginhoux et al., 2010). Ginhoux and colleagues showed that microglia start appearing in the brain at E9.0-9.5 and that specific depletion of YS macrophages, but not circulating monocytes, dramatically reduces their number in the brain (Ginhoux et al., 2010). These data are confirmed also in zebrafish, where loss-of-function mutation in fms (the zebrafish orthologue of CSF-1R) impairs macrophages migration from the YS throughout the embryo, resulting in defective microglia brain colonization. However, normal numbers of microglia are restored at larval stages (Herbomel et al., 2001). Recently, our group identified Slc7a7, a Leucine/Arginine amino acid transporter, as a marker for microglia precursors; interestingly, at 22 hours post fertilization (hpf), only a restricted subset of YS macrophages expresses this gene and mutants lacking Slc7a7 have no microglia in the brain, but a normal number and distribution of other tissue macrophages (Rossi et al., 2015). Furthermore, in zebrafish, it has been shown that the establishment of the microglial population is linked to the rate and distribution of developmental apoptosis in the brain. Neuronal apoptosis promotes the entry and positioning of microglia by nucleotide signalling and Lysophosphatidylcholine (Casano et al., 2016; Xu et al., 2016).

1.5.3 MICROGLIA FUNCTIONS

It is clear that microglia are extremely versatile cells: the heterogeneity of their transcriptional profile, their different morphologies, their migratory capacity and their high motility are suggestive of the importance of microglia in brain development and homeostasis. Indeed, these macrophages are involved in many regulatory processes necessary for development, homeostasis, response to injury, infection and subsequent repair. Microglia are responsible for the rapid and efficient clearance of unwanted cells and debris and they react to damage signals (Ransohoff and Khoury, 2016) by migrating over long distances and by producing chemokines, cytokines and other pro- and anti- inflammatory signals to promote repair and homeostatic maintenance (Lenz and Nelson, 2018). In support of the important role of microglia, there is

the fact that deletion of microglia-related genes severely compromises proper brain functionality leading to altered brain wiring and producing behavioural deficits associated with neurodevelopmental and neuropsychiatric disorders (Chen et al., 2010a; Frost and Schafer, 2016; Holstege et al., 2008; Parkhurst et al., 2013).

Thanks to their phagocytic activity, microglia are involved in refinement of neuronal connectivity and spatial patterning. It has been shown that brain macrophages sculpt synaptic connectivity by engulfing the neuronal terminal that form synapses, a process known as synaptic pruning (Hong et al., 2016b; Paolicelli et al., 2011; Schafer et al., 2012; Stevens et al., 2007; Tremblay et al., 2010). More recent studies confirmed this hypothesis by suggesting a model by which microglia would remodel synapsis through a process of trogocytosis (or nibbling) of synaptic structures rather than the engulfment of entire synapses (Weinhard et al., 2018). On the other hand, the role of microglial phagocytosis in sculpting the brain tissue is doubtless. As the local phagocyte of the brain, microglia engulf apoptotic neurons during the embryonic development (Casano et al., 2016; Sierra et al., 2010) and also in adult neurogenesis (Ekdahl et al., 2003; Monje et al., 2003). Furthermore, microglia are thought to actively take part in the shaping of organs by promoting apoptosis directly. This process is known as "phagoptosis" and it has been demonstrated for Purkinje cells (Marin-Teva et al., 2004), granular cells in the hippocampus (Dalmau et al., 1997), and ganglionic cells in the avian retina (Navascués et al., 1995).

1.5.3.1 Phagocytic microglia

A driving force behind many microglial activities is phagocytosis. This is a key function of immune cells in health and disease and microglial cells are a great model for studying this process. Indeed, programmed cell death in the CNS is central in establishing the brain cytoarchitecture, and microglia play a key role in removing apoptotic neurons preventing the leakage of harmful contents and suppressing unwanted immune responses. Microglial involvement in the physiologic removal of apoptotic cells has been first suggested by Perry and Ashwell, who documented the round and ameboid shape of microglia and their distribution preferentially in pyknotic areas of the developing mouse brain (Ashwell, 1990; Perry et al., 1985). Similarly, also in avians, embryonic brain macrophages accumulate in areas characterized by high levels of cell death and show dense phagosome inclusions containing fragments of dead cells at different stages of digestion (Cuadros et al., 1993). Although the

importance of microglial phagocytosis is broadly recognized, factors involved in this process remain largely unknown. The engulfment of apoptotic neurons by microglia follows the multi-step process described for all phagocytes and involves a well conserved molecular machinery across different species such as mouse and zebrafish (Davalos et al., 2005; Haynes et al., 2006; Mazaheri et al., 2014; Ravichandran, 2011; Sieger and Peri, 2012; Sieger et al., 2012). Other than being essential for proper tissue homeostasis, the ingestion and degradation of cells have several indirect consequences for both the phagocyte and the surrounding tissue. Indeed, phagocytosis triggers the activation of several pathways and microglia receive an incredible metabolic load leading to changes in the lipid, cholesterol and glucose metabolism (Han and Ravichandran, 2011).

Overall, microglial phagocytosis is considered a beneficial phenomenon and defects have been linked to autoimmune and neurodegenerative diseases (Nagata et al., 2010; Neumann, 2013). Already Río-Hortega in his fourth paper of 1919 described the high migratory and phagocytic activity of microglia under pathological conditions (Sierra et al., 2016). Neurodegeneration by apoptosis is a major part of several brain diseases such as epilepsy, stroke, Alzheimer's disease (AD) and Parkinson's disease (PD) and the role of microglial phagocytosis in these conditions still remain controversial. For example, in AD microglia are thought to play a detrimental role by removing healthy neurons and synapses (Hong et al., 2016a; Sanagi et al., 2010). Conversely, microglia are thought to play a beneficial role after traumatic brain injuries where they support subsequent recovery by removing cell corpses and debris (Donat et al., 2017; Loane and Kumar, 2016).

Thus, understanding the mechanisms by which microglia migrate, engulf and digest their prays is of great importance and interest in biology and also for developing novel therapeutical approaches to modulate microglia phagocytosis in different contexts.

1.6 ZEBRAFISH AS A MODEL SYSTEM TO STUDY MICROGLIA

Since the work of Streisinger and colleagues in 1980s, zebrafish, Danio rerio, has emerged as an excellent model organism for biological studies (Streisinger et al., 1981). Today, zebrafish is widely used to study, for example, embryonic development, neurobiology and for mechanistic *in vivo* investigations in vertebrates (Amatruda et al., 2002; Dooley and Zon, 2000; Lele and Krone, 1996). This small tropical fish is relatively cheap to raise and maintain, it is easy to handle and breeds rapidly, laying per clutch around 100 embryos which develop rapidly and synchronously outside the mother.

A great advantage of this model system, is its genetic accessibility. Originally, the zebrafish has been extensively used as a tool for large-scale forward genetic approaches. These screens typically are based on adding N-ethyl-N-nitrosourea (ENU) to the water of male zebrafish to induce in premeiotic spermatogonia random point mutations, which are then transmitted to the progeny. In this way stable mutant lines can be generated and used for the unbiased identification of new genes and genetic functions (Driever et al., 1996; Haffter et al., 1996; Meireles et al., 2014; Mullins et al., 1994; Patton and Zon, 2001; Rossi, 2013).

Complementary to forward genetic approaches, with sequencing of the zebrafish genome, a collection of reverse genetics tools has been developed for studying the function of specific genes. Widely used are morpholinos (MOs), antisense oligonucleotides that knock down gene expression by affecting splicing or translation of mRNA. While in mouse antisense oligonucleotides are rapidly diluted during development, in zebrafish the effect of morpholinos can persist up to 5 days post fertilization (dpf), allowing the functional characterization of gene activity *in vivo* (Bedell et al., 2011). To overcome the transient nature of MOs and allow the generation of stable zebrafish mutant lines, engineered endonucleases including ZFNs (zinc finger nucleases), and TALENs (transcription activator-like effector nucleases) have been generated starting in 2008 (Doyon et al., 2008; Huang et al., 2011; Meng et al., 2008; Sander et al., 2011). Those methods allowed to achieve directly site-specific genome modification based on the induction of double strand breaks (DSB) in target genes. These induce non-homologous end joining (NHEJ), an endogenous DSB repair response that results in small insertions and/or deletions. Alternatively, homology-directed repair (HDR) can occur if a template is supplied resulting in the generation of engineered alleles at the break site. However, those systems even though innovative and promising require time and skill. More

recently, the CRISPR-Cas9 (Clustered Regularly Interspaced Short Palindromic Repeats) system has been introduced and this has been immediately recognized as a game-changing advance in directed mutagenesis experiments since it is faster, easier and inexpensive compared to ZFNs and TALENs (Hwang et al., 2013a; 2013b; Sander and Joung, 2014). CRISPR-Cas are RNA-directed endonucleases systems which evolved in bacteria and archaea as a mechanism of defence to silence foreign nucleic acids. These have been engineered to create single guide RNAs (sgRNAs) capable of directing site specific DNA cleavage by the Cas9 nuclease which has been modified by the addition of nuclear localization sequences (NLSs) to target the endonuclease activity to the nucleus in eukaryotes. The endonuclease-generated DSB repair can be manipulated so that the gene function is lost (targeted gene knock-out) or to add a new function (targeted knock-in) by taking advantage of NHEJ or HDR respectively.

There is no doubt that one of the most remarkable advantages of the zebrafish model system is its transparency during embryonic stages. The use of vital dyes and the generation of transgenic lines that label different cell types combined with recent advances in light microscopy allows the monitoring and characterization of complex biological and developmental processes at an unprecedented spatial and temporal resolution *in vivo* (Casano et al., 2016; Huang et al., 2012; Mazaheri et al., 2014; Meireles et al., 2014; Morsch et al., 2015; Peri and Nüsslein-Volhard, 2008).

A great innovation in zebrafish research has been introduced in 2010 thanks to the use of the site-specific recombinases (SSRs) PhiC31 (Hu et al., 2011; Lister, 2010; 2011; Lu et al., 2010; Mosimann et al., 2013). This recombinase mediates an integration reaction between heterotypic binding sites termed attB (attachment site Bacterium) and attP (attachment site Phage) without requirement for any accessory factors (Groth, 2004). The completed attP/attB recombination results in hybrid attL and attR (Left and Right) sites that are incompatible with the phiC31 integrase, thus rendering the recombination irreversible (Groth, 2000). The use of SSRs for generation of proteins' live reporters allows to overcome some limitations such as possible overexpression phenotypes or the variable expression intensity and patterns among different transgenic lines allowing quantitative and qualitative evaluation of transgene expression.

Another recent development that is perfectly suited for zebrafish is optogenetics, an approach that has revolutionized the toolbox arsenal that biologist possess to investigate basic fundamental processes *in vivo*. In fact, the genetic encoding of light-sensitive proteins that

activate or deactivate signalling pathways in response to light allows to monitor, control and perturb tissue and cellular dynamics. Its first application was the use of light-gated ion channels to manipulate the excitability of neuronal cells (Boyden et al., 2005), today the molecular engineering has also enabled optogenetic control of well-defined biochemical events (Airan et al., 2009; Toettcher et al., 2010; Wu et al., 2009). For example, early in 2009 Airan and colleagues described optical control of distinct G protein-coupled receptors (GPCR) biochemical pathways using vertebrate rhodopsin-GPCR chimeras (optoXRs), which recruit pathways that are governed by distinct heterotrimeric G-proteins (G_q and G_s) (Airan et al., 2009).

Relevant for this thesis is the fact that the immune system of the zebrafish closely resembles that of higher vertebrates or mammals, qualifying it as a valid model organism for comparative studies of macrophages, microglia and their interactions with the surrounding environment in the developing living organism (Ellett et al., 2011; Niethammer et al., 2009; Peri and Nüsslein-Volhard, 2008; Renshaw and Trede, 2011; Sieger et al., 2012).

Thus, in the last decade the zebrafish has emerged as a powerful and well-established model system for *in vivo* studies.

2 AIM OF THE PROJECT

The aim of this thesis was to take advantage of the optical transparency of the zebrafish larva and to combine genetical and chemical perturbations to investigate how microglia and macrophages process the ingested cargo. In particular, we aimed to determine the fate of mature phagosomes and understand how their processing impacts back on the phagocytic activity. The starting point of this work has been the identification during a previous genetic screen of a mutant in which microglia are round and bloated.

Former PhD students in the lab contributed to this project. Specifically, Katrin Henke identified the *blb* mutant and mapped the mutations and Christian Moritz performed initial investigative experiments. This work has been conducted in collaboration with my colleague Jørgen Benjaminsen, who in particular focused on the ultrastructural characterizations of macrophages and microglia.

3 RESULTS

3.1 IDENTIFICATION OF A ZEBRAFISH MUTANT WITH AN ABERRANT MICROGLIA PHENOTYPE

Previous work has shown that aberrant morphology of microglia or their phagocytic compartments can be indicative of defects in phagocytosis, such as the fusion between phagosomes and lysosomes (Peri and Nüsslein-Volhard, 2008) or proper lysosomes functionality (Shen et al., 2016). Thus, in order to investigate the mechanisms behind intracellular processing of the material engulfed and phagosomal resolution in brain macrophages, we revisited a large ENU mutagenesis screen that was carried out in 2005-2006 at the MPI in Tubingen, looking for altered microglia morphologies. This was the first screen addressing specifically microglial phenotypes in a vertebrate system. By the use of Neutral Red (NR), a pH indicator staining in the brain microglia, we isolated a class of mutants characterised by an altered morphology (Henke, 2011). This mutant was named *bubblebrain* (*blb*), because of the enlarged, bloated morphology of microglia.

The mutant cells were swollen and had a bubble-like morphology, visible already with low magnification at the stereomicroscope (Figure 3.1 A-D). In order to investigate this phenotype, stable transgenic lines expressing different fluorescent markers were used. In particular, viable *blb* homozygous mutants where crossed with lines labelling all macrophages (*Tg(spi1b:Gal4,UAS:eGFP)*; *Tg(spi1b:Gal4,UAS:TagRFP)* and *Tg(mpeg1:eGFP-caax)*) (Ellett et al., 2011; Peri and Nüsslein-Volhard, 2008; Sieger et al., 2012), or specific for microglia (*Tg(ApoE:lyn-eGFP)*) (Peri and Nüsslein-Volhard, 2008). Then, crosses of these animals with *Tg(NBT:dsRed)* (Peri and Nüsslein-Volhard, 2008) and *Tg(NBT:secA5-BFP)* (Mazaheri et al., 2014) allowed labelling at the same time of macrophages/microglia and neurons or apoptotic neurons respectively. These crosses allowed live imaging of mutant microglia, and confocal microscopy of 4 dpf *blb* embryos revealed that the aberrant morphology observed from the bright field and NR staining was caused by the presence of a single, large vesicle that could reach up to 40 µm in diameter (Figure 3.1 F, H and J). Most of the cell body, indeed, was occupied by this large vesicle (*blb* "vacuole") and it was left with very little cytoplasm.

Moreover, the bubble morphology was accompanied by an important loss of ramifications (Figure 3.1 compare J to I).

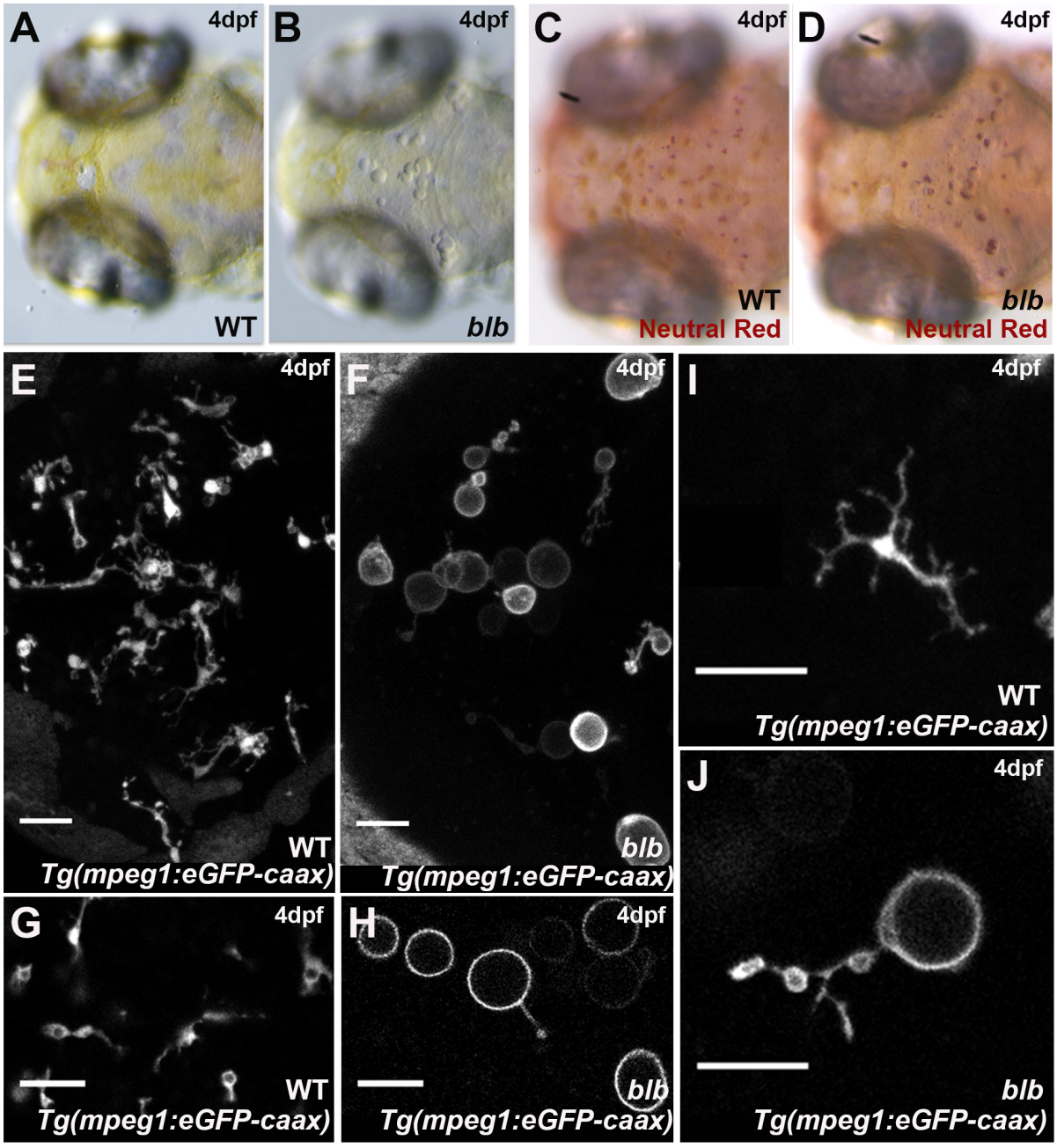

Figure 3.1. Characterization of *bubblebrain* (*blb*), a mutant with bloated microglia.

(**A and B**) Bright field view of the dorsal side of a 4 dpf wild type (A) and blb^{NY007} (B) embryo.
(**C and D**) Neutral Red staining in a 4 dpf wild type (C) and blb^{NY007} (D) embryo.
(**E-J**) Microglia cells labelled with *Tg(mpeg1:eGFP-caax)* in 4 dpf wild type (E, G and I) and blb^{NY007} (F, H and J) embryos. (E and F) Maximum intensity projections of the optic tectum of wild type (E) and blb^{NY007} (F) embryo, scale bar 30 µm. (G and H) Single plans of an optic tectum region of wild type (G) and blb^{NY007} (H) embryo, scale bar 30 µm. (I and J) Microglia cell of wild type (I) and blb^{NY007} (J) embryo, scale bar 30 µm.

3.2 MUTANT MICROGLIA ARE PHAGOCYTIC AND THE PHENOTYPE INCREASES OVER TIME

During brain development, the main function of microglia is the clearance of apoptotic neurons. To determine whether these cells are also phagocytically active in *blb* we took advantage of the *Tg(NBT:secA5-BFP)* line, which labels apoptotic neurons with BFP. In particular, by using this PS reporter (Mazaheri et al., 2014) it was possible to progressively localize apoptotic neurons in 4 dpf mutant embryos. Interestingly, this approach showed that the *blb* vacuole is filled up with apoptotic neuronal material (Figure 3.2 A), suggesting that mutant microglia are phagocytically active.

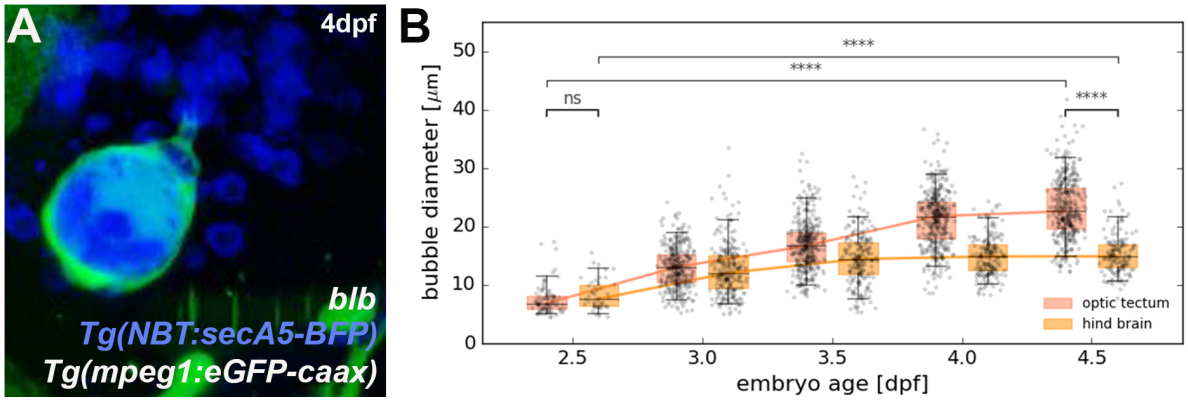

Figure 3.2. Mutant microglia are phagocytic and the *blb* vacuole grows over time.

(**A**) Microglia cell labelled with *Tg(mpeg1:eGFP-caax)* and *Tg(NBT:secA5-BFP)* to visualize apoptotic neurons in a 4 dpf blb^{NY007} embryo.
(**B**) Quantification of the "bubble" size in blb^{NY007} embryos from 2.5 to 4.5 dpf in optic tectum (OT, red plots) and in the hindbrain (HB, orange plots). P value < 0.0001. N reported in Table 3.1.

The characterization of *blb* microglia in terms of morphology and content was performed at 4 dpf, when the brain is fully populated by microglia (Casano et al., 2016). The presence of apoptotic neuronal material inside the *blb* vacuole suggests that the bubble-morphology could be acquired by phagocytosis over time. Thus, to investigate the progression of the *blb* phenotype, we followed those cells during development. In particular, we imaged at the confocal microscope *blb* embryos at different time points, starting at 2.5 dpf when microglia just started entering the brain, through 3, 3.5, 4 dpf till 4.5 dpf when the entire microglia population is established. For each time point, we imaged several embryos (Table 3.1) and we acquired full brain stacks. The analysis was performed by measuring the diameter of the *blb* vacuole in the different brain regions imaged, such as optic tectum (OT) and hind brain (HB).

Indeed, this revealed that the *blb* phenotype progresses over time. At 2.5 dpf few cells were identified with a bubble morphology and the diameter of the vacuole was 3 times smaller than the one observed at the latest time point. From the earliest time point, the size of the bubble increased progressively in all brain regions (Figure 3.2 B). Previous work in the lab showed that different areas in the brain are characterised by different levels of apoptosis (Casano et al., 2016), in particular cell death is significantly less in the HB than in the OT. Our data showed that even though in both regions the bubble diameter increased over time, the growth of the *blb* vacuole was significantly higher in the OT than in the HB (Figure 3.2 B compare red to orange), suggesting a correlation between apoptosis/phagocytosis and progression of the phenotype in *blb*.

Together these results show that the mutant microglia are phagocytically active, as they contain apoptotic neurons, and that the *blb* vacuole grows progressively, in particular in brain regions characterised by high level of neuronal PCD.

Localization	OT	OT	OT	OT	OT	HB	HB	HB	HB	HB
dpf (approx.)	2.5	3	3.5	4	4.5	2.5	3	3.5	4	4.5
N (fish)	11	54	48	44	44	11	54	48	44	44
n (cells)	92	333	372	391	389	48	253	208	198	158

Table 3.1. N and n quantification in Figure 3.2 B

Number of embryos and cells analysed at each time point for the quantification of the bubble growth.

3.3 THE *BLB* PHENOTYPE RESULTS FROM DEFECTS IN PROCESSING OF THE ENGULFED MATERIAL

The bloated phenotype observed in *blb* microglia and the accumulation of apoptotic material in those cells could be the consequence of increased phagocytic activity. This might be induced by higher levels of neuronal apoptosis, therefore we investigated whether programmed cell death was altered in *blb* mutants. The number of apoptotic cells was quantified in living samples by staining with Acridine Orange (AO). This is an intercalating agent that binds to the fragmented DNA of apoptotic cells and has been widely used for fast labelling and analysis of cell apoptosis *in vivo* (Abrams et al., 1993; Casano et al., 2016; Mazaheri et al., 2014; Paquet et al., 2009). In particular, for a proper estimation of the absolute amounts of dead cells accumulated in the brain, phagocytic microglia were genetically depleted in *blb* and wild type controls. This was achieved via a morpholino approach, by knocking down the myeloid transcription factor pU.1, which impairs the production of macrophages and microglia (Peri and Nüsslein-Volhard, 2008; Rhodes et al., 2005). This approach revealed that apoptosis occurs at a normal rate in mutant embryos as numbers of apoptotic nuclei in embryos lacking microglia are comparable between wild type and *blb* (Figure 3.3 A-C).

Then, we asked if the phagocytic activity was affected in *blb* mutants, and to achieve this we used two different approaches. First, we performed AO staining in wild type and *blb* embryos in the presence of phagocytic microglia and we quantified the number of uncollected apoptotic neurons. Contrary to what expected, this showed that the amount of un-engulfed apoptotic cells is significantly higher in *blb* when compared to wild type embryos (Figure 3.3 D). These data suggest that in *blb* while neuronal cell death is normal, the clearance of apoptotic neurons is defective. To test this, we took an *in vivo* approach by using live reporters labelling microglia and apoptotic neurons. Time lapse imaging in wild type and *blb* embryos were quantified by counting the number of phagocytic events over time. This showed that *blb* microglia engulf fewer neurons per hour when compared to wild type cells (Figure 3.3 E).

Collectively, these findings excluded that the *blb*-bloated morphology was caused by increased apoptosis or engulfment. Therefore, we asked if the *blb* defect would occur downstream of these events, in the processing of dead neurons. To test this, different approaches were used to manipulate brain apoptosis or microglia engulfment and monitor the effects on *blb* microglia morphology.

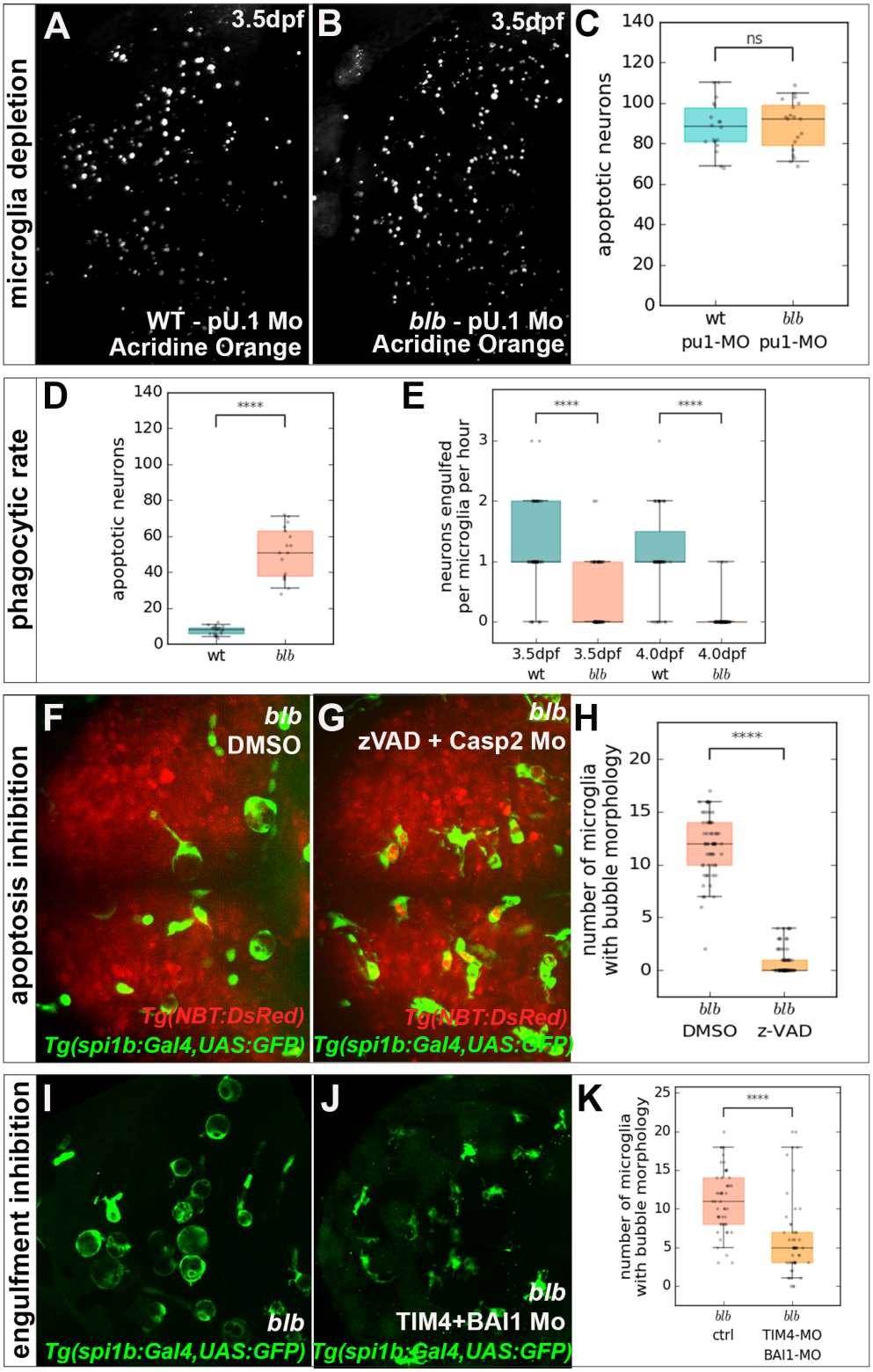

Figure 3.3. *Bubblebrain* functions downstream of cell death and engulfment.

(**A-C**) Microglia depletion in wild type and blb^{NY007} embryos and Acridine Orange (AO) staining for apoptosis quantification. (A and B) Dorsal view of a 3.5 dpf wild type (A) and blb^{NY007} (B) embryo injected with the pU1 morpholino to deplete microglia and stained with AO to visualize apoptotic neurons. (C) Quantification of apoptotic neurons visualized by AO in wild type (n=18) and blb^{NY007} (n=19) injected with the pU1 morpholino to deplete microglia in 3.5 dpf embryos; representative images in (A) and (B).

(**D and E**) Analysis of the phagocytic rate of wild type and blb^{NY007} embryos. (D) Quantification of uncollected apoptotic neurons visualized by AO in wild type (n=20) and blb^{NY007} (n=17) embryos. P value < 0.0001. (E) Quantifications of phagocytic events per cell per hour in wild type (n=50;47) and blb^{NY007} (n=61;77) embryos at 3.5 dpf and 4dpf, respectively. P value <0.0001.
(**F-H**) Analysis of *blb* microglial morphology upon apoptosis inhibition. Dorsal view of blb^{NY007}; *Tg(spi1b:Gal4,UAS:GFP)*; *Tg(NBT:DsRed)* (F) and blb^{NY007}; *Tg(spi1b:Gal4,UAS:GFP)*; *Tg(NBT:DsRed)* injected with a Caspase 3 morpholino and treated with Z-VAD to reduce apoptosis (G), representative images quantified in (H). (H) Quantification of (F) and (G). Number of microglia with bubble morphology in blb^{NY007} (n=61) and blb^{NY007} with reduced apoptosis (n=61). P value < 0.0001.
(**I-K**) Analysis of *blb* microglial morphology upon engulfment inhibition. (I and J) Microglial cells labelled with *Tg(spi1:Gal4,UAS:GFP)* in 4 dpf blb^{NY007} (I) and in blb^{NY007} injected with morpholinos against BAI1 and TIM4 to reduce engulfment (J), representative images quantified in (K). (K) Quantification of (I) and (J). Number of microglia with bubble morphology in blb^{NY007} (n=50) and blb^{NY007} injected with BAI1+TIM4 morpholino to reduce engulfment (n=50) P value < 0.0001.

First, we decreased cell death. The pathway of apoptosis is incredibly conserved between mammals and fish, and many of its core components can be compared between the two groups of vertebrates (Eimon and Ashkenazi, 2010). Thus, cell death reduction was achieved by targeting the effector caspase-3, a critical executioner of apoptosis, using a morpholino-mediated knock down and the irreversible caspase inhibitor Z-VAD-fmk (Williams and Holder, 2000; Yamashita et al., 2008). Previous work in the lab showed that those treatments combined were efficient in reducing of 50% apoptosis levels (Casano et al., 2016). Here, quantification of the number of microglia with a bubble morphology, showed a significantly lower number of bloated microglia in *blb* embryos in which we reduced apoptosis as described above (Figure 3.3 F-H).

Next, we inhibited microglial engulfment. In particular, we targeted simultaneously two PS receptors, BAI1 and TIM4, which are highly expressed on microglia and are involved in phagocytic cup formation and phagosome stabilization respectively (Mazaheri et al., 2014). Previous work in the lab demonstrated that morpholino knock down of both PS receptors leads to a significant decrease in engulfment (Mazaheri et al., 2014). Here, similarly to the result obtained for apoptosis inhibition, also the down regulation of engulfment receptors decreased significantly the number of visible bubble-like microglia in the brain of *blb* (Figure 3.3 I-K). Therefore, apoptosis inhibition and engulfment down regulation prevented the formation of the typical bubble-like morphology in *blb*.

The data presented above identify *blb* as a factor required in microglia for intracellular processing downstream of apoptotic cell engulfment.

3.4 THE *BLB* PHENOTYPE IS NOT RESTRICTED TO MICROGLIA BUT AFFECTS ALL MACROPHAGES

To determine whether the *blb* phenotype was restricted to microglia or if other professional phagocytes display a similar bloated morphology, we examined other tissue resident macrophages. The use of the transgenic line *Tg(mpeg1:eGFP-caax)* labelling all macrophages allowed live imaging of trunk macrophages which exhibited a normal morphology at physiological conditions (Figure 3.4 A). It has been previously shown that in the trunk apoptotic levels are low (Cole and Ross, 2001; Yamashita, 2003), therefore the normal macrophages' phenotype could be due to their lower phagocytic activity compared to microglia. To test this, we induced all macrophages to engulf more by elevating cell death. In particular, we induced ectopic apoptosis by treating the zebrafish embryos (*blb* and wild type controls) with the drug Camptothecin (CPT) (Li et al., 2017). CPT is an alkaloid which reversibly binds DNA-topoisomerase-I complexes, but not the enzyme or DNA alone, inducing apoptosis in dividing cells. This treatment resulted in *blb* trunk macrophages developing a bubble-like morphology similar to that of microglia (Figure 3.4 B). Similarly, trunk macrophages developed the characteristic *blb* microglia phenotype when induced to phagocyte more in response to a tissue damage induced with either laser ablation or mechanical injury by forceps (data not shown).

These data indicate that the *blb* phenotype is not restricted to the brain, but it can affect all phagocytically active macrophages in the body.

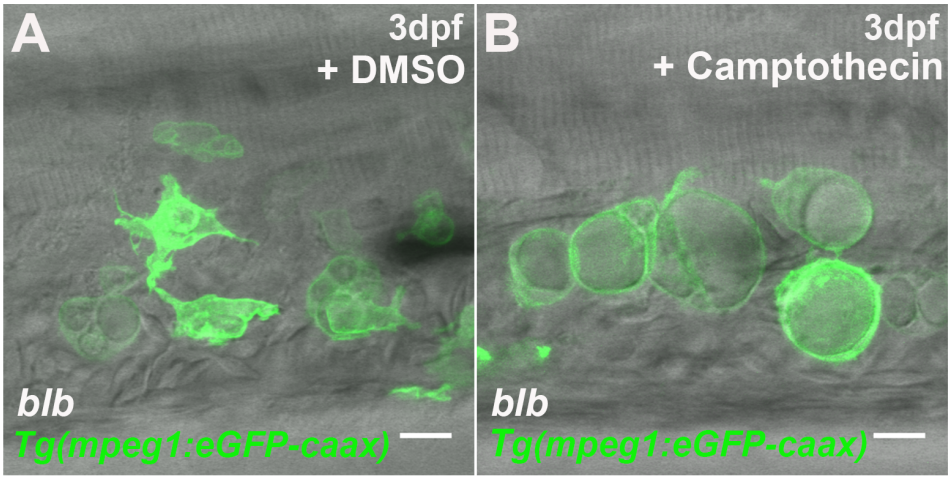

Figure 3.4. The mutant phenotype affects all macrophages.

(**A and B**) Representative examples of trunk 4dpf macrophages in blb^{NY007} (A) and blb^{NY007} treated with Camptothecin to increase apoptosis (B). Scale bar 10µm.

3.5 THE *BLB* VACUOLE IS CHARACTERIZED BY A DISTINCT ULTRA-STRUCTURE

The most striking feature of the *blb* mutant was the presence of a single large vesicle per cell. As described earlier, at 4 dpf, the identification of mutant microglia is straightforward even without any fluorescent labelling observing the zebrafish head at low magnification at the stereomicroscope. Thus, we aimed to describe the ultrastructure of this vesicle which grows over time upon phagocytic activity. Electron microscopy (EM) is a major analytical method, with significant higher resolution compared to confocal microscopy, and commonly used in biology to investigate the structure and content of a wide range of biological samples and compartments. Thus, by taking an EM approach we described the morphology and content of the *blb* vacuole and the general ultrastructure of mutant microglia. As observed by live imaging, this approach confirmed that *blb* microglia have a very limited cytoplasm as most of the cell volume is occupied by one large vesicle. In addition, this approach revealed that this big vesicle is surrounded by a single lipid bilayer and has a strikingly electron lucent, clear lumen that contains sparse membrane debris (Figure 3.5). Interestingly, we couldn't find any description in the literature of such a compartment in microglia or macrophages.

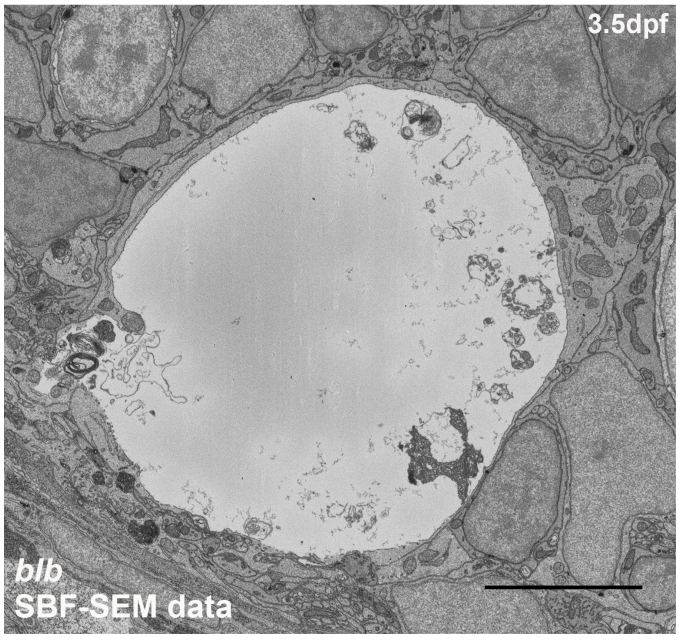

Figure 3.5. The *blb* vacuole has a distinct ultrastructure.

Electron micrograph of a representative blb^{NY007} microglia at 3.5 dpf. Scale bar 5µm.

3.6 GENETIC MAPPING OF *BLB* REVEALS THAT THE UNDERLYING GENE ENCODES FOR SOLUTE CARRIER FAMILY 37 MEMBER 2 (SLC37A2)

Previous work in the lab has mapped the *blb* mutation on chromosome 5, in an interval that includes the gene Slc37a2 (Figure 3.6 A). This is a solute carrier transporter predicted to harbour 12 transmembrane α helixes and responsible for glucose-6-phosphate (G6P) transport. In particular, two non-complementing mutant alleles - NY007 (blb^{t30301}) and NI150 (blb^{t30913}) - characterized by a C to T transition at bp +442 and a T to A transition at bp +1016 respectively have been identified. In both cases, the point mutations lead to the formation of premature stop-codons and the consequential production of a truncated, potentially non-functional protein (Figure 3.6 A) (Henke, 2011).

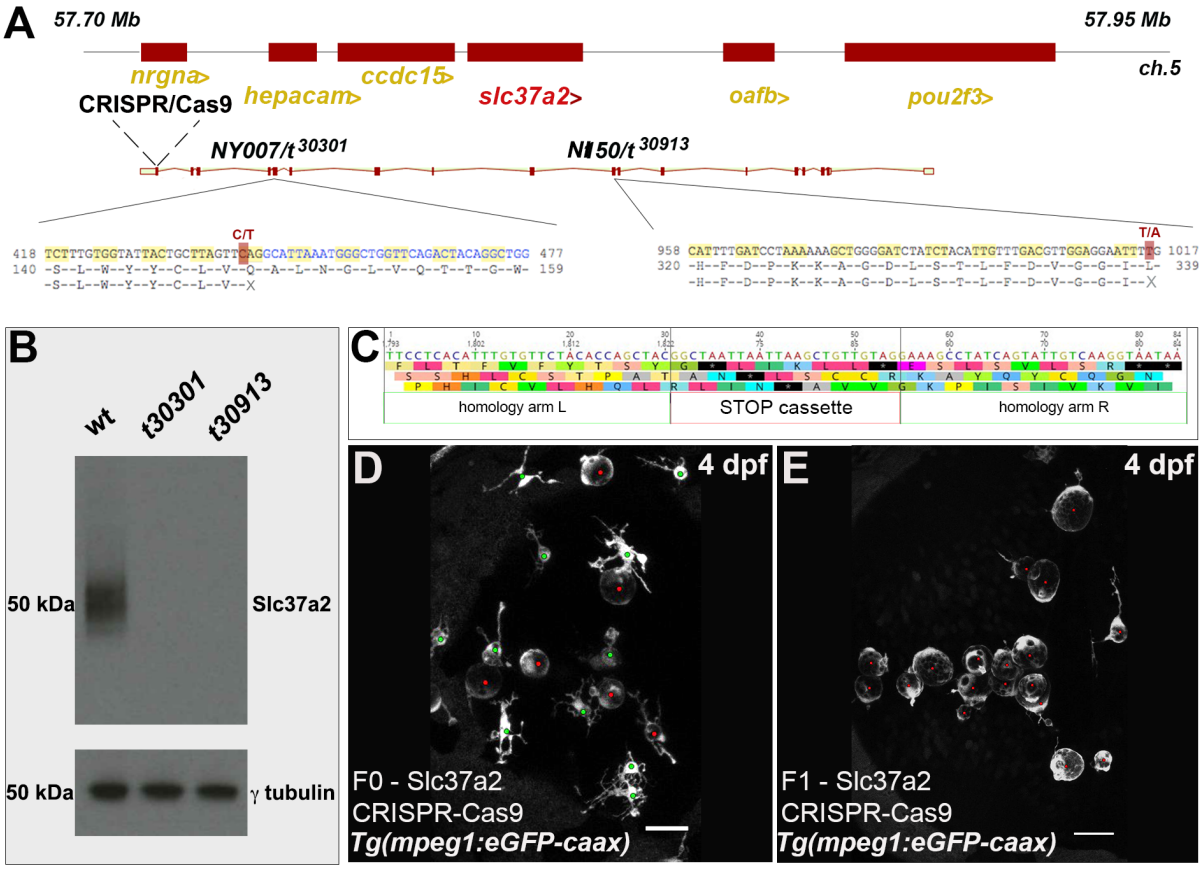

Figure 3.6. Cloning and characterization of Slc37a2, the gene underlying the *blb* phenotype.

(**A**) Schematic of the *slc37a2* locus. Sequences of the NY007/t^{30301}allele (C/T mutation) and NI150/t^{30913} allele (T/A mutation).
(**B**) Western blot analysis of Slc37a2 (55kDa) and γTubulin (48kDa) in wild type, blb^{NY007} and blb^{NI150} total lysates.

(**C**) Sequence with annotations of the STOP-cassette injected in wild type *Tg(mpeg1:eGFP-caax)* labelled embryos to generate the Slc37a2-CRISPR knock-out via CRISPR-Cas9.
(**D and E**) Dorsal view of 4 dpf Slc37a2 CRISPR knock-out embryo generated as shown in (A and C) labelled with *Tg(mpeg1:eGFP-caax)*. Red dots indicate microglia with bubble morphology, green dots indicate microglia with normal morphology. Scale bar 30 µm. (D) Embryo injected with CRISPR-Cas9 targeting Slc37a2 in combination with the STOP-cassette. F0 generation. (E) F1 generation of (D) obtained by incross.

To investigate the expression and localization of Slc37a2 protein, a mouse monoclonal antibody was raised against the fish epitope. In particular, we selected 32 aa (aa 236-267) in the loop between transmembrane domain 6 and 7, as the stretch of this protein is predicted to be exposed, enabling binding of the antibody. First, we used this monoclonal antibody for western blot (WB) analysis to determine the Slc37a2 protein expression in wild types, NY007 and NI150 embryos. To this aim, 4 dpf embryos were homogenised and proteins were obtained by using a lysis buffer optimized for extraction of transmembrane proteins (Fiorotto et al., 2016). The samples were run on a gel and transferred on a membrane for immunoblot with Slc37a2 and γ-tubulin antibodies. The Slc37a2 protein is post-translationally modified with the addition of N-linked glycans and migrates as a heterogeneous species of 50-75 kDa, while γ-tubulin is a 50 kDa protein commonly used as housekeeping protein for the positive control. As expected, wild type lysates showed both bands at the proper molecular weights, while NY007 and NI150 extracts had a comparable γ-tubulin band, but absence of the Slc37a2 one. This showed that protein extraction and immunoblot were successful in all samples, but both *blb* mutants lacked Slc37a2 protein (Figure 3.6 B). These data supported the conclusion that both *blb* mutations are null alleles for Slc37a2.

Commonly, to confirm the phenotype of interest is actually caused by the lack of the identified protein, cloning is used to test whether gene overexpression does rescue the observed phenotype. Unfortunately, we were never able to clone the fish Slc37a2 gene as this turned out to be highly toxic to several different bacteria strains, regardless the method of cloning and/or culturing. To overcome this problem, we adopted an opposite approach and, by taking advantage of reverse genetics, we knocked out Slc37a2 gene in wild type embryos and characterized microglial cells. In particular, we used CRISPR-Cas9 technology to introduce a DSB at the beginning of the gene and induce HDR to introduce stop codons. By using the software CHOPCHOP we designed a sgRNA targeting the first exon of the gene (bp +108); this, co-injected in one cell stage wild type embryos together with Cas9 protein, introduced DSB at the desired position (Figure 3.6 A). To generate a knock out gene, we co-injected a short

nucleotides sequence containing STOP codons in every reading frame and homology arms to mediate HDR (Figure 3.6 C). Already F_0 injected embryos displayed a mosaic expression of the *blb* phenotype clearly visible both at the stereomicroscope and confocal microscope (Figure 3.6 D). Embryos from F_1 generation obtained by incross of injected F_0, had all microglia showing the typical bubble-like morphology and were indistinguishable from blb^{t30301} and blb^{t30913} mutants (Figure 3.6 E, compare with Figure 3.1 F).

3.7 LACK OF SLC37A2 CAUSES SUGAR BUILD-UP AND OSMOTIC STRESS IN MACROPHAGES

Slc37a2 belongs to the Slc37 family which consists of four members, a1, a2, a3 and a4. The latter, also known as glucose-6-phosphate (G6P) transporter (G6PT), is the best characterized. It has been shown that G6PT coupled with G6Pase-α or G6Pase-β maintains blood glucose homeostasis or neutrophils energy homeostasis and functionality, respectively (Chou et al., 2010a; 2010b; Jun et al., 2010). Deficiency in sugar transport or processing can severely affect homeostasis, leading to pathological conditions. Mutations in Slc37a4 have been associated with various forms of glycogen storage disease. Indeed, Chou and colleagues showed that lack of G6PT causes glycogen storage disease 1b, a metabolic and immune disorder (Chou et al., 2010a; 2010b).

While the role of Slc37a4 is clear, very little is known about Slc37a2. It was first identified by Takahashi and colleagues in RAW 264.7 macrophages as a cAMP-inducible gene (Takahashi et al., 2000). This, together with the finding by Kim and colleagues that Slc37a2 is highly expressed in macrophages in white adipose tissue of obese mice (Kim et al., 2007), suggests a macrophage specific function for the gene. Subsequent studies *in vitro* identified Slc37a2 as a protein anchored to the endoplasmic reticulum and functioning as a phosphate-link G6P antiporter catalysing G6P:P_i and P_i:P_i exchanges (Bartoloni and Antonarakis, 2004; Chou et al., 2013; Pan et al., 2011). Thus, lack of G6P:P_i transport might lead to G6P accumulation followed by an influx of water.

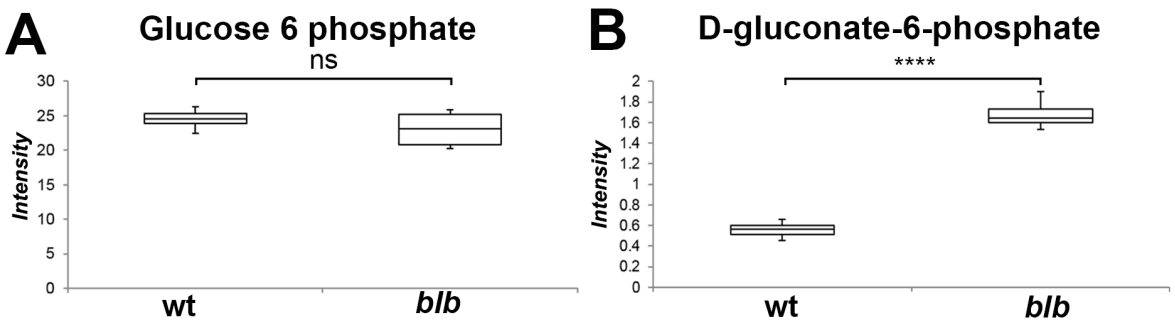

Figure 3.7. Heads of *blb* embryos show an accumulation of D-gluconate-6-phsphate.

(**A and B**) Mass-spectrometry data showing normalised intensities of glucose 6-phosphate (A) not significant, and D-gluconate-6-phosphate (B) significant in wild type and blb^{NY007}. P value < 0.0001.

To investigate the substrate of Slc37a2 transporter *in vivo*, we took a mass spectrometry approach. To this aim, we compared levels of sugars in the heads of wild type and *blb* embryos.

Interestingly, while we couldn't detect any significant difference in the levels of G6P (Figure 3.7 A), this approach revealed in mutant heads a significant enrichment in D-gluconate-6-phosphate, a well-known by product of G6P in the pentose phosphate pathway (Figure 3.7 B). Thus, lack of Slc37a2 is likely to cause a build-up of D-gluconate-6-phosphate that cannot be extracted from the phagocyte. This sugar accumulation might induce an osmotic stress which induce microglia to swallow. In line with this, injection of a saturated glucose solution locally in the brain of mutant embryos led to the complete collapse of *blb* microglia, indicating that those cells are indeed subjected to osmotic stress (Moritz, 2014).

3.8 SLC37A2 LOCALIZES TO PHAGOSOMES IN MICROGLIA AND MACROPHAGES

As previously shown, the *blb* phenotype is not restricted to microglia, but affects all phagocytically active macrophages in the body (Figure 3.4 B). The expression of Slc37a2 in macrophages is in line with its first identification in RAW 264.7, one of the most commonly used lines of mouse macrophages (Takahashi et al., 2000) and the identification of this protein highly expressed in the macrophages of obese mice (Kim et al., 2007). In order to determine the subcellular localization of Slc37a2, we performed whole mount immunohistochemistry in 3 and 4 dpf wild type embryos. In particular, we used the monoclonal antibody directed against the fish epitope and performed double labelling experiments in wild type *Tg(mpeg1:eGFP-caax)* transgenic embryos to visualize at the same time Slc37a2 and macrophages. This showed that, in the brain, Slc37a2 localizes specifically on microglia (Figure 3.8 A). Higher magnification of the stained tissue showed that in particular Slc37a2 localizes around phagosomes (Figure 3.8 B).

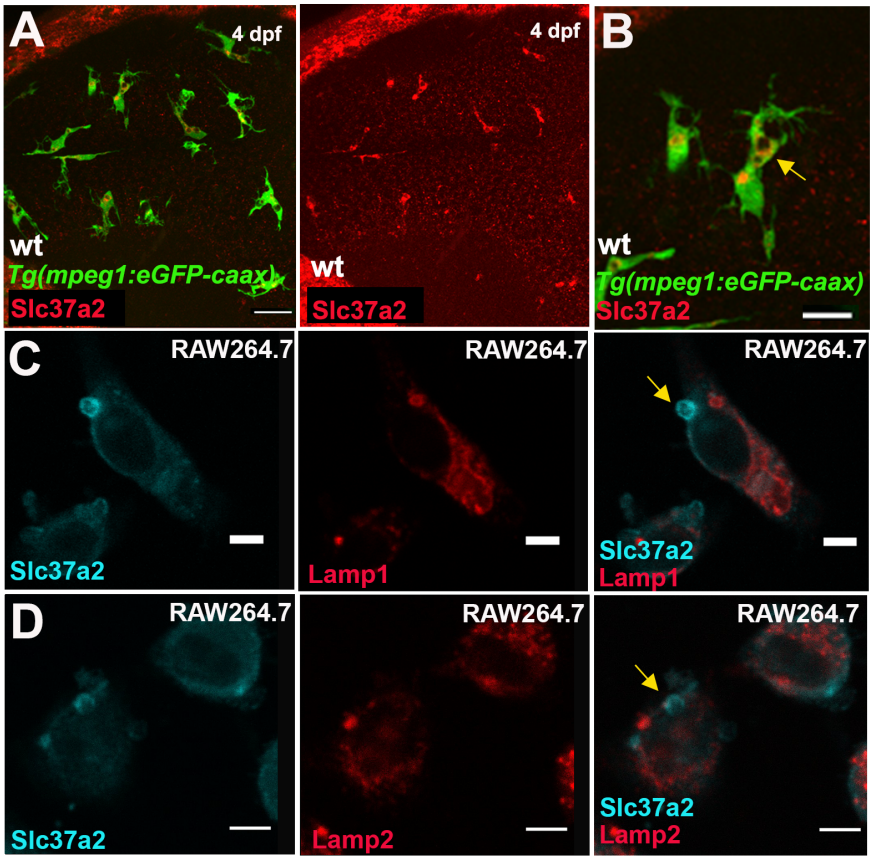

Figure 3.8. Subcellular localization of Slc37a2 in fish microglia and mouse macrophages.

(**A and B**) Dorsal view of a representative immunostaining of a 4 dpf wild type embryo where microglia are in green *Tg(mpeg:GFP-caax)* and Slc37a2 in red. Scale bar 30µm. (B) Magnification of (A). Scale bar 15µm. The yellow arrow points to a phagosome positive for Slc32a2.

(C and D) Immunostaining in RAW 264.7 cells. The yellow arrows point to phagosomes positive for Slc37a2. Scale bar 5 µm. (C) Immunostaining of Slc37a2 (cyan) and Lamp1 (red). (D) Immunostaining of Slc37a2 (cyan) and Lamp2 (red).

Slc37a2 localization around phagosomes suggested a role for this protein in the phagocytic pathway. However, a limitation of the zebrafish model system is the poor availability of antibodies. For this reason, to better characterize Slc37a2 and its relation with other phagocytic markers, we investigated the localization of this protein in RAW 264.7. Immunofluorescence staining on RAW 264.7 by using a commercial antibody against the mouse protein (see material and methods), showed that -similarly to what observed in fish microglia- Slc37a2 localizes to vesicles inside the phagocyte (Figure 3.8 C and D, cyan). Interestingly, the Slc37a2-positive vesicles were negative for Lamp1 and Lamp2, two classical lysosomal markers (Figure 3.8 C and D, red).

The data reported here showed that Slc37a2, a sugar transporter, is localized on the membrane of phagosomes in microglia and macrophages. Here, it is likely to mediate the export of sugar(s) deriving from engulfed material (such as apoptotic neurons), participating at the phagosomal maturation.

3.9 *IN VIVO* TRACKING OF PHAGOSOMES SHOWS THAT PROCESSING OF APOPTOTIC NEURONS REQUIRES SLC37A2-MEDIATED COMPACTION

Previous work in the lab has shown that in the developing zebrafish embryo, the higher level of apoptosis in the brain are observed at 3 dpf (Casano et al., 2016), which therefore is the stage when microglia are most phagocytically active. The data presented above identified Slc37a2 as a protein localized on phagosomes in microglia, however its lack induces the enlargement of a single vesicle in the cell. To understand the consequences of lack of Slc37a2 on phagosomes within microglia, we took a quantitative approach. To this aim, we imaged by confocal microscopy several wild type and *blb* embryos at 3 dpf taking full brain stacks. In line with the previously quantified phagocytic activity (Figure 3.3 D), *blb* showed less phagosomes per cell when compared to wild type (Figure 3.9 A). Moreover, measurement of phagosomal diameter revealed a significant difference in vesicles size between wild type and *blb*, with the latter having, on average, bigger phagosomes (around 5 µm, Figure 3.9 B). However, the distribution of phagosomes diameter in both genotypes revealed that while in *blb* all phagosomes are around the same size (approximately 5 µm), in wild type the range of size was much broader, varying from 1 to 6 µm, with two high-density-areas around 2 µm and 4-5 µm respectively (Figure 3.9 B).

To understand the dynamics behind the difference in phagosomal size distribution we took a live imaging approach. In particular, we aimed to image wild type and *blb* brains at high temporal and spatial resolution in order to describe the process of microglial phagocytosis in great detail. Noteworthy, the light excitation during live imaging is associated with phototoxicity which increases with higher thickness of the sample and faster temporal resolution. At 3 dpf, the transparent larval tectum is 300-400 µm and populated by 20-30 cells (Peri and Nüsslein-Volhard, 2008). Here, to minimize phototoxicity and photobleaching without compromising on the imaging resolution, we took advantage of Single Plane Illumination Microscopy (SPIM). This approach allowed us to acquire the entire brain volume of 3 dpf living embryos in thin sections (0.5 µm) and at fast temporal resolution (15-30 seconds) for several hours. Interestingly, SPIM imaging in wild type and *blb* embryos showed that neuronal engulfment results in the formation of phagosomes of similar size (around 5µm, Figure 3.9 C), further supporting the conclusion that defects lie downstream of engulfment. Moreover, we tracked newly formed phagosomes and measured their diameter over time. This

revealed that wild type phagosomes are highly dynamic compartments that undergo a progressive shrinkage corresponding to a reduction of 34% of their initial volume, on average (Figure 3.9 D, green line). By contrast, *blb* phagosomes maintain their initial size (Figure 3.9 D, red line). These results explain the different distribution in phagosomal size and suggest the requirement of Slc37a2 in wild type phagosomal size reduction.

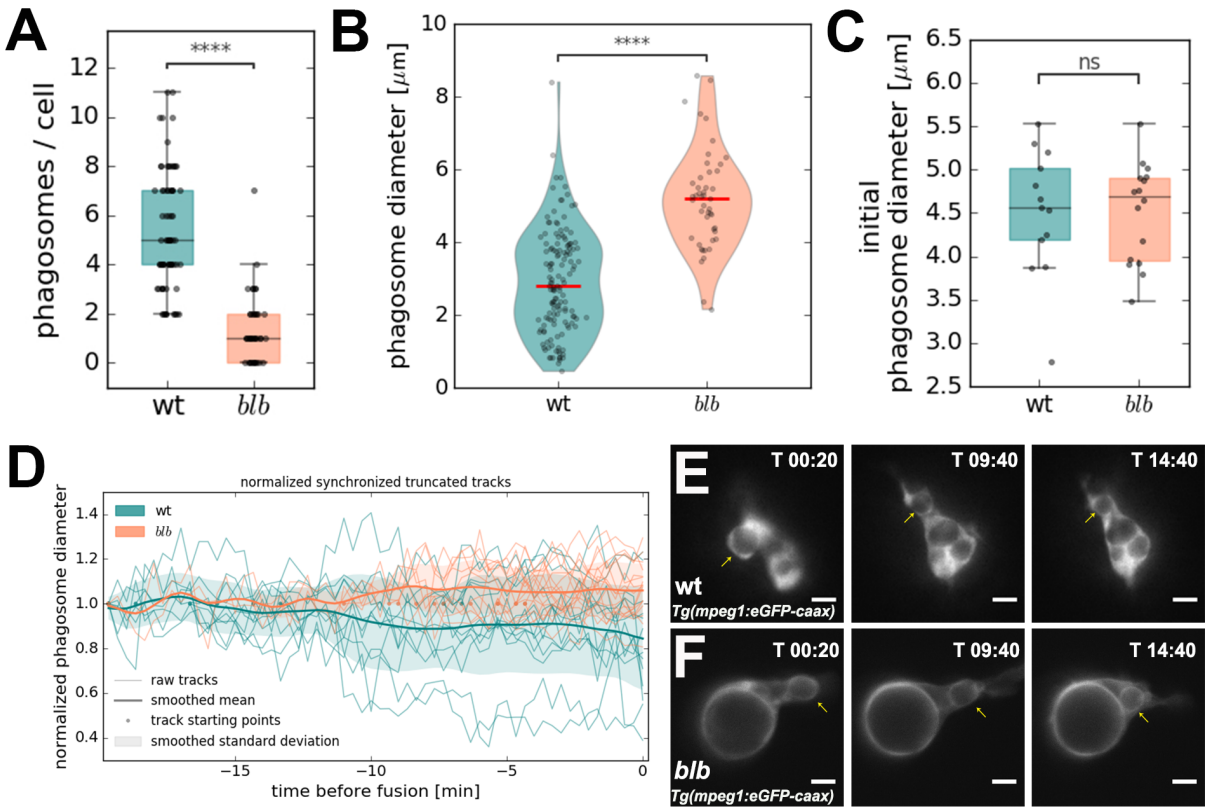

Figure 3.9. Tracking of phagosomes reveals that these shrink in a Slc37a2-dependent manner.

(**A**) Box plot showing the number of phagosomes per cell in wild type (N=9; n=72) and blb^{NY007} (N=9; n=40) at 3 dpf. P value < 0.0001.
(**B**) V-plot showing size distribution of phagosomes in wild type (N=27; n=141) and blb^{NY007} (N= 27; n=47) at 3 dpf. P value < 0.0001.
(**C**) Quantification of the size of newly formed phagosomes in 3 dpf wild type (n=13) and in blb^{NY007} (n=16).
(**D**) Quantification of relative vesicle diameter over time in 3 dpf wild type (n=13) and blb^{NY007} (n=16). T0 corresponds to first fusion event. Data are normalized against the initial size.
(**E and F**) Representative time-lapse of phagosomal tracking in 3 dpf wild type (E) and blb^{NY007} (F). Microglia are labelled with *Tg(mpeg1:eGFP-caax)*. Scale bar 5µm.

3.10 PHAGOSOMES CONVERGE INTO A UNIQUE CELLULAR COMPARTMENT

Continuous imaging of newly formed phagosomes in wild type revealed two important phagosomal behaviours. First, as described before, that those vesicles significantly reduce their size along maturation; second, that tracks of phagosomes terminate with fusion events with other vesicles (Figure 3.10 A). In *blb*, quantification of the bubble growth along development, showed that the typical mutant morphology is an acquired phenotype that progresses over time rather than being intrinsic of *blb* microglia (Figure 3.2 B). In line with this, laser depletion of all microglia in *blb* zebrafish embryos at 3 dpf led to the repopulation by new macrophages that at first were small and highly branched, and progressively enlarged acquiring the round phenotype with a single, big vesicle (Moritz, 2014). To investigate the genesis of this compartment, we imaged the brains of *blb* embryos at early developmental stages (2.5 dpf) when microglia just entered the brain. Previous work in the lab has shown that brain macrophages derive from a sub-population in the YS that invade the CNS entering from the frontal part of the head and then differentiate into microglia (Rossi et al., 2015). Thus, we once again took advantage of SPIM microscopy, which allows to acquire large volumes of sample with very limited phototoxicity and high temporal resolution. In this way, we were able to image the entire zebrafish head which gradually, during imaging, got populated by microglia. This approach revealed that, at early stages, mutant microglia are indistinguishable from wild type as they are highly branched and dynamic, actively involved in the clearance of apoptotic cells. Tracking of un-compacted 5 µm phagosomes at early time points (2.5 dpf) showed that phagosomes converge into a receiving compartment that expands progressively, taking over gradually most of the cell volume (Figure 3.10 B and C).

These data showed that the *blb* phenotype develops as a consequence of phagosomal fusion with a receiving compartment, which as a consequence keeps expanding. Previously, it has been shown that vesicular fusion in microglia is mediated by the v0-ATPase a1 subunit, a function that is independent of its proton pump activity (Peri and Nüsslein-Volhard, 2008). To further prove that vesicular fusion is at the basis of *blb* morphology, we blocked this process by knocking down the a1 subunit of the vATPase via morpholino injection in *blb* (Peri and Nüsslein-Volhard, 2008). This, indeed, prevented the bubble formation in *blb* and resulted instead in mutant microglia with many individual vesicles (Figure 3.10 D and E).

Noteworthy, newly formed phagosomes along their maturation process fuse with lysosomes. This event allows phagosomal acidification and therefore degradation of the engulfed material. Different live pH indicators, such as lysotracker and lysosensor, can be used to track fusion events between phagosomes and lysosomes and in general to label acidic compartments (Peri and Nüsslein-Volhard, 2008). Here, we showed that the *blb* phenotype develops as a consequence of fusion events between phagosomes and a receiving compartment. To investigate the involvement of lysosomes and acidification in this process, we combined SPIM imaging with lysotracker staining in *blb*. Interestingly, this live staining showed that in *blb*, un-shrunk 5 µm phagosomes fuse with the collecting compartment after acidification (Figure 3.10 F). Fusion with lysosomes and acidification are commonly considered the last steps of the pathway, indeed phagolysosomes are referred to as terminal phagocytic compartments. Hence, this result opens the possibility to a scenario where the existence of specialized post-lysosomal compartments might play important roles in phagocytosis resolution.

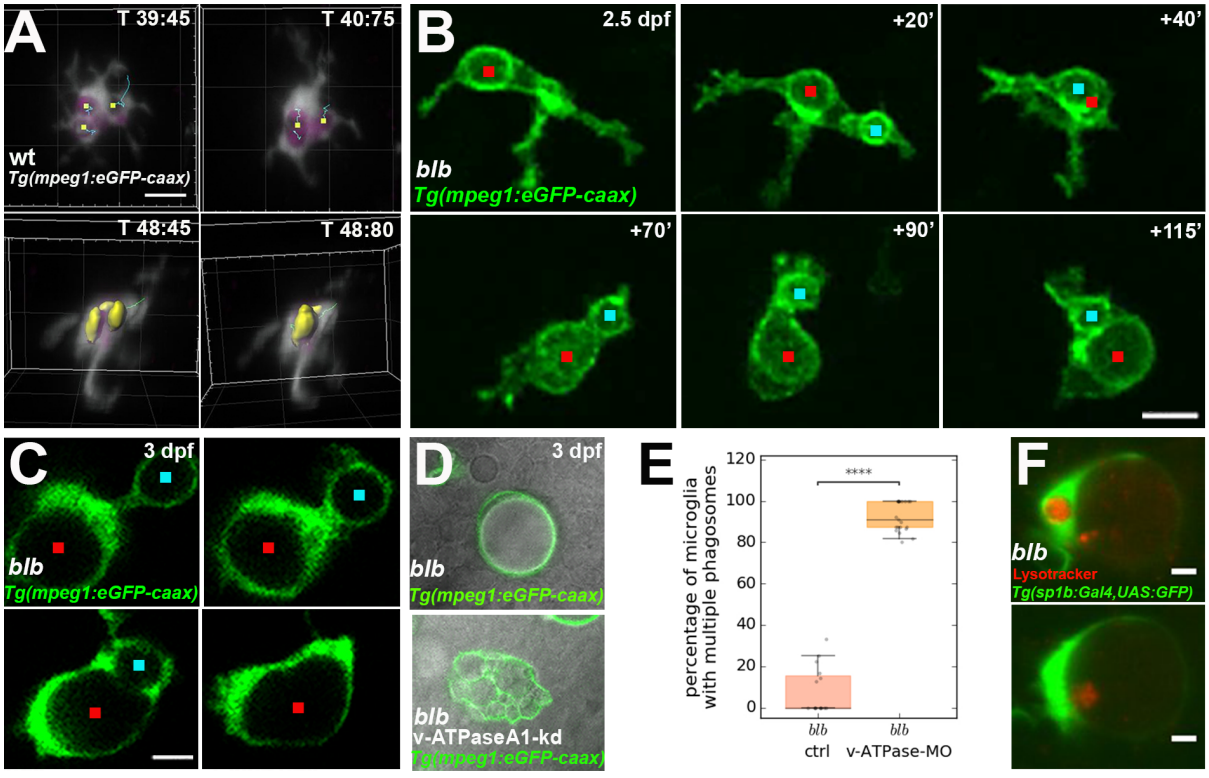

Figure 3.10. Tracking of phagosomes *in vivo* reveal that these converge into one cellular compartment.

(**A**) SPIM time-lapse of wild type microglia labelled in *Tg(mpeg1:eGFP-caax)*. Tracking highlights fusion events, in yellow phagosomes segmentation. Time in minutes. Scale bar 5µm.

(**B and C**) SPIM time-lapse of blb^{NY007} microglia labelled with *Tg(mpeg1:eGFP-caax)* at different time points. The red dot marks the growing vesicle, the cyan dot marks incoming phagosomes. (B) 2.5 dpf blb^{NY007}

microglia. Time indicated in minutes. Scale bar 10µm. (C) A representative fusion event in a 3 dpf blb^{NY007} microglia. Scale bar 5µm.
(**D and E**) Representative examples of microglia labelled with *Tg(mpeg1:eGFP-caax)* in blb^{NY007} (D, top panel) and in blb^{NY007} injected with a morpholino against the a1-vATPase (D, bottom panel) to prevent vesicular fusion. (E) Quantification of experiment in (D). Percentage of microglia with more than 1 vesicle per cell, in blb^{NY007} (n=15) and blb^{NY007} injected with a morpholino against the a1-vATPase (n=21). P value < 0.0001.
(**F**) Time-lapse of a representative fusion event in blb^{NY007} microglia labelled with *Tg(mpeg1:eGFP-caax)* and Lysotracker (in red) to visualize acidification. Scale bar 5µm.

The currently accepted view of phagocytosis proposes that mature phagolysosomes act autonomously, with each vesicle processing and recycling its own cargo independently. Here, however, imaging and genetic data suggest an alternative model where these vesicles fuse into a single post-lysosomal compartment. To further investigate this, we developed an *in vitro* assay to track the fate of wild type phagosomes and their cargos (Figure 3.11 E). Specifically, we used mammalian RAW 264.7 macrophages which we showed have Slc37a2 positive phagosomes (Figure 3.8 C and D). In particular, we co-cultured on glass coverslips RAW macrophages together with nuclear-labelled red and green HeLa cells (1:1 ratio). Approximately 12 hours after seeding, when cells reached 60-80% confluence, HeLa cells were selectively killed via apoptosis using the anti-tumoral drug TRAIL (Steven R Wiley et al., 1995). This triggered the engulfment of the dying HeLa labelled with green or red nucleus. The coverslips were fixed at different time points (3, 6 and 9 hours after apoptosis induction), and at every time point it was possible to identify in RAW macrophages vesicles containing the HeLa apoptotic fluorescent material engulfed. This showed that RAW macrophages which engulfed both red and green HeLa cells, at early time points (3 hours after apoptosis induction) contained several distinct red and green fluorescent vesicles (Figure 3.11 A). At the next time point (6 hours after apoptosis induction) there was the appearance of a single yellow vesicle per cell, together with red and green fluorescent phagosomes (Figure 3.11 B). However, at the latest time point (9 hours after apoptosis induction), this yellow vesicle was the only fluorescent compartment visible in RAW cells which engulfed both red and green labelled apoptotic HeLa (Figure 3.11 C).

The existence of a single yellow vesicle supports a model where wild type phagosomes fuse and converge into a collecting compartment (Figure 3.11 E). This was fluorescent only when RAW macrophages were fed with labelled apoptotic HeLa (Figure 3.11 D). Interestingly, this compartment always appeared to be highly light scattering and easily visible from the bright field, a feature that might be related with the content of the compartment itself.

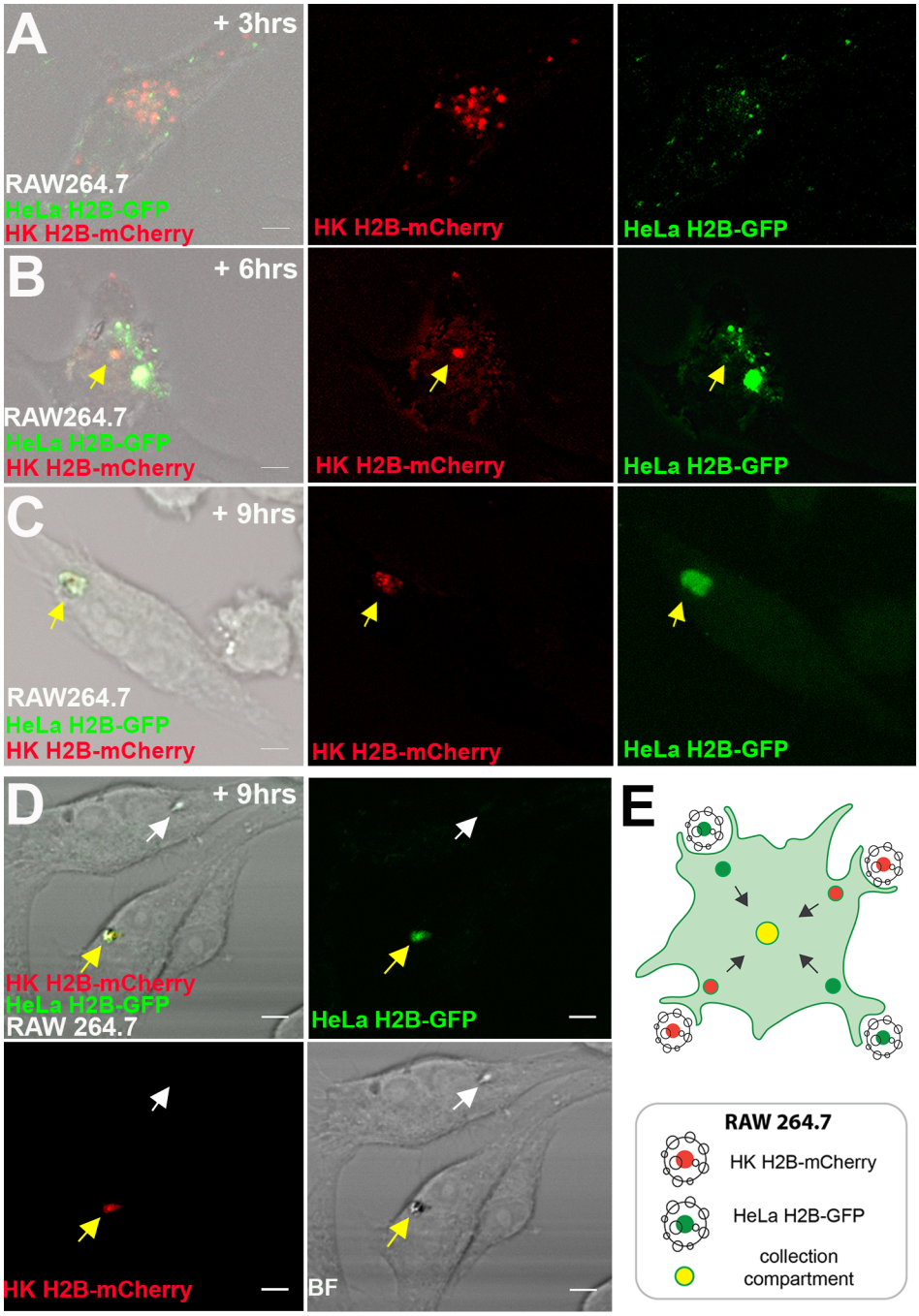

Figure 3.11. *In vitro* phagocytic assay on mammalian macrophages show that phagosomes converge into one cellular compartment.

(**A-C**) Fixed RAW264.7 macrophages, co-cultured with HK H2B-mCherry (red) and HeLa H2B-GFP (green), 3hrs (A), 6hrs (B) and 9hrs (C) after induction of apoptosis in HeLa and HK. The yellow arrow indicates the collection compartment.
(**D**) RAW264.7 macrophages fixed 9 hours after apoptosis induction. The image shows two adjacent cells with a collection compartment each. One is fluorescently labelled (yellow arrow) while the other is not (white arrow). Scale bars 5µm.
(**E**) Schematic representation of the experiment in (A-C).

3.11 THE COLLECTING COMPARTMENT IS IDENTIFIED IN MOUSE MACROPHAGES AND ZEBRAFISH MICROGLIA AND HAS A DISTINCT ULTRA-STRUCTURE

The ability to fluorescently label this compartment specifically allowed the investigation of its ultrastructure by using Correlative Light Electron Microscopy approach (CLEM). To this aim, the experiment was conducted on glass bottom gridded dishes as described above, and cells were fixed 9 hours after apoptosis induction for CLEM. Cells of interest, namely macrophages containing a yellow vesicle, were identified by confocal microscopy. Then, we performed EM to study their ultrastructure. This revealed that the yellow compartment identified in phagocytic RAW macrophages was a large, single membrane vesicle with an electron-lucent lumen containing what appears to be cellular debris (Figure 3.12 A-C). As mentioned earlier, the collecting compartment always appeared to be easily visible in fixed samples without the use of fluorescence. In this context, we also investigated this compartment for its morphology and characteristics visible from the bright field. Interestingly, also EM directed on this resulted in the identification of the same ultra-structure. Therefore, after several verifications, this feature has been used in later experiments to identify the compartment of interest from the bright field.

This experiment allowed us to identify in mouse macrophages fed with apoptotic cells a compartment highly resembling the collecting compartment identified in zebrafish *blb* microglia. Hence, both in mutant zebrafish and wild type mouse macrophages, we identified a compartment that receives the cargo of all incoming phagosomes and is characterised by a distinct ultrastructure.

This prompted us to investigate the ultrastructure of wild type zebrafish microglia. To this aim, we developed a CLEM pipeline for the zebrafish brain, using near infrared branding (NIRB) to introduce fiducial markers in fixed samples and precisely map fluorescently labelled microglia in EM preparations (Figure 3.12 D). Scanning at high resolution by SBF-SEM (Figure 3.12 E and F) allowed the unbiased exploration of entire wild type microglia volume in zebrafish embryos at 3 dpf. Thanks to this method that we developed, we were able to reconstruct wild type phagocytic microglia from an *in vivo* unperturbed context, describing the ultrastructure of the cell and its subcellular compartments. This revealed the identification of several phagosomes per cell, which appeared highly electron-dense and packed with digested material (Figure 3.12, yellow vesicles in E and structure marked as “P” in F). Contrary to those, in each microglia we

identified a single electron-lucent compartment containing debris of membranes and digested material and clearly distinguishable from the surrounding more electron-opaque cytoplasm (Figure 3.12 F). Interestingly, we could always identify one vesicle with such characteristics per cell and the high conservation of features suggests this is the same compartment identified in fed mouse macrophages (compare Figure 3.12 F and C) and that expands so dramatically in *blb* microglia (compare Figure 3.12 F and Figure 3.5).

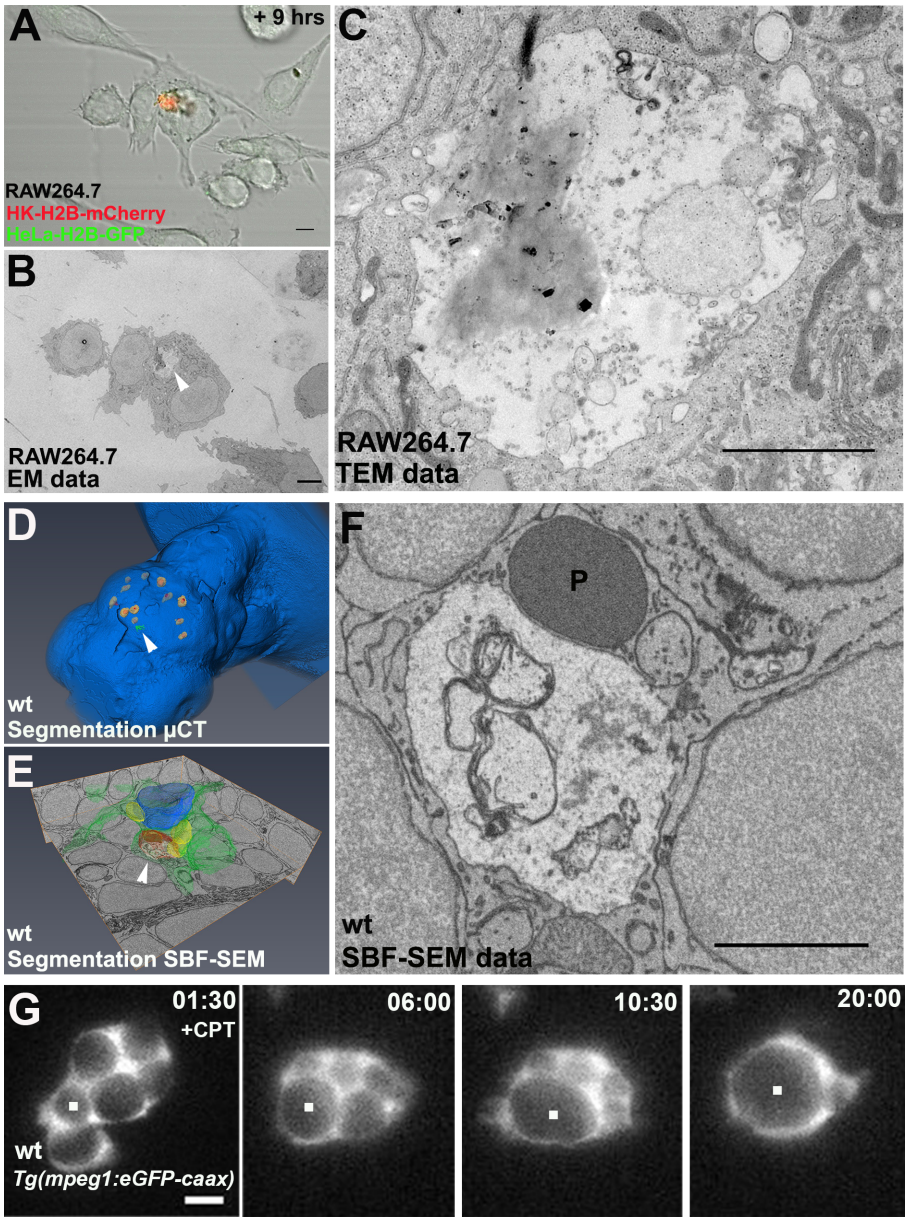

Figure 3.12. Structural characterization of the gastrosome.

(**A-C**) CLEM of RAW264.7 macrophages fixed 9 hours after induction of apoptosis in HK H2B-mCherry (red) and HeLa H2B-GFP (green). (A) Confocal microscopy data. Scale bar 5µm. (B) Low magnification EM data. White arrowhead points to the compartment of interest. Scale bar 5µm. (C) High magnification of the compartment of interest in TEM data. Scale bar 2µm.

(**D-F**) CLEM on wild type zebrafish. (D) Segmentation of µCT data. 4dpf zebrafish embryo outline is in blue. Yellow and red mark near-infra-red-branding as detected by 2-photon microscopy and µCT, respectively. Outline of the microglial cell of interest is in green. (E) Segmentation of the cell of interest. Green outlines the cell body. Blue marks the nucleus. Phagosomes are in yellow. The receiving compartment (gastrosome) is in red, white arrowhead points towards it. (F) High magnification of the gastrosome in SBF-SEM data. P indicates a phagosome. Scale bar 2µm.
(**G**) SPIM time-lapse of a representative 3dpf wild type *Tg(mpeg1:eGFP-caax)* microglia in an embryo treated with Camptothecin to increase apoptosis. Scale bar 5µm.

Thus, phagocytosis in microglia and macrophages relies on the existence of a collecting compartment where phagosomes fuse and converge, which we termed "gastrosome" as, similar to a stomach, it receives ingested material. In microglia, the existence of the gastrosome, only became apparent through a genetic approach where the absence of a solute carrier transporter normally expressed on phagosomes caused its massive and obvious expansion (Figure 3.1 and Figure 3.6). Our data showed that there is a correlation between phagocytosis and gastrosomal expansion, in particular, we showed that the *blb* phenotype is the result of defects in the intracellular processing of the engulfed material (Figure 3.3). Thus, we asked if gastrosomal expansion could also be triggered via non-genetic routes, for example by elevating cell death by using CPT, which -as shown earlier - results in macrophages engulfing more apoptotic cells (Figure 3.4). Indeed, increased engulfment led to the rapid expansion of a single vesicle which enlarged as a consequence of phagosomal income (Figure 3.12 G). CPT treated wild type embryos developed a microglia phenotype which, at the cellular level, highly resembles the one of *blb* (compare Figure 3.12 G with Figure 3.1 J).
Together this data revealed a new step in the phagocytic pathway, namely the existence of a new post-lysosomal compartment, which collect all phagosomes and is characterised by a distinct ultrastructure. This appeared to be conserved across vertebrates and represents a critical bottleneck in the processing of engulfed material.

3.12 THE GASTROSOME IS CHARACTERIZED BY A DISTINCT MOLECULAR SIGNATURE

To better characterize the identity of the gastrosome and establish its molecular signature we stained RAW 264.7 macrophages fed with apoptotic HeLa with a variety of endocytic, phagosomal and lysosomal markers. This revealed that the collecting compartment has a hybrid nature that differs from that of classical phagolysosomes. Indeed, the gastrosome proved to be positive for Rab7, Lamp1, Lamp2 and LBPA, which are all well-known late endosomal or lysosomal markers (Figure 3.13 A-D). On the contrary, the gastrosome was negative for Cathepsin D (Figure 3.13 E), a proteolytic enzyme normally expressed in lysosome and as a consequence traceable in phagolysosomes, and classically used as a marker of proteolytic-lysosomal activity and late marker of phagocytosis (Garin et al., 2001; Yeung et al., 2006). Interestingly, Slc37a2 is not localised on the gastrosome (Figure 3.13 F).

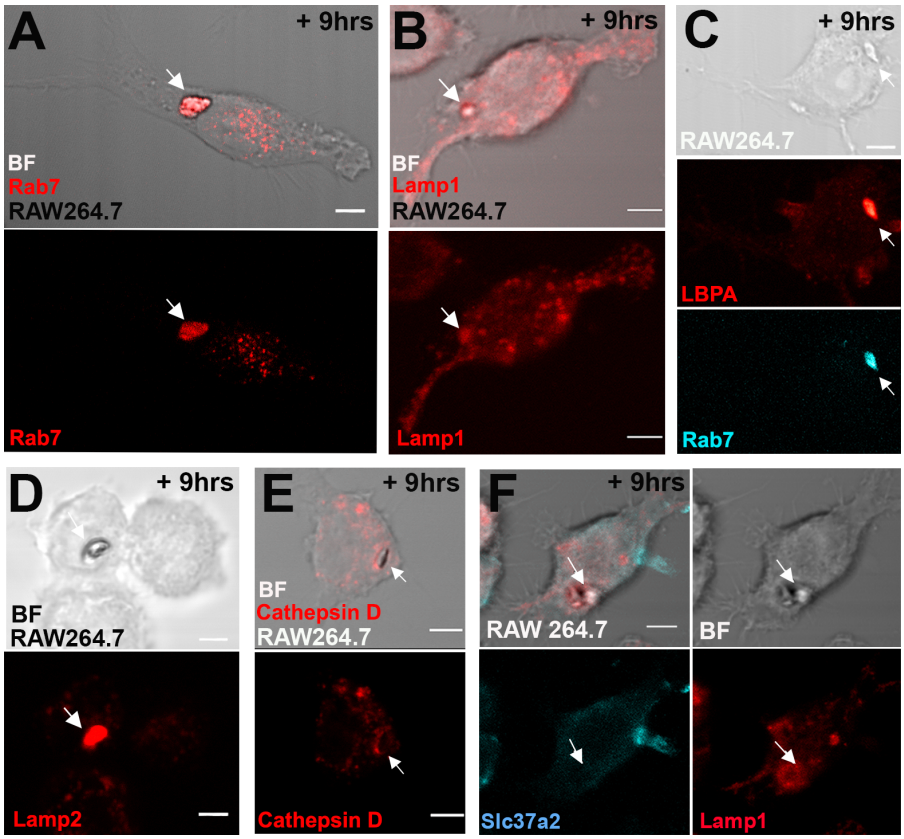

Figure 3.13. Molecular characterization of the gastrosome.

(**A**) RAW264.7 macrophages fixed 9 hours after apoptosis induction of unlabelled HeLa cells. Immunostaining against Rab7 (red). The white arrow indicates the collection compartment (gastrosome). Scale bars 10µm. (**B**) RAW264.7 macrophages fixed 9 hours after apoptosis induction of unlabelled HeLa cells. Immunostaining against Lamp1 (red). The white arrow indicates the collection compartment (gastrosome). Scale bars 5µm.

(**C**) Fixed RAW264.7 macrophages, 9hrs after apoptosis of unlabelled HeLa cells. Immunostaining against LBPA (red) and Rab7 (cyan). The white arrow indicates the collection compartment (gastrosome). Scale bars 5µm.
(**D**) RAW264.7 macrophages fixed 9 hours after apoptosis induction of unlabelled HeLa cells. Immunostaining against Lamp2 (red). The white arrow indicates the collection compartment (gastrosome). Scale bars 5µm.
(**E**) RAW264.7 macrophages fixed 9 hours after apoptosis induction of unlabelled HeLa cells. Immunostaining against Cathepsin D (red). The white arrow indicates the collection compartment (gastrosome). Scale bars 5µm.
(**F**) RAW264.7 macrophages fixed 9 hours after apoptosis induction of unlabelled HeLa cells. Immunostaining of Lamp1 (red) and Slc37a2 (cyan). The white arrow points to a collection compartment (gastrosome) that is Lamp1 positive and Slc37a2 negative. Scale bar 5µm.

The distinct ultrastructure and the hybrid molecular signature identify the gastrosome as a new compartment. The existence of an additional step following the phagolysosome formation, namely the fusion of phagosomes with the gastrosome, suggests a possible need for further degradation or disposal of the digested target.

The EM analysis in fish (both wild type and *blb*) and in the fed mammalian macrophages indicated that the gastrosome contains sparse membranous debris. This prompt us to screen a panel of lipid dyes differentially staining different kind of lipids, with the aim of describing the gastrosomal content and therefore speculate on its possible function. In particular, we stained both fed RAW 264.7 and zebrafish *blb* microglia with wheat germ agglutin (WGA) that is classically used for labelling plasma membrane by detecting glycoconjugates residues on it, the lipophilic dye Nile Red and Bodipy 493/503 to detect neutral lipids and lipid droplets and finally with Nile Blue Chloride which is a pH sensitive dye detecting DNA and lipids. All probes labelled the gastrosome in both models, indicating its content is indeed lipidic (Figure 3.14 A-H). Interestingly, these dyes do not give a uniform labelling of the gastrosomal lumen in *blb*, but rather highlight discrete structures within this compartment. We next asked if a similar staining could be observed also in wild type microglia, and to this aim we repeated the CPT experiment to induce gastrosomal expansion without perturbing the expression of Slc37a2. Upon increase of apoptosis by CPT treatment, the wild type enlarged gastrosome was labelled with Nile Blue which, once again, reveals the presence of circular structures within the lumen (Figure 3.14 I and J). We conclude that the gastrosome is a previously un-described phagocytic compartment that contains lipids and membrane structures and that responds dynamically to changes in microglial phagocytosis.

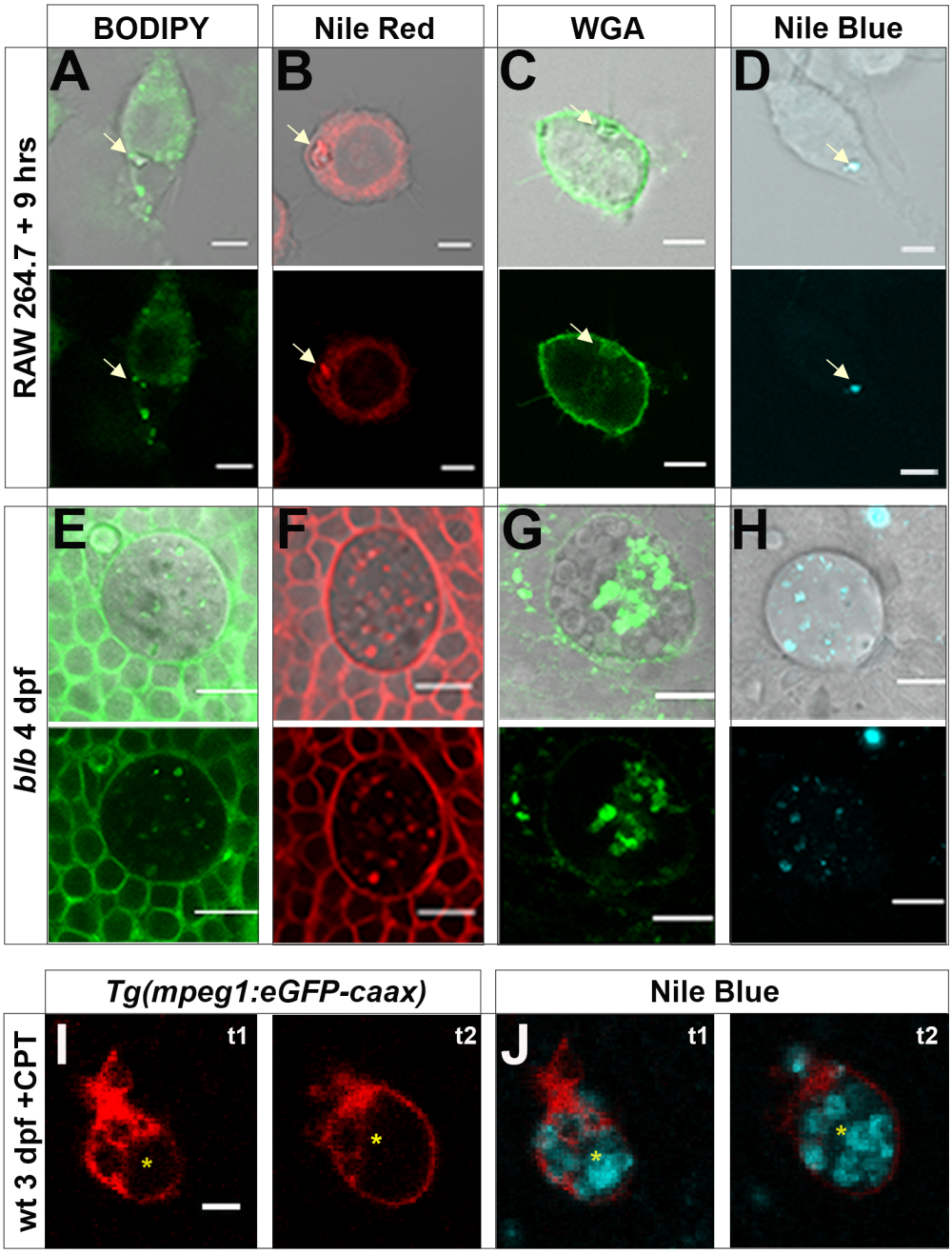

Figure 3.14. In macrophages and microglia the gastrosome contains lipids and membranes.

(**A-D**) RAW264.7 macrophages fixed 9 hours after apoptosis induction of unlabelled HeLa cells. Stained with BODIPY (A), Nile red (B), WGA (C) and Nile Blue (D). The white arrow points to the gastrosome. Scale bar 5 µm.

(**E-H**) 4pf *blb* microglia stained with BODIPY (E), Nile red (F), WGA (G) and Nile Blue (H). Scale bar 10 µm.

(**I and J**) 3 dpf wild type *Tg(mpeg1:eGFP-caax)* microglia (red) (I and J) stained with Nile Blue (cyan) (J) in an embryo treated with Camptothecin to increase apoptosis. Scale bar 5µm. The asterisk marks the gastrosome.

3.13 GASTROSOMAL EXPANSION AFFECTS MICROGLIAL MORPHOLOGY AND FUNCTIONALITY

In highly phagocytic microglia the gastrosome constitutes a critical bottleneck in the phagocytic pathway that, by altering the cellular morphology, could also affect microglial functionality. One of the strengths of our *in vivo* system is that we can directly address the impact of gastrosomal expansion on higher order microglial functions, such as their ability to migrate and engulf apoptotic neurons. It is clear that *blb* microglia are less efficient in phagocytosis when compared to wild type. Indeed, as previously shown, mutant microglia remove fewer neurons per hour (Figure 3.3 E) and have less phagosomes per cell (Figure 3.9 A). Moreover, we quantified the length of each phagocytic event in wild type and *blb* by measuring the time intercurrent between phagosome formation and retraction of the branch to the cell body. This analysis showed that not only *blb* engulf fewer targets over time, but also that each phagocytic event lasts significantly longer than in wild type embryos (Figure 3.15 A).

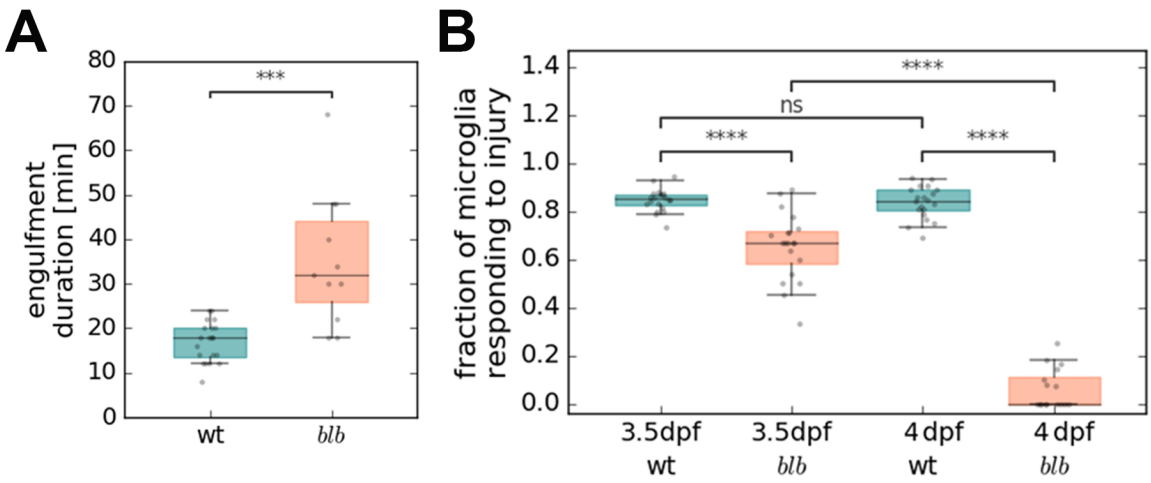

Figure 3.15. Gastrosomal defects affect microglial functionality.

(**A**) Quantification of engulfment duration in wild type (n=20) and blb^{NY007} microglia (n=11). P value < 0.001. (**B**) Quantification of microglia responding to an injury in wild type and blb^{NY007} microglia at different developmental stages; n(wt, 3.5 dpf)=20; n(blb^{NY007}, 3.5 dpf)=20; n(wt, 4 dpf)=20; n(blb^{NY007}, 4 dpf)=16. P value < 0.0001.

Finally, we asked to which extent the enlarged gastrosome affects microglia functionality. To test this, we measured the ability of *blb* microglia to react to injuries. In particular, a pulsed 532 nm cutting laser attached to a commercial Olympus FluoView 1200 was used to generate spatiotemporally controlled cell death in the brain. The ablation protocol was set up to kill

around 200 neurons without perturbing the blood brain barrier and influencing the larval development (Sieger et al., 2012). We induced laser ablation at the brain midline, a protocol which was previously shown to induce microglia of both hemispheres to migrate towards the site of injury at a speed of around 3.3 µm/min in wild type (Sieger et al., 2012). Here, while in wild type microglia reacted and migrated by 30 minutes from injury induction, in *blb* these cells were unable to migrate (Figure 3.15 B). The migration defect correlated with the progression of the phenotype. At earlier developmental time points (such as 3 dpf), when mutant microglia have a smaller gastrosome (Figure 3.2 B), they were still partially able to respond to injuries (Figure 3.15 B) even though with reduced efficiency. However, upon further gastrosomal expansion (4 dpf, Figure 3.2 B) mutant microglia were completely unable to migrate to the site of injury (Figure 3.15 B). This is consistent with a scenario where the expansion of the newly identified gastrosome has a dramatic impact on microglia functionality. Thus, the discovery of this new cellular compartment constitutes a new potential entry point for microglia manipulation, as interfering with its morphology directly impacts on microglia activity and functionality.

4 DISCUSSION

Although much is known about the complex mechanisms that control phagosome maturation and fusion with lysosomes (Kinchen and Ravichandran, 2008; Levin et al., 2016), we know very little about the final stages of cargo degradation, including export of resulting macromolecules and the processing of membranes.

In this study we have described *bubblebrain* (*blb*) a zebrafish mutant in the solute carrier transporter Slc37a2 that is characterized by microglia with a dramatically enlarged morphology. In Slc37a2 knock outs the cell body of microglia is occupied by a single large compartment which keeps expanding upon phagocytosis due to a defect in the processing of the engulfed material. *In vivo* imaging of mutant microglia at high temporal and spatial resolution allowed the discovery of several novel and important aspects of phagocytosis (Figure 4.1). These results were also validated *in vitro* using mouse RAW 264.7 macrophages.

First, we discovered a process by which phagosomes shrink progressively. This is mediated by Slc37a2, a putative glucose-6-phosphate transporter that we showed is localized on phagosomes both in fish microglia and mouse macrophages. Second, we identified a novel step in the phagocytic pathway, namely the existence of a post lysosomal compartment which we termed *gastrosome*. Indeed, we showed that in zebrafish and mammalian macrophages phagosomes do not act autonomously, but they rather converge into a collecting compartment which is characterized by a distinct ultrastructure and by a hybrid distinct molecular signature. Third, we investigated the impact of gastrosomal disfunction on microglial activities, such as migration or phagocytosis. Finally, our *in vivo* data showed that increased levels of phagocytosis result in a dramatic gastrosomal expansion that affects microglial cell morphology to an unprecedented level.

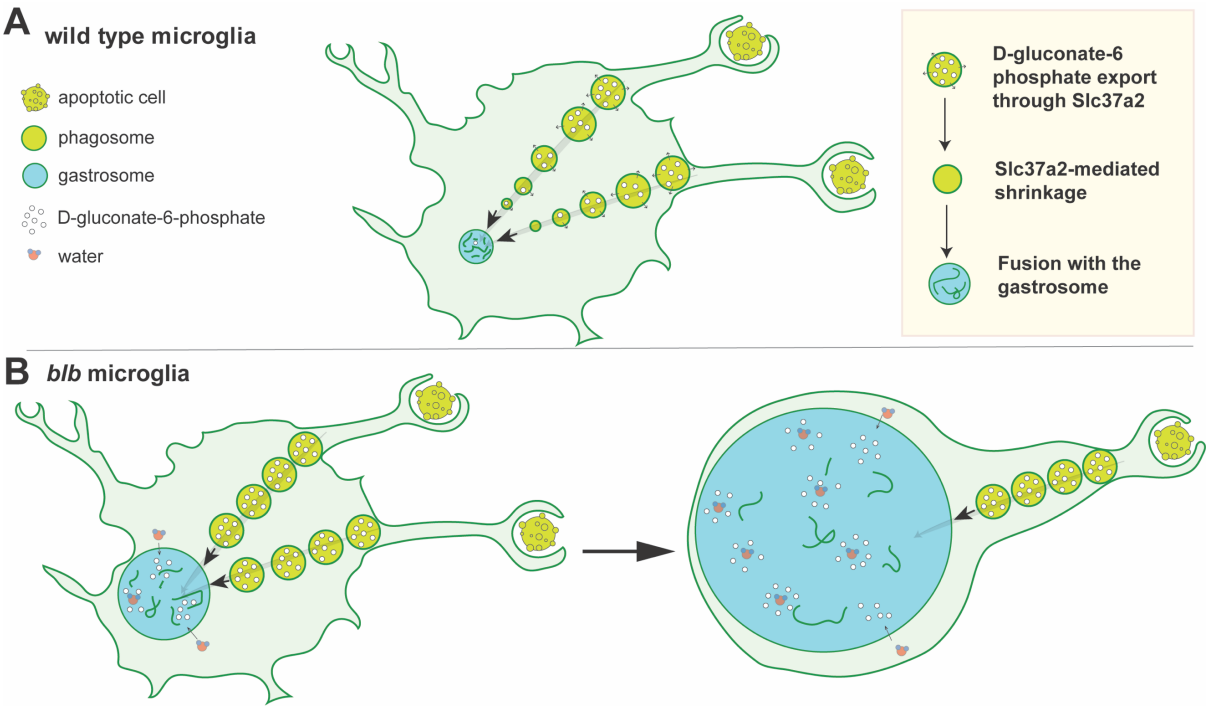

Figure 4.1. Results summary: schematic comparison between wild type and *blb* microglia.

(**A**) During phagosomal maturation, D-gluconate-6-phosphate is exported from the phagosomes through the solute carrier transporter Slc37a2, a process responsible for phagosomal shrinkage. Moreover, phagosomes fuse and converge in the gastrosome, a unique cellular compartment rich in lipids and membranes.
(**B**) Lack of Slc37a2 prevents export of D-gluconate-6-phosphate and therefore phagosomal shrinkage. The fusion of un-shrunk phagosomes with the gastrosome mediates its expansion caused by osmotic stress. Gastrosomal expansion drastically affect microglia morphology and phagocytic activity.

4.1 PHAGOSOMAL MATURATION INVOLVES SLC37A2-MEDIATED SHRINKAGE

The removal of apoptotic cells by phagocytosis is an essential cell biological process involved in development, homeostasis and disease. Since the first description of phagocytosis in 1883 by Elie Metchnikoff, our knowledge about this process grew exponentially, however many aspects remain unknown or are still highly debated. In particular, our understanding of phagosomal resolution is fragmented and incomplete and very often what we know comes from studying other endocytic processes (Levin et al., 2016).

Today, it is well accepted that the lumen of a nascent phagosome lacks degradation capacity. Shortly after its formation, the young phagosome undergoes maturation, a process that leads to the degradation of its cargo. Indeed, fusion events between the phagosome and organelles of the endocytic pathway, such as early endosomes, late endosomes and eventually lysosomes, allow the acquisition of digestive enzymes necessary for the degradation (Kinchen and Ravichandran, 2008; Vieira et al., 2002). Interestingly, data presented here show that phagosomes, during their maturation, undergo a dramatic size reduction and that this shrinkage depends on the activity of the solute carrier transporter Slc37a2. Growing evidence shows that solute carrier transporters are essential cellular components, in particular for supporting lysosomal functions, by localizing on these vesicles (Bissa et al., 2016). Here, we show that both in zebrafish microglia and mouse macrophages Slc37a2, a putative Glucose-6-phosphate-transporter, is localized on phagosomes. The size of these vesicles (~5µm) and lack of Lamp1 suggest that these vesicles are phagosomes and not lysosomes. Lack of Slc37a2 leads to accumulation of D-gluconate 6 phosphate in the zebrafish head, and it affects phagosomal maturation. Indeed, while wild type phagosomes reduce their size significantly, lack of Slc37a2 prevent this shrinkage. The molecular mechanisms that pair Slc37a2-mediated transport with vesicular contraction are of course of great interest, also because recent reports have shown that phagosomal size can influence the transport and the behaviour of these vesicles inside the cell (Keller et al., 2017). A mechanism reported to be involved in phagosome remodelling and size maintenance is the formation of intraluminal vesicles (ILVs). By delivering vesicles to the lumen of the phagolysosome, this process allows the degradation of integral membrane components. However, some ILVs seem to undergo back-fusion with the phagosomal membrane. (Fairn and Grinstein, 2012). Work in bacteria and plants show that formation of micro-lumina and finger-like protrusions reduces membrane length, allowing the resizing of

vesicles and cells. Those vesicular size adjustments are observed downstream of osmotic variations and solute trafficking and could represent a possible mechanism for phagosomal shrinkage (Claessens et al., 2008). Similar size reduction is observed during the maturation of the entotic vacuole by the Overholtzer group (Krajcovic et al., 2013). Here the authors show that entotic vacuoles undergo a late maturation step characterized by mTOR-mediated fission, which redistributes vacuolar contents in the lysosomal network. More recently the same group identified the lipid kinase PIKfyve as a regulator of an alternative pathway that distributes engulfed contents in support of intracellular macromolecule synthesis during different endocytic pathways (Krishna et al., 2016). Our *in vivo* data clearly identify Slc37a2 as a key molecule mediating phagosomal shrinkage during apoptotic cells digestion in microglia.

4.2 THE DISCOVERY OF THE GASTROSOME, A POST-LYSOSOMAL COMPARTMENT

During phagosomal maturation the engulfed cargo get degraded thanks to the activity of enzymes which typically activate at acidic pH. The phagocytic target is typically complex and rich in different macromolecules. It is clear that the phagolysosome can catabolize its content thanks to the presence of a diverse arsenal of hydrolytic enzymes acquired by fusing with the lysosomes. However, the products of this digestion have to be processed for the phagocyte to return to homeostasis, and it is unclear how phagolysosomes get reabsorbed and resolved. More than 20 years ago, *in vitro* experiments based on engulfment of latex beads and sucrose indicated the possibility of retrograde fusion events between "terminal lysosomes" and the late endosomal compartment via the microtubule network (Jahraus et al., 1994). Similarly, retrograde transport of undigested cargo through phosphatidylinositol 3-phosphate (PtdIns(3)P) has been observed from early endosomes to the trans-Golgi network (TGN) (Cullen and Korswagen, 2012). More recently, Krajcovic and colleagues predicted continual fusion/fission between lysosomes and the shrinking entotic vacuole (Krajcovic et al., 2013). Finally, the Desjardins group observed that small endosomes fuse with each other. In particular, they fed small latex beads (LBs) to cultured J774 macrophages and showed that while LBs are initially internalized individually in small vesicles, within 15 minutes from internalization bigger endosomes are containing a larger number of LBs, suggesting the coalescence of multiple small vesicles containing single beads (Duclos et al., 2011). However, a clear evidence of how the phagolysosomes are resolved is still missing.

In this work, we identified a previously undescribed step in the phagocytic pathway subsequent the formation of phagolysosomes. Combining *in vivo* studies in zebrafish microglia with an *in vitro* approach using mammalian macrophages we uncovered a new compartment, the gastrosome, to whom phagosomes fuse and deliver their content. Given the huge biological and medical importance of phagocytosis, it is surprising that today it is still possible to discover un-described steps in this pathway. One possible explanation for why this has gone unnoticed so far, could come from the fact that previous studies have been conducted mostly in cultured phagocytes fed with either bacteria or undigestible beads. The first have been extremely useful in uncovering the immune relevance of phagocytosis during infection, however many microorganisms developed mechanisms to escape the phagocytic system making impossible to follow their degradation over time. On the other hand, gold or latex beads are artificial prays

that by definition are indigestible, and therefore can "clog" the system. While these approaches have been fundamental for the identification of key molecular players and early steps in phagosomal maturation, they are perhaps not perfectly suited for addressing how these vesicles are resolved. Here, we investigated the fate of apoptotic cell components *in vivo* in an unperturbed, physiological context namely the developing brain. The identification of the gastrosome was first possible thanks to the study of a zebrafish mutant where this compartment enlarges upon phagocytic activity. Here, *in vivo* tracking of newly formed phagosomes at high temporal resolution showed that those vesicles, after acidification, merge with one compartment which keeps enlarging upon fusion. Acidification was visualized by Lyso-Tracker, a vital dye which becomes fluorescent at acidic pH, a feature acquired by phagosomes after fusion with lysosomes. This observation shed light on the existence of an undescribed post lysosomal compartment, the gastrosome. This was confirmed also by the development of an *in vitro* phagocytic assay that we developed to monitor the fate of apoptotic cells engulfed by mammalian wild type macrophages. This confirmed that phagosomes converge into a single compartment in the cell.

The discovery of the gastrosome is in partial contrast with the current view that phagosomes and phagolysosomes are autonomous terminal organelles. Indeed, we show that they have a "collective" behaviour and that they all converge into the same vesicle. This vesicle is characterized by a unique combinatorial molecular signature and by a distinct ultrastructure that we determined via an unbiased exploration and reconstruction of wild type microglia. Both phagocytic microglia and macrophages have a single gastrosome, this has a peri-nuclear localization and it is delimited by a single membrane surrounding an electron-lucent lumen containing lipids and membranous structures.

4.3 CHARACTERIZATION OF PHAGOCYTIC COMPARTMENTS

The discovery of a new step during phagocytosis more than a century after the first description of this process, is certainly surprising and of a certain significance. While we can clearly demonstrate the importance of the gastrosome for phagocytosis and for microglia functionality (see below), today we failed to identify a specific marker for this compartment and we still do not know its exact function. In this section, I would like to discuss these two aspects in the light of what is currently known about the phagocytic pathway.

4.3.1 THE CLASSICAL VIEW: ENDOCYTIC MARKERS RUNNING IN ORDER

During maturation, phagosomes actively remodel the membrane-associated proteins and lipids. Great advances in this field have been obtained thanks to proteomic studies of isolated phagosomes which revealed the identities of hundreds of proteins associated with phagocytic compartments (Boulais et al., 2010; Campbell-Valois et al., 2012; Garin et al., 2001; Griffiths and Mayorga, 2007; Shui et al., 2008). The continuous alteration of phagosomal-associating molecules is believed to enable the phagosomes to preferentially interact with distinct endocytic organelles driving phagosome maturation in a stepwise manner. Among several molecules identified, some are considered classical markers of specific stages of maturation. For example, the lipid second messenger PtdIns(3)P and the small GTPase Rab5 are considered early markers of phagosomal maturation. In particular Rab5, localized on early phagosomes and early endosomes, has been shown to be essential for endosome-phagosome fusion (Fairn and Grinstein, 2012; Kinchen and Ravichandran, 2008). Recycling events are primarily mediated by Rab GTPases, specifically Rab11 and Rab4 have been shown to be involved in slow and fast recycling respectively (Garin et al., 2001; Levin et al., 2016). Additionally, Rab10 has also been implicated in phagosomal recycling and maturation upstream of Rab5 (Cardoso et al., 2010). A key event in phagosome maturation is the rapid removal of Rab5 from the phagosomal membrane and its exchange with the later marker Rab7. This protein is typically localized on late endosomes and late phagosomes and mediates the recruitment of lysosomes. Fusion between late phagosomes and lysosomes leads to the formation of phagolysosomes which are enriched in lysosomal markers Lamp1 and Lamp2. The phagosomal lumen is continuously acidified owing to the activity of the vATPase which is acquired already at early stages, until reaching below 5.0 at the phago-lysosomal stage. Here, thanks to the oxidation

and acidification, the hydrolases carried by the lysosomes are fully activated and result in the degradation of the phagocytic cargos (Levin et al., 2016).

4.3.2 THE ALTERNATIVE VIEW: PHAGOCYTOSIS AS A DYNAMIC PROCESS RELYING ON CONSTANT INTERACTION BETWEEN DIFFERENT COMPARTMENTS

The identification of protein markers for early and late phagocytic compartments surely allowed the description of phagosomal maturation and its key players. However, in the last 30 years it became clear that phagocytosis and its compartments are much more dynamic than previously expected. Already the intrinsic nature of an early phagosome, late phagosome or phagolysosome is per se a clear example of the impossibility to assign exclusive markers to each of this compartment. Indeed, during phagosome maturation the nascent phagosomes acquire properties from the donor organelles including distinct membrane markers and acidity. Another interesting aspect to consider is the localization pattern of distinct Rab proteins: while some markers (such as Rab5, Rab2 and Rab14) are relatively transient and identified exclusively in early phagosomes and endosomes (Bin He et al., 2010; Guo et al., 2010; Mangahas et al., 2008), Rab7, once recruited, maintains its association with the phagosome until the cargo is completely degraded (Yu et al., 2008). Consequently, Rab7 is not an exclusive marker for late phagosomes and endosomes. Moreover, also the terminology used for lysosomes is highly confusing (Griffiths, 1996). Since the late 1980s lysosomes have been defined as the terminal compartment of the endocytic and phagocytic pathways devoid of recycling receptor molecules (Griffiths, 1996; Jahraus et al., 1994; Kornfeld and Mellman, 1989). They are enriched in specific molecules such as Lamps and hydrolases, which are, however, also found in late endosomes. A recent work from Cheng and colleagues also comments on the use of so-called lysosomal markers (such as Lamp1/2) and they suggest that labelling a set of lysosomal hydrolases combined with various endosomal markers would be more accurate than simply relying on a single “classical” staining to assess the nature of a compartment and its functions.

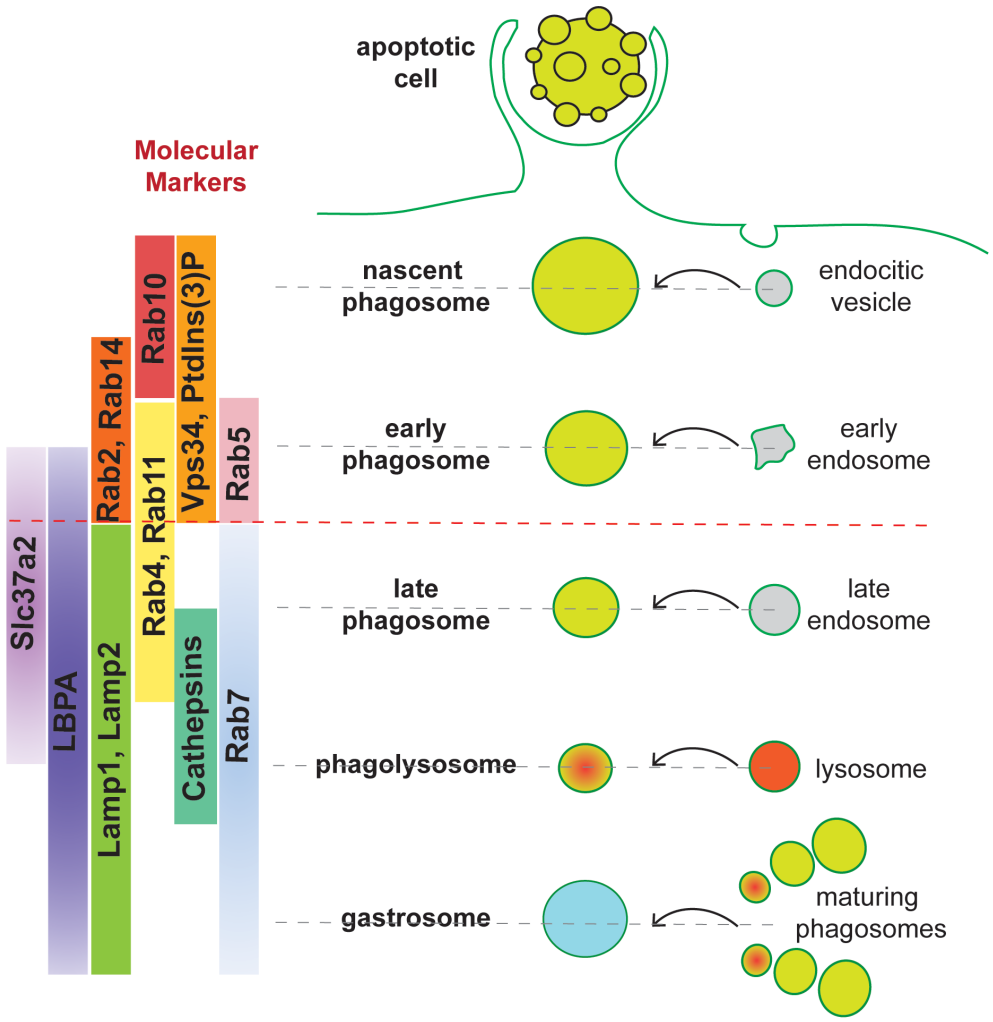

Figure 4.2. Phagosomal maturation and resolution: multi-step processes defined by fusion events and hybrid molecular signatures.

Phagosomal maturation relies on a series of fusion and fission events between the phagocytic and endocytic pathways. Those give rise to new hybrid compartments at every step of maturation, which are characterized by overlapping molecular signatures. While molecular markers can be divided into "early" and "late" (see red dotted line), it is not possible to identify exclusive markers for each stage of maturation (see grey dotted lines). Here we encourage a description of the phagocytic compartments based on a combinatorial molecular signature (i.e. the gastrosome is Rab7, Lamp1/2 and LBPA positive but Cathepsin D and Slc37a2 negative), and their ultrastructure which describe the content of each compartment, a valuable readout of cargo degradation.

Thus, all these aspects support a view where the different phagocytic compartments are in close relation with each other and therefore give rise, after every interaction, to hybrid compartments that acquire new functions along the pathway (Figure 4.2) (Lu and Zhou, 2012; Vieira et al., 2002). In our work we identify a new compartment, the gastrosome, which fuses with other phagocytic organelles. Thus, to identify the gastrosomal molecular signature, we stained macrophages fed with apoptotic cells with a panel of known phagocytic markers. This

showed that the gastrosome is a late compartment that is positive for Rab7, Lamp1/2 and LBPA. On the other hand, the gastrosome is different from a classical phagosome or phagolysosome as it lacks Slc37a2 and Cathepsin D, molecules that localize on phagosomes and lysosomes, respectively (Figure 3.13 and Figure 4.2).

4.3.3 A POSSIBLE ROLE FOR THE GASTROSOME IN LIPID DIGESTION AND MEMBRANE RECYCLING

As mentioned earlier, a second important aspect is to determine the function of the newly identified gastrosome. What is clear already from this first study is that the gastrosome contains membrane debris and lipids as revealed by electron microscopy and fluorescent lipid dyes, indicating a possible role in membrane recycling or metabolism. In support of this hypothesis there is also the gastrosomal localization of LBPA. This lipid has been shown to be enriched in late endosomes and phagosomes where it mediates cholesterol efflux (Kobayashi et al., 1999) and it may play a similar role in phagosomes. Finally, LBPA has been described as involved in lipid digestion and ILV formation (Matsuo et al., 2004). The Gruenberg group showed that LBPA can be visualized in late endosomes and phagosomes and it is highly enriched in ILVs, suggesting its involvement in their formation.

Previous studies have shown that degrading enzymes in the lumen of lysosomes and phagolysosomes are responsible for digestion and recycling of lipids (Kolter and Sandhoff, 2010; Linke et al., 2001). Membranes are essentially composed of amphiphilic acids and proteins, and obviously complex lipids have to be degraded within the phagocytosis process so that the final degradation products can leave the compartment, either as waste or for recycling. It has been shown that lysosomal digestion of membranes allows break-down of glycosphingolipids which are continuously recycled and reutilized in salvage process (Tettamanti et al., 2003). Proteins such as NPC1 and NPC2 have been proposed as possible exporters of sphingosine from lysosome and phagolysosomes, however the observed endosomal accumulation associated with lack of this transporters (Niemann-Pick type C disease) may be an indirect consequence of excessive cholesterol accumulation (Lloyd-Evans et al., 2008). ABC transporters similar to those that transport cholesterol at the plasma membrane have been identified in lysosomal compartments, but whether they play a role in the export of cholesterol from the phagosome is unclear (van der Kant et al., 2013). There are enzymes which has been reported to be highly expressed in macrophages and found in

phagosomes able to catabolize lipids, however, the mechanisms whereby lipids are processed after traversing the phagolysosomal membrane are virtually unknown (Levin et al., 2016).

Careful delineation of gastrosomal functions will require extensive further investigation. However, the existence of an additional compartment containing membrane debris suggests that lysosomes and phagolysosomes are not the sole organelles responsible for (lipid) housekeeping functions in the cell. Located at the end of the phagocytic pathway, the gastrosome may constitute a centre for lipid degradation, sorting and/or recycling.

4.4 PHAGOCYTOSIS AS A SOURCE OF NUTRIENTS AND ITS METABOLIC IMPACT

Billions of cells die via apoptosis daily and are efficiently removed. Moreover, it appears that there are fewer phagocytes than apoptotic cells in a tissue, meaning that phagocytes have to engulf multiple targets. During this process, the phagocyte essentially doubles its content of protein, carbohydrates, nucleotides, lipids and other cellular materials. An interesting but largely unanswered question is how does the phagocyte handle this excess. It is noteworthy that culturing phagocytes in a uncomplete nutrient environment, such as low glucose, tends to promote apoptotic clearance, while a high glucose environment reduces uptake (Park et al., 2011). Glycolysis is the major catabolic pathway that supplies cellular energy, therefore it is possible that the products of corpses digestion could modify the levels of glucose in the phagocyte and affect cellular glucose transport and synthesis. One pathway that might be of interest, in particular, is the pentose phosphate pathway, in which the products NADPH and pentoses are used for the synthesis of nucleic acids and amino acids. Slc37a2, localized on the phagosomal membrane, could play an important role in the extraction of sugars from the engulfed target and in the maintenance of glucose homeostasis. Notably, the majority of sugar in a cell is converted to glucose 6 phosphate by phosphorylation, and this sugar, transported by Slc37a2, lays at the start of the two major metabolic pathways: glycolysis and the pentose phosphate pathway. In addition, this sugar can also be converted to glycogen for cellular storage.

Solute carrier membrane transporters control essential physiological functions, including nutrients uptake, ion transport and waste removal. Expressed in different cell types, SLCs regulate the chemical exchange with the environment and the transport of small molecules keeping the internal physiology. It is surprising how, despite its clear relevance to health and disease, the SLC protein family is comparatively less well studied than other gene families. Indeed, 76% of SLCs with an already identified disease have no associated compound yet (César-Razquin et al., 2015) and this may be due to a number of technical barriers. Specifically, acquiring competent biological reagents for SLC study can be highly challenging as those are integral membrane proteins difficult to express and purify and very often poorly detected by typical mass spectrometry protocols (César-Razquin et al., 2015). Loss or gain of function studies can be confounded by endogenous SLC with overlapping specificities and high-quality antibodies are available only for few SLCs. In phagocytic cells, different SLCs have been

reported to localize to lysosomes and endosomes where they mediate the transport of essential molecules deriving from the ingested cargo. For example, Slc38a9 has been identified as an arginine sensor at the lysosomal membrane (Wang et al., 2015) and its modulation has been proposed as a new therapeutic intervention in neurodegenerative and aging disorders. Phagocytosis was not always used for immunity, but rather to intake nutrients from the environment. Therefore, is not surprising how this complex intracellular machinery is suited for nutrients extraction from the cargo digestion and homeostasis maintenance.

Proteomic studies recently described in macrophages and dendritic cells (DC) a high enrichment of transporters, in particular from the SLC family (Duclos et al., 2011). Interestingly, while pumps of the vATPase family have been shown to only localize to late endosomes and lysosomes, SLC transporters are differentially distributed between early, late endosomes and lysosomes (Duclos et al., 2011). There, the authors suggest that those transporters might participate in distinct functions performed by macrophages and DC and they define these molecules as potential differentiation or activation markers in those immune cells. Here, we identify Slc37a2 as a sugar transporter localized on phagosomes and essential for their maturation, as its absence prevents phagosomal size reduction. Finally, the gastrosome could also play an important role in lipids and membranes recycling and in the phagocyte homeostasis as defects strongly affect cellular behaviour and functionality.

4.5 INSIGHTS INTO A NEW WAY OF CLASSIFYING MICROGLIA

An interesting aspect of the Slc37a2 phenotype is that *blb* microglia display an aberrant bloated morphology that we show is associated with a migratory defect and low rate of engulfment. By contrast, in the microglial field, round morphologies are often used as a measure of cellular "activation" with round microglia being considered highly active and phagocytic. On the contrary, even though it is clear that ramified microglia are not inactive, they are usually associated with a surveillance rather than a phagocytic state. A careful delineation of microglial morphology, regional heterogeneity, transcriptome and turnover is emerging greatly. For example, in the adult human cortex, microglia acquire a ramified morphology when surveying the environment and an amoeboid morphology with retracted processes when they are removing the debris of dying neurons or reacting to a foreign body (Gomez-Nicola and Perry, 2015).

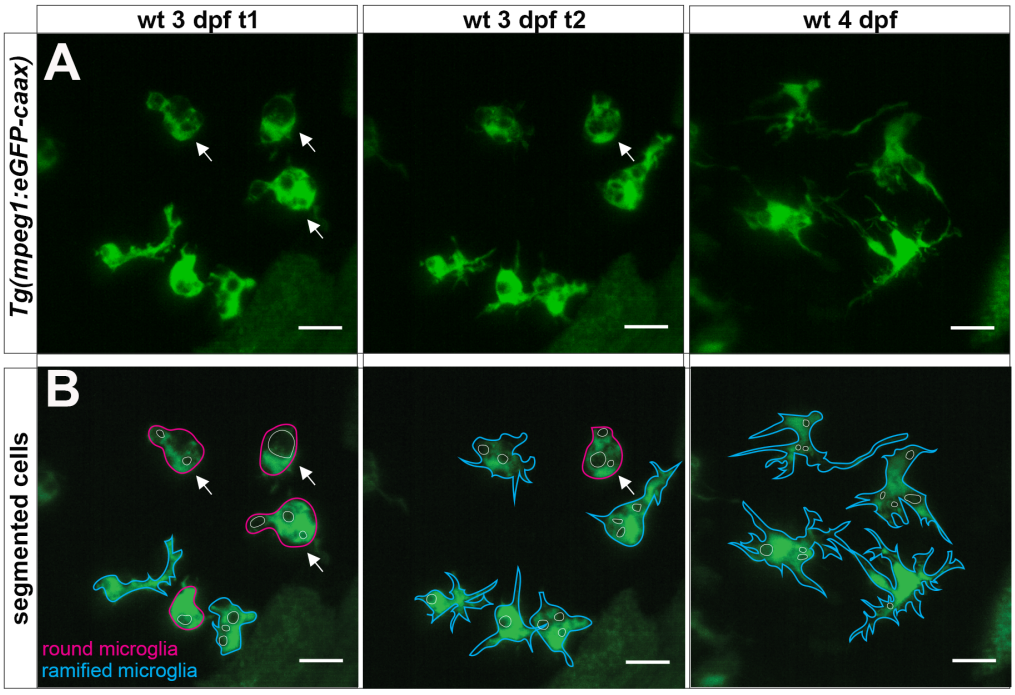

Figure 4.3. Highly phagocytic wild type microglia are rounded and can develop bubble-like morphology.

(**A and B**) SPIM time-lapse of a representative wild type embryo labelled with *Tg(mpeg1:eGFP-caax)* at different developmental stages. Microglia at 3 dpf are highly dynamic, assume rounded morphology (see white arrows) and dynamically recover a more ramified shape (compare 3 dpf t1 and 3 dpf t2). Microglia at 4 dpf are ramified. (B) Segmentation of the cells in (A), magenta line indicates round microglia, the blue line indicates ramified microglia. Scale bar 30 µm.

Our work, without being in contrast with the current classification of microglia morphology, adds a new level of complexity to it. Indeed, the Slc37a2 knockout phenotype reveals that defects in intracellular processing also lead to enlarged microglia. Our data show that the bubble morphology in *blb* is acquired over time and that it depends on the phagocytic activity. In line with this, inhibition of phagocytosis prevents the development of the characteristic *blb* phenotype. In addition, when wild type microglia are exposed to higher level of apoptosis, they also develop the same rounded phenotype. Most importantly, we showed that once microglia become so enlarged, they are less efficient phagocytes and unable to migrate and to engulf new targets.

Untreated zebrafish wild type microglia at 3 dpf when level of apoptosis in the brain are high (Casano et al., 2016), are on average rounded and some can develop a bubble morphology (Figure 4.3). This phenotype is transient, and wild type microglia can actively and dynamically revert this morphology. In physiologic conditions, a dynamic equilibrium is maintained, however, defects in the intracellular processing of the engulfed material, such as in *blb*, can lead to an irreversible bubble morphology which is associated with low microglia functionality. This calls for a new way of classifying these cells and their activity (Figure 4.4).

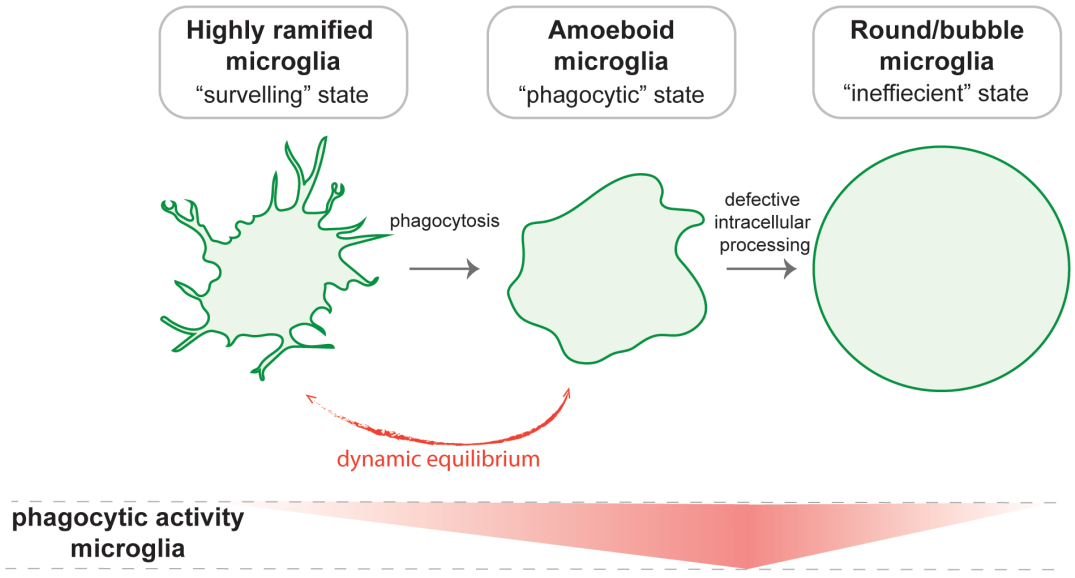

Figure 4.4. Microglia morphology model.

Microglia are highly dynamic cells. Highly ramified microglia are considered in a surveillance state. Upon increase of phagocytic activity, microglia assume an amoeboid shape. Those morphologies exist in a dynamic equilibrium. When microglia are highly phagocytic can transiently assume a bubble-like morphology, which can also occur when the intracellular processing of the ingested material is defective. A bubble-like shape is indicative of an inefficient cell, characterized by low phagocytic activity.

4.6 GASTROSOMAL ENLARGEMENT AFFECTS MICROGLIA MIGRATION AND ENGULFMENT AND COULD CONTRIBUTE TO THE PATHOGENESIS OF LYSOSOMAL STORAGE DISORDERS

Defects in either engulfment or degradation of apoptotic cells contribute to different conditions such as autoimmune diseases, suggesting that both eating and digesting apoptotic cells are essential for proper immune responses (Elliott and Ravichandran, 2010; Nagata et al., 2010). Kawane and colleagues showed the importance of apoptotic cell degradation by studying the DNase II knockout mice which lack the lysosomal enzyme responsible for the degradation of nuclear DNA of the engulfed cells (Kawane et al., 2001). Those mice suffer of improper activation of innate immunity and die at birth because of severe anaemia (Yoshida et al., 2005a; 2005b). Phagocytes such as professional macrophages are interested by a specific family of disorders known as Lysosomal Storage Diseases (LSDs). LSDs represent a group of about 50 genetic disorders caused by deficiencies of lysosomal and non-lysosomal proteins. Here, enzymes required for the degradation of specific compounds are lacking, leading to their accumulation in lysosomal and non-lysosomal compartments. LSDs have been shown to reduce macrophages endocytic recycling capabilities and migration to the target (Berg et al., 2016).

In our study, by characterizing *blb*, a zebrafish mutant lacking a sugar transporter where phagosome do not reduce their size during maturation, we identify the gastrosome as a new phagocytic compartment which dynamically respond to the phagocyte's activity and feeds back to it. In this mutant, the gastrosome keeps enlarging upon phagocytosis transforming microglia into large, poor phagocytes. It is surprising however how no diseases related with Slc37a2 transporter or gastrosomal expansion have been reported yet. Surprisingly, zebrafish homozygous knockouts for Slc37a2 are viable and their lifespan is comparable to those of wild type. As in the mutant, the bubble-like phenotype is visible only in the brain while trunk macrophage can develop this morphology only by increasing the level of apoptosis in the embryo, we hypothesize that the immune system can cope and handle the phagocytic requirements. Mutant microglia grow over time reading a peak at 4 dpf. At later time points levels of apoptosis in the brain are significantly reduced. Moreover, in other tissues the number of macrophages is much higher than in the brain while levels of apoptosis are significantly lower (Casano et al., 2016) preventing the development of the *blb* phenotype in the other tissue resident macrophages. Finally, Slc37a2 has been shown to localize specifically on

macrophages (Kim et al., 2007), meaning that other phagocytic cells should not be affected. Thus, we would assume that, at least in absence of further external challenges (such as injuries, infections etc.), the immune system of Slc37a2 knock out organisms could be able to handle the physiological levels of apoptotic cell clearance, explaining why mutations in this gene might have gone unnoticed so far.

In our work, the injury experiments and quantifications of the phagocytic activity in *blb* clearly highlight the importance of the gastrosome in phagocytosis as interfering with its function affects microglia morphology and behaviour. Moreover, the finding that this compartment expands dynamically in response to elevated apoptosis in wild type embryos raises the possibility of an entry-point for manipulating microglial cellular morphology and modulating the impact that these cells have in the context of many neurodegenerative disorders.

5 MATERIAL AND METHODS

5.1 FISH REARING AND HANDLING

5.1.1 ZEBRAFISH STRAINS AND TRANSGENIC LINES

For this study, Golden, Tübingen and TLF fish were used as wild types. Macrophages and microglia were visualized by using either a *Tg(spi1b:GAL4,UAS:EGFP)*, a *Tg(spi1b:GAL4,UAS:TagRFP)* line (Peri and Nüsslein-Volhard, 2008; Sieger et al., 2012) or a *Tg(mpeg1:eGFP-caax)*. In the first two lines, the yeast-derived transcription activation factor Gal4 is expressed under the control of the pU.1 promoter and specifically binds UAS (Upstream Activation Sequence). This allows a stable labelling of all myeloid cells and their progeny even when the activity of the original promoter is weak or active for a restricted period of time. In the *Tg(mpeg1:eGFP-caax)* line, the eGFP-caax fusion protein was cloned downstream of the macrophage mpeg1 promoter (Ellett et al., 2011) using the Gateway cloning kit from Thermo Fisher Scientific to label the plasma membrane of all macrophages.

Microglia were as well specifically labelled using the *Tg(apoeb:lyn-eGFP)* line (Peri and Nüsslein-Volhard, 2008). Here the membrane bound fluorescent marker was cloned in the Apolipoprotein-E locus and a BAC line was generated.

To visualize neurons a *Tg(NBT:DsRed)* line was used, where DsRed expression is under the control of the Xenopus neural beta-tubulin (nbt) promoter (Peri and Nüsslein-Volhard, 2008). To monitor neuronal apoptosis *in vivo* a *Tg(nbt:DLexPR:SecA5-TagBFP)* line was used (Mazaheri et al., 2014). Here the fluorescent protein TagBFP was cloned downstream of Secreted Annexin-V. The expression of this construct was driven by the NBT promoter and DLexPR (a constitutively active form of the inducible LexPR system).

5.1.2 FISH HUSBANDRY

Zebrafish were raised and maintained as indicated in “Zebrafish – A practical approach” (Nüsslein-Volhard and Dahm, 2002). Adult zebrafish were kept in aquaria from Aquaschwarz Aquarienbau (Gottingen, Germany) and Muller & Pfleger (Rockenhause, Germany), at 27-28°C in a 14 hours light and 10 hours dark cycle. System water was desalted and adjusted to pH ~7

and conductivity of 400 ± 50 µS. Embryos were obtained by pairs of males and females naturally mating and after collection they were kept in E3 medium 1x (pH 7.2) at 28°C. Embryos were either analysed at the desired stage or bleached for rising. Staging was done according to Kimmel at al., 1995 (Kimmel et al., 1995).

Medium	*Composition*	*Concentration*
E3 60x	NaCl	3 mM
	KCl	0.17 mM
	$CaCl_2 \cdot 2H_2O$	0.33 mM
	MgSO4·6H2O	0.33 mM
PBS 1x pH 7.4	NaCl	137 mM
	KCl	2.7 mM
	$Na_2 \cdot HPO_4$	10 mM
	KH_2PO_4	2 mM

5.1.3 BLEACHING PROCEDURE

To reduce the risk of pathogen contamination, embryos to be raised were disinfected by bleaching using sodium hypochlorite 10-15% according to Nüsslein-Volhard and Dahm, 2002 (Nüsslein-Volhard and Dahm, 2002). Briefly, embryos were incubated in bleaching solution for 5min and then rinsed in E3 + dH_2O for additional 5min. This procedure was repeated twice, finally followed by a last rinsing step. After bleaching, the eggs were placed in a new Petri dish and 10 µg/ml pronase was added to help the embryos hatching from the bleached egg. As recommended, bleaching was performed only on embryos up to 28hpf.

Reagent	*Stock Solution*	*Supplier (cat.no.)*
Sodium hypochlorite solution	10-15% NaOCl, store at 4°C	Sigma (425044)
Pronase	30 mg/ml, store 1 ml aliquots at -20°C	Roche (11459643001)

5.1.4 PTU TREATMENT

To avoid pigmentation of the larvae which starts from 24-28 hpf, embryos were kept in E3 medium containing 1% v/v of N-Phenylthiourea (PTU). Since PTU blocks the process of melanogenesis only transiently, it had to be applied at a constant rate with every exchange of medium, but only after 6 hpf, as if applied before it could lead to heart oedema and developmental delays. PTU stock solution was prepared as following.

Reagent	*Stock Solution*	*Supplier (cat.no.)*
PTU	100x solution: dissolve 750 g in 250 ml of PBS medium. Warm up to 60°C and stir to dissolve. Store at 28°C.	Sigma (P7629)

5.1.5 ANAESTHESIA OF ZEBRAFISH EMBRYOS

Prior manipulation, embryos were anesthetized by adding Ethyl 3-aminobenzoate methanesulfonate salt (Tricaine) to the E3 medium. Tricaine stock solution was prepared as following and kept at 4°C.

Reagent	*Stock Solution*	*Supplier (cat.no.)*
Tricaine	100x solution: dissolve 2g Tricaine in 489.5 ml autoclaved water + 10.5 ml Tris 1M pH 9.5. Adjust pH to ~7	Sigma (A5040)

5.1.6 MOUNTING EMBRYOS FOR LIVE IMAGING

Embryos to be imaged under the confocal or light sheet microscope were anaesthetized and screened based on the expression of the desired fluorescent labelling, using the stereoscope Olympus SZX16. Selected embryos were then embedded in 1.3% low-melting agarose, dissolved in E3 medium and tricaine and mounted on a glass bottom dish. The dish was then filled with E3 medium containing PTU and tricaine for imaging.

Material	*Supplier (cat.no.)*
peqGOLD Low Melt Agarose	peqLab Biotechnologie GmbH (35-2030)
Glass bottom Microwell Dishes	MatTek Corporation (P35G-1.5-10-C)

5.2 CELL CULTURE

RAW 264.7 cells were cultured in Dulbecco's Modified Eagle's Medium (DMEM) High Glucose wilt L-glutamine plus 10% Heat Inactivated Fetal Bovine Serum (FBS). HeLa Kyoto H2B-EGFP and HeLa Kyoto H2B-mCherry were cultured in DMEM-1g/L D-Glucose, Pyruvate plus 10% FBS, 1% Penicillin/Streptomycin and 1% GlutMAX-l 100x. Cells were cultured in a cell culture incubator (5% CO_2, 37°C) and handled in a sterile cell culture hood. Cells were grown to 70-80% confluency, rinsed with 1x PBS, trypsinized with 0.05% Trypsin-EDTA 1x, washed with complete culture medium and introduced into a culture flask (10-30% confluency) or seeded for co-culture experiments.

Reagent/Material	*Supplier (cat.no)*
RAW 264.7	ATCC (TIB-71)
HeLa Kyoto H2B-EGFP	Gift from Lars Velten and Lars Steinmetz, EMBL
HeLa Kyoto H2B-mCherry	Gift from the Mitocheck consortium, EMBL
DMEM High Glucose, L-Glutamine	ATCC (30-2002)
DMEM 1g/L D-Glucose, Pyruvate	Gibco (11880-028)
Heat Inactivated FBS	Gibco (10500-064)
Penicillin/Streptomycin	Gibco (15140-122)
GlutMAX-l (100x)	Gibco (35050-061)
0.05% Trypsin-EDTA (1x)	Gibco (25300-054)

5.2.1 PHAGOCYTOSIS ASSAY

For phagocytosis experiments, cells were co-cultured in RAW 264.7 medium on glass coverslips (22 mm) in a 1:1 (RAW264.7:HeLa) ratio until 50% confluence. To induce HeLa-specific apoptosis, we used a medium containing Recombinant Human TRAIL/TNFSF10 (80 ng/ml, (Steven R Wiley et al., 1995)), a homologous of Fas ligand able to induce rapid apoptosis in cancer cells. After 1 hour, the drug was removed and fresh medium was added. Cells were kept in the incubator, then rinsed with PBS 1x and fixed with 4% Paraformaldehyde (PFA) after 3, 6 or 9 hours from treatment. Coverslips were incubated overnight at 4°C before antibody or dyes staining.

Reagent	*Stock Solution*	*Supplier (cat.no.)*
TRAIL/TNFSF10	10 μg /ml stock solution: resuspend 20 μg in 1 ml of filtered PBS 0.5% BSA. Store 20 μl aliquots at -20°C, up to 1 month.	R&D Systems (375-TEC-010)
PFA, prills, 95%	4% Solution: Dissolve 1g PFA powder in 15 ml PBS 1x pre-heated at 60°C. Add NaOH dropwise until the solution clears. Adjust pH to ~7 and bring to a final volume of 25 ml with PBS 1x.	Sigma (441244)

5.3 MOLECULAR BIOLOGY TECHNIQUES

5.3.1 CRISPR/CAS9 GENOME EDITING

5.3.1.1 Target design

CRISPR-Cas9 has been used to genetically modify the genes of interest. CRISPR-Cas9 is a technology based on a bacterial system of programmable DNA endonucleases. By the use of a sgRNA complementary to a specific sequence on the genome, Cas9 endonuclease is able to induce very efficiently and quickly a cleavage of the double strand DNA, 4 base pairs upstream of the so-called PAM sequence (NGG). The cell will repair the double strand brake in the DNA by either non-homologous end joining (NHEJ) or by homology directed repair (HDR) when homology sequences are present. NEHJ is an error-prone repair mechanism that result in insertions and deletions that often disrupt the gene, reason why it is often used to generate knock outs. On the other hand, HDR uses homology recombination leading to a precise repair on the cut double strand and this repair mechanism can be used to insert small pieces of DNA into the cleavage. Here, HDR has been used to introduce specific sequences (cassettes) in the loci of interest. In particular, the first exon of Slc37a2 has been targeted to introduce a short sequence which, whatever the reading frame, will lead to the introduction of a STOP codon (STOP cassette). On the other hand, P2Y6, P2Y12 and P2Y13 loci have been targeted at 50-100 bp from the ATG to introduce a STOP cassette plus the landing site for PhiC31 integrase recombination (attB/STOP cassette) which will allow the generation of knock ins.

The sgRNAs were designed using the CRISPR-Cas9 target online predictor CHOPCHOP (http://chopchop.cbu.uib.no) based on the ENSEMBL Transcript ID. Only coding regions were considered as targets, and the sgRNA were designed 20 nucleotides long + full PAM sequence (NGG) at the 3'. The sgRNA targets were selected based on their position in the gene (by 100 bp from ATG), GC percentage (ideally between 60-70%) and the target score which takes into consideration self-complementary, efficiency and absence of predicted off-targets.

Gene	*Transcript ID*	*sgRNA (5'-3')*	*Cutting site position*
Slc37a2	ENSDART00000038602.6	TGATAGGCTTTCGAGAGAGA	108 nucleotides after ATG
P2Y6	XM_689367.6	GAAGGCCGAAGATGAAGACC	93 nucleotides after ATG
P2Y12	ENSDART00000154780	AGTTCATCCTGTTCTCGAGA	61 nucleotides after ATG
P2Y13	ENSDART00000155392	GAAGTGTGAGCGGGACACTC	42 nucleotides after ATG

Cassette name	*Cassette sequence*
STOP	GGCTAATTAATTAAGCTGTTGTAG
attB/STOP	GGTGCCAGGGCGTGCCCTTGGGCTCCCCGGGCGCGGGCTAATTAATTAAGCTGTTGTAG

The cassettes were ordered as oligos purified by HPLC through Sigma. Those were designed by flanking the STOP or attB/STOP cassette by 30 nucleotides specific for the target. In particular, from the Cas9 cutting site (4 nucleotides before the PAM sequence), 5 nucleotides were left to each side and then 30 bp left and right were taken as homology arms flanking the cassette of interest. 5.4 μM stocks of cassettes were prepared for each gene.

5.3.1.2 sgRNA synthesis

A PCR was used to generate the DNA template for the sgRNA which will be generated by retro-transcription. This PCR take advantage of the use of three common (66F, 66R and 67R) and one specific primers which partially overlap (Figure 5.1). All oligos are ordered as highly purified primers (purified by high performance liquid chromatography, HPLC). The specific oligo, always 81 nucleotides long, mediates the overlap among the 4 primers working as a template for the PCR. In particular, it contains the T7 promoter sequence (21 nucleotides) followed by the target sequence (5'-3', 20 nucleotides) and a 40 nucleotides long tail common in every sgRNA.

Primer name	*length*	*Primer sequence / structure (5'-3')*
Specific oligo	81 nt	GCGTAATACGACTCACTATAGNNNNNNNNNNNNNNNNNNNNGTTTTAGAGCTAGAAATAGCAAGTTAAAATAAGGCTAGTC
66F	20 nt	GCGTAATACGACTCACTATA
66R	20 nt	GCACCGAGTCGGTGCGGATC
67R	81 nt	GATCCGCACCGACTCGGTGCCACTTTTTCAAGTTGATAACGGACTAGCCTTATTTTAACTTGCTATTTCTAGCTCTAAAAC

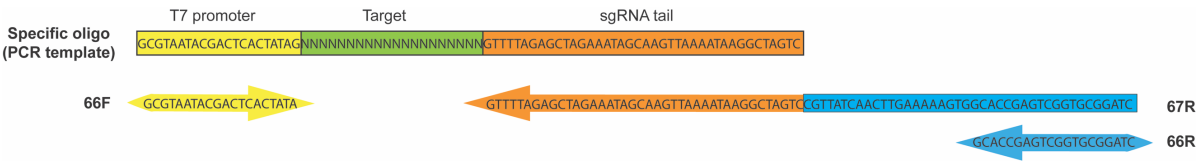

Figure 5.1. Schematic representation of the oligos for the synthesis of sgRNAs.

Three partially overlapping primers (66F, 66R and 67R) are used for the synthesis of every sgRNA. A specific oligo is designed for the target of interest. This include the T7 promoter sequence (yellow) where 66F binds and used for the RNA synthesis, the specific sequence of the target (green) and the sgRNA tail shared by all sgRNA for Cas9 recognition (orange) where 66R and 67R primers bind.

50 µl of PCR mix for the synthesis of the sgRNA template was done as following.

Reagent	*Volume (x1)*	*Supplier (cat.no.)*
Buffer 10x	5 µl	Genaxxon Bioscience (M3454)
X7 Pfu polymerase	0.5 µl	Protein Expression and Purification Facility, EMBL, Heidelberg, Germany
10 mM dNTPs	1 µl	Thermo Fisher Scientific (R0192)
100 µM specific oligo	0.4 µl	Sigma
100 µM 67R	0.4 µl	Sigma
100 µM 66F	2.5 µl	Sigma
100 µM 66R	2.5 µl	Sigma
H2O	37.7 µl	

PCR Conditions		
94°C	3 min	
94°C	15 sec	40x
50°C	15 sec	
72°C	15 sec	
72°C	5 min	
4°C	hold	
Storage at 4°C		

The successful amplification of the template was tested by electrophoresis. 3 µl of PCR (plus 6x dye) were run on a 1.5% agarose gel in TAE 1x. Nucleotides were visualized by SYBR safe and a DNA ladder was used as a molecular weight reference. After the 122 bp fragment was visualized by gel, the PCR product was purified by column using QIAquick PCR Purification Kit according to the manufacturer's instructions.

The concentration of the purified PCR product was then measured by Nanodrop (NanoDrop 8000 Spectrophotometer, Thermo Fisher Scientific), and the RNA was synthetized *in vitro* taking advantage of the T7 promoter by using the MEGAshortscript T7 kit according to the manufacturer's instructions. The freshly synthetized sgRNA was then purified by column using the miRNeasy Mini Kit following instruction from step 6 of the manufacturer's protocol and the purified sgRNA was eluted in 60 µl of RNAse free water.

After purification, 1 µl of sgRNA plus 1 µl 6x dye and 10 µl water was heated up at 70°C for 5 min, then kept 2 minutes on ice and immediately loaded on a 2% agarose gel and run for 10 min at 140V to check for integrity. Finally, the concentration was measured by Nanodrop and a stock of 600 ng/µl was prepared for each sgRNA.

Reagent/Material	*Stock Solution*	*Supplier (cat.no.)*
TAE	50x stock solution: 121g TRIZMA base + 50 ml EDTA 0.5M (pH 8.0) + 28.55 ml glacial acetic acid. Bring to 500 ml with Millipore H2O and autoclave before use. Store at room temperature.	Stock solution prepared by EMBL laboratory kitchen
Agarose	-	Sigma (A9539)
SYBR Safe DNA gel stain	10000x	Thermo Fisher Scientific (S33102)
GeneRuler 100 bp DNA ladder	-	Thermo Fisher Scientific (SM0241)
6x DNA loading Dye	6x	Thermo Fisher Scientific (R0611)
QIAquick PCR Purification Kit	-	Qiagen (28104)
MEGAshortscript T7	-	Thermo Fisher Scientific (AM1354)
miRNeasy Mini Kit	-	Qiagen (217004)

5.3.2 MICROINJECTIONS OF ZEBRAFISH EMBRYOS

Injection plates were prepared as indicated in Nüsslein-Volhard and Dahm, 2002 (Nüsslein-Volhard and Dahm, 2002) with 2% Agarose in E3, and freshly laid zebrafish eggs were placed and aligned in the groves. 1-cell stage embryos were injected with a Pneumatic PicoPump microinjector (WPI, SYS-PV820). The capillaries (Harvard Apparatus No. 30-0035) were pulled using a Sutter P9 Micropipette Puller (Sutter) (pulling conditions: heat 630, pull 80, velocity 75, time 90). After the injection the embryos were transferred into a fresh petri dish with E3 and placed in 28°C incubator. About 7 hours later, unfertilized eggs were sorted out.

5.3.2.1 Morpholino knock-downs

For morpholino-mediated knockdown, 1-cell stage embryos were injected into the yolk. Morpholinos (Gene Tools, LLC. Oregon, USA) were diluted in dH_2O as stock solutions and co-injected with 0.1M KCl and 0.2% Phenol red (Sigma) at the desired concentration.

Gene	*Sequence (5'-3')*	*Working Concentration*	*Reference*
pU.1	GATATACTGATACTCCATTGGTGGT	0.5 mM	(Rhodes et al., 2005)
Caspase 3	TTGCGTCCACACAGTCTCCGTTCAT	0.1 mM	(Yamashita, 2003)
BAI-1	CTAGAACTCTAACACACTTACTCAT	1 mM	(Mazaheri et al., 2014)
TIM4	CATAGTTTATCAACACTTACCATCA	0.7 mM	(Mazaheri et al., 2014)
a1vATPase	CCTCGCTACGAAACAGCTCCCCCAT	0.4 mM	(Peri and Nüsslein-Volhard, 2008)

5.3.2.2 sgRNA and Cas9 injection

To induce Cas9-double strand break and the insertion of the cassette by homologous recombination, an injection mix was prepared as follow and incubated for 20 minutes at 37°C to allow Cas9 protein (Protein Expression and Purification Core Facility, EMBL Heidelberg) re-folding before injection into the single cell of freshly laid zebrafish embryos.

Composition	*[Stock]*	*[Use]*	*Volume (x1)*
sgRNA	600 ng/µl	200 ng/µl	1.36 µl
Cassette	5.4 µM	1 µM	0.74 µl
KCl	1M	300 mM	0.9 µl
Cas9	4000 ng/µl	1000 ng/µl	1 µl

5.3.3 GENOTYPING

5.3.3.1 Fin Clip

To collect tissue from adult fish for genotyping, fish were transferred in 250 ml fish water containing 6 ml of Tricaine 100x. As soon as the righting reflex was lost, a small piece of fish tail was cut and collected in a PCR tube. The sedated fish was immediately moved to fresh water in a screening tank numbered in the same way as the PCR tube containing the fish tissue.

5.3.3.2 DNA extraction

To identify F_0 founders carrying the cassette in the germline, offspring of the outcross between adult F_0 injected fish and with wild types were genotyped (single embryos). From F_1 onwards, fish were genotyped by fin clipping (as described above). The total genomic DNA was extracted by adding 25 µl to single embryos or 40 µl to fin-tissue from adult fish (fin clip) of Quick Extract

Solution. The samples were incubated for 15 minutes at room temperature, vortexed for 10 seconds and transferred for 5 minutes at 65°C. After mixing 10 seconds by vortex, samples were incubated at 95°C for 2 minutes and transferred at 4°C or -20°C for long storage. Before use, the genomic DNA was spin down by centrifuge.

Reagent	*Supplier*
QuickExtract DNA Extraction Solution	Epicentre (QE09050)

5.3.3.3 Polymerase chain reaction (PCR)

To determine the genotype of the samples, the sequence of interest was amplified from the total genomic extract. In particular, two different PCRs were performed per gene: one having the forward primer binding on the cassette inserted by HDR and the reverse primer on the gene, the second having both primers binding on the gene, outside the inserted cassette. The first PCR was used to determine whether the cassette of interest was inserted by the presence (or absence) of the proper length band. The second PCR product was used to verify proper insertion by evaluating the size of the fragment amplified but especially by analysing the amplified product by sequencing. The following PCR mix, cycles and primers pairs were used.

PCR Mix	*Volume (x1)*
Buffer 10x	2 µl
Taq Polymerase	0.4 µl
10 µM Frw primer	0.4 µl
10 µM Rev Primer	0.4 µl
10 mM dNTPs	0.4 µl
Genomic DNA	2 µl
H2O	14.4 µl

PCR Conditions		
95°C	2 min	
95°C	30 sec	40x
Tm	30 sec	
72°C	30 sec	
72°C	2 min	
4°C	hold	
Storage at 4°C		

Primer pair; Tm	*Target*	*Amplificate size*
20F/7R; 60°C	attB/STOP cassette P2Y12	538 bp (if with cassette)
20F/9R; 60°C	attB/STOP cassette P2Y13	231 bp (if with cassette)
20F/19R; 60°C	attB/STOP cassette P2Y6	385 bp (if with cassette)
7F/7R; 65°C	P2Y12, for sequencing	643 bp
9-10F/9R; 64.1°C	P2Y13, for sequencing	338 bp
19F/19R; 65°C	P2Y6, for sequencing	519 bp

5.3.3.4 Sequencing

To analyse the sequence of the fish on genotyping, the PCR product of interest was first tested on 1% agarose gel (2 μl to verify the length of the amplificated), then purified by column using the QIAquick PCR Purification Kit according to manufacturer's instructions. Sequencing on purified PCR products was outsourced to GATC Biotech (Konstanz, Germany) by providing an aliquot of 10 μM forward primer. Sequencing results were analysed using Geneious Software (Biomatters, New Zealand).

5.3.4 PROTEIN EXTRACTION

To obtain whole-embryo protein lysate, 50 wild type or *blb* (NY007 and NI150) embryos at 4 dpf were anesthetized in 0.01% tricaine and resuspended in 200 μl of lysis buffer (Fiorotto et al., 2016) supplemented with protease inhibitor cocktail tablets (1 tablet/10 ml; Roche). Embryos were homogenized with a microfuge pestle until uniform consistency and lysates were incubated for 30 min at 4°C under rotation. The samples were centrifuged at 10000g for 30 min at 4°C, then the supernatant was transferred to a new tube and the total protein extract was measured by Coomassie Protein Assay Reagent (Thermo Fisher Scientific, 1856209) using a spectrophotometer (Eppendorf BioPhotometer plus).

Lysis Buffer composition	*Concentration*	*Supplier (cat.no.)*
Tris-HCl [1M, pH 7.5]	50 mM	
EDTA [10mM]	1 mM	
Octyl β-D-glucopyranoside	2%	Sigma (O8001)
2-Mercaptoethanol	5 mM	Sigma (M6250)
NaCl [3M]	0.25 M	Merck (1.06404.1000)
Na3VO4	1 mM	Sigma (S6508)
NaF	20 mM	Sigma (201154)
Glycerol	5%	Merck (1.04093.1000)
Triton X-100	100 μL	Sigma (T9284)

5.3.5 SDS-POLYACRYLAMIDE GEL ELECTROPHORESIS (-PAGE)

Discontinuous gel electrophoresis under denaturing conditions was used for protein separation of zebrafish lysates. Therefore, 800 μg of sample protein were solubilized in 20 μl of 1x Laemmli buffer-10% 2-Mercaptoethanol and warmed up for 10 min and 37°C. Proteins

were separated electrophoretically based on their molecular size using precast polyacrylamide gels for 1.5 hours at 200V and MOPS or MES buffers for big or small proteins respectively.

Reagent	*Supplier (cat.no.)*
Laemmli Buffer 4x	Biorad (161-0747)
2-Mercaptoethanol	Sigma (M6250)
NuPAGE 4-12% Bis-Tris Protein Gels	Novex (NP0321BOX)
NuPAGE MOPS SDS Running Buffer (20x)	Novex (NP0001)
NuPAGE MES SDS Running Buffer (20x)	Novex (NP0002)

5.3.6 IMMUNOBLOTTING

Immunoblotting was used to identify specific proteins recognized by antibodies. To this aim, proteins separated by SDS-PAGE were transferred electrophoretically onto nitrocellulose membranes. Prior to blotting membranes, filter paper, fiber pads and gels were equilibrated in transfer buffer 1x prepared according to the manufacturer's instructions and the gel-membrane transfer sandwich was assembled. Proteins were transferred at room temperature for 1 hour at 170 mA. Membranes were first rinsed with TBS-T (0.1% Tween-20), then free binding sites were blocked by immersing the membrane in 5% fat-free milk powder in TBS-T for 1 hour at room temperature. Primary antibodies (Table 5.1) were diluted in blocking buffer and incubated overnight at 4°C with constant gentle agitation. Membranes were washed thoroughly at least 3 times in TBS-T buffer for at least 10 minutes each. Washing was followed by incubation with the appropriate fluorescent secondary antibody, diluted 1:2500 in blocking buffer for 1 hour at RT. Membranes were again washed for at least 30 min with several times changed TBS-T buffer before HRP detection systems and autoradiography films according to the manufacturer's instructions.

Reagent/Materials	*Supplier (cat.no.)*
Nitrocellulose membranes, 0.2 μm pore size	Novex (LC2000)
NuPAGE transfer buffer 20x	Novex (NP0006)
Tween-20	Sigma (P9416)
Immobilion Western	Millipore (WBKLS0500)
Super signal West Pico PLUS	Thermo Fisher Scientific (34579)
Amersham Hyperfilm MP	GE Healthcare (28906845)

PRIMARY ANTIBODY	SPECIES	SUPPLIER (CAT.NO.)	APPLICATION/DILUTION
Anti-fish Slc37a2*	Mouse, monoclonal	EMBL Rome	WB (1:100); IF (1:20)
Anti-mouse Slc37a2	Rabbit, polyclonal	Invitrogen (PA5-20916)	IF (1:100)
Anti-mouse Rab7	Rabbit, monoclonal	Abcam (Ab137029)	IF (1:100)
Anti-mouse LBPA	Hamster, monoclonal	Millipore (MABT837)	IF (1:100)
Anti-mouse Lamp1	Rat, monoclonal	Abcam (Ab25245)	IF (1:100)
Anti-mouse Lamp2	Rat, monoclonal	Abcam (Ab25339)	IF (1:100)
Anti-mouse γ-Tubulin	Mouse, monoclonal	Sigma (T6557)	WB (1:2000)
Anti-rat Cathepsin D	Rabbit	Gift from Bernard Hoflack	IF (1:100)

Table 5.1. List of Primary Antibodies used in this Thesis.

Antibodies with their characteristics including supplier and specific information about their application are listed in this table.

* Generation of the monoclonal antibody for Slc37a2

A monoclonal antibody against Slc37a2 was raised in mouse at the Monoclonal Antibodies Core Facility (MACF) at the EMBL outstation in Rome, Italy. The following epitope was selected: CTAPQHHERVEEEPLLRNSSTNEEIFNSHTST (236-267). This is located in the loop between transmembrane domains 6 and 7 of the protein.

5.4 HISTOLOGICAL METHODS

5.4.1 ACRIDINE ORANGE

Acridine Orange (AO) is an organic compound used as a nucleic acid-selective fluorescent dye. AO selectively penetrate cells undergoing programmed cell death, therefore it was used to visualize apoptotic cells *in vivo*. Embryos were incubated with 10µg/ml AO in E3/PTU for 1h and extensively washed with fresh E3 prior live imaging microscopy. Since AO is light sensitive, embryos were kept in the dark during the procedure.

Reagent	*Stock Solution*	*Supplier (cat.no.)*
Acridine Orange hemi(zinc chloride) salt	Dissolve 10 mg/ml in double distilled water. Store at 4°C	Sigma (A6014)

5.4.2 NEUTRAL RED STAINING

Neutral Red (NR) is a dye used to stain acidic compartments (such as lysosomes). NR staining was used to visualize microglia in the living zebrafish embryo, since during development those are the cells containing acidic compartments. For the staining, Neutral Red was added to a final concentration of 5 µg/ml to the larvae in E3/PTU. After 2 h in the staining solution at 28 °C, the larvae were transferred to new E3, washed several times with E3, anesthetized and analysed under a stereomicroscope (Olympus SZX16, Olympus) and/or mounted and imaged at a confocal microscope (Olympus FV 1200).

Reagent	*Stock Solution*	*Supplier (cat.no.)*
Neutral Red	Dissolve 500 µg/ml in autoclaved water. Store at 4°C	Sigma (N4638)

5.4.3 LYSO-TRACKER STAINING

LysoTracker Red DND-99 is a weakly basic amine that selectively accumulates in cellular compartments with low internal pH. It can be used as a vital stain to label lysosomes and phago-lysosomes. For staining, 12 µl were added to 30 ml E3/PTU 1% DMSO and the embryos

were stained for 1 hour, in the dark at 28 °C. Before mounting for confocal microscopy fish were washed several times with fresh E3.

Reagent	*Supplier (cat.no.)*
LysoTracker Red DND-99	Thermo Fisher Scientific (L7528)

5.4.4 LIPID STAINING

To stain membranes and lipids, a panel of different lipidic dyes was used on both cell culture and zebrafish embryos. In particular, BODIPY 493/503 and Nile Red were used for neutral lipid staining, Wheat germ agglutinin (WGA) was used to stain lectins and Nile Blue Chloride to visualize lipids and DNA.

Reagent	*Stock*	*Use*	*Supplier (cat.no.)*
BODIPY 493/503	1 mg/ml in DMSO	1µg/ml	Thermo Fisher (D3922)
Nile red	1 mg/ml in DMSO	5µg/ml	Thermo Fisher (N-1142)
Nile Blue Chloride	1 mg/ml in H_2O	5-10µg/ml	Sigma (222550)
WGA, AF 488	1 mg/ml in PBS	5µg/ml	Thermo Fisher (W11261)

On cell culture, stainings were performed after phagocytosis experiments on samples fixed 9 hours after apoptosis induction. The fixed co-culture was first washed with PBS 1x, then directly incubated with the dyes dissolved in PBS 1x for 30 minutes at room temperature. Stained co-cultures were washed 3 times for 5 minutes with PBS 1x and mounted using a Vectashield Kit (Vector Laboratories, Inc., Burlingame, CA) for confocal imaging.

For staining on zebrafish embryos, the live dyes (BODIPY 493/503, Nile Red and Nile Blue) were added to the medium of 4 dpf Zebrafish embryos for 30 minutes at 28°C. After incubation with the dye, the embryos were rinsed extensively with E3 medium, anesthetized with 0.01% Tricaine and mounted in 1.3% low-melting agar for confocal imaging.

For staining on fixed samples, Zebrafish embryos at 4 dpf were anesthetized with 0.01% tricaine and fixed overnight at 4°C in freshly prepared 4% PFA. Fixed embryos were extensively permeabilized by washing 5x30 minutes with PBS-Tx100 0.8%. Embryos were incubated with WGA for 30 min at room temperature after permeabilization. Subsequently they were rinsed with PBS and mounted in 1.3% low-melting agar for confocal imaging.

5.4.5 IMMUNOHISTOCHEMISTRY ON ZEBRAFISH EMBRYOS

For whole mount antibody staining, *Tg(mpeg1:eGFP-caax)* Zebrafish embryos at the desired stage of development were anesthetized with 0.01% tricaine and fixed overnight at 4°C in freshly prepared 4% PFA. Embryos were then extensively permeabilized by washing 5x30 minutes with permeabilizing solution. Subsequently they were rinsed with 10x blocking buffer and incubated with blocking solution 10x for 1 hour at room temperature. The primary antibody was added (Table 5.1) in blocking buffer 1x overnight at 4°C with gentle rocking. On the next day, embryos were washed extensively in PBS-Tx100 rinsed with 10x blocking buffer and then blocked for 1 hour at room temperature. The secondary antibody (1:500) and GFP booster (1:200, Chromotek GBA488-100) to enhance the green fluorescence of the microglia were added in blocking buffer 1x and incubated overnight at 4°C with gentle rocking. Embryos were washed extensively (3x30 minutes) in PBS-Tx100 and mounted in 1.3% low-melting agar for confocal imaging. To avoid bleaching it is advised to protect the sample from light during the whole procedure.

Reagent	*Composition*
Permeabilizing Solution	PBS-Tx100 0.8% (800 μl in 100ml)
Blocking Solution 10x	10% NGS in permeabilizing solution (600 μl in 6 ml)
Blocking solution 1x	Dilute 1:10 the blocking solution 10x

5.4.6 IMMUNOHISTOCHEMISTRY ON CELL CULTURE

Antibody stainings were performed on glass coverslips with co-cultures of HeLa and RAW 264.7 cells prior and after apoptosis induction fixed at different time points depending on the experiment set up. Cells were fixed overnight with freshly prepared 4% PFA, washed with 3 times for 5 minutes with PBS 1x and permeabilized for 7 minutes. After 1 hour blocking at room temperature with gentle rocking, cells were incubated overnight at 4°C with primary antibody (Table 5.1) in blocking buffer. The next day, cells were washed 3 times for 5 minutes with PBS 1x and incubated at room temperature with the appropriate secondary antibody. After 1 hour, unbound antibody was removed by washing in PBS 1x and coverslips were mounted using a Vectashield Kit (Vector Laboratories, Inc., Burlingame, CA).

Reagent	*Composition*
Permeabilizing Solution	PBS-TritonX-100 0.2% (200 μl in 100 ml)
Blocking Solution	PBS-0.2%TritonX-100-3%BSA (3g BSA in 100 ml permeabilizing solution)

Reagents/Materials	*Supplier (cat.no.)*
Triton X-100	Sigma (T9284)
Bovine Serum Albumine	Sigma (A2153)
Normal Goat Serum (NGS)	Merck (S26)

5.5 CHEMICAL TREATMENTS

5.5.1 Z-VAD-FMK TREATMENT

The drug Z-VAD-fmk (Carbobenzoxy-valyl-alanyl-aspartyl-[O-methyl]-fluoromethylketone) was used to reduce the levels of apoptosis in the zebrafish embryo. To facilitate uptake, it was dissolved to its final concentration (300 µM) in E3 medium containing 1% DMSO

Reagent	*Stock Solution*	*Supplier*
Z-VAD-fmk	20 mM stock solution: Dissolve 5 mg of Z-VAD-fmk in 535 µl of sterile DMSO. Store at -20°C.	Bachem (4027403)

5.5.2 CAMPTOTHECIN TREATMENT

The drug Camptothecin (CPT) was used to increase apoptosis level in the embryos and therefore further enhance microglia and macrophages phagocytosis. CPT was dissolved in E3 with 1% DMSO at a final concentration of 1 µM.

Reagent	*Stock Solution*	*Supplier*
(S)-(+)-Camptothecin	25 mM stock solution: Dissolve 100 mg of CPT powder in 11.5 ml of sterile DMSO in sterile conditions. A second dilution in DMSO was done to prepare 1 mM stock aliquots. Store at -20°C.	Sigma (C9911)

5.6 MICROSCOPY AND IMAGE ANALYSIS

5.6.1 LIVE IMAGING

For live imaging, zebrafish embryos were anesthetized in 0.01% tricaine and embedded in 1.3% low-melting-point agarose. Imaging was performed using the Olympus FV1200, the Leica SP8 and the Andor Spinning disk with 40x/NA1.15 and 20x/NA0.7 objectives. For full brain imaging an average of 30-40 stacks were captured, with a z-step of 1.5 µm. Live imaging at high temporal resolution to track phagosomes was performed using the Zeiss Lightsheet Z.1 with a 20x detection objective, the Leica SP8 DLS and the Luxendo MuVi SPIM with a 25x detection objective, at a temporal resolution between 15 and 30 seconds. All images and videos were analysed in Fiji and Imaris.

5.6.2 LASER INDUCED INJURY

Injuries were performed using the 532 nm cutting laser attached to the FV1000 or the 355 nm cutting laser attached to the Andor Spinning Disk confocal microscope. Using the FV1000, the tornado tool was used with 40-45 % laser intensity in a ROI of 30x30 pixels. On the Spinning Disk microscope, injuries were induced using a frequency of 2500 Hz, 100 % laser intensity and 1000 pulses/point. To induce smaller injuries, the laser intensity was decreased.

5.6.3 MICROSCOPY FOR FIXED MATERIAL

Confocal analysis of fixed cells was performed using the Olympus FV1200 and Leica SP8 with a 40x/NA1.15 water objective. 0.5µm serial optical sections were collected for analysis. All images were analysed in Fiji.

5.6.4 CORRELATIVE LIGHT ELECTRON MICROSCOPY (CLEM)

My colleague Jørgen Benjaminsen performed EM and CLEM to describe the ultrastructure of the gastrosome. Here I report the methods he used both for cell culture and zebrafish embryos.

5.6.4.1 Cell culture

Cells were cultured in dishes marked with a coordinate system (MatTek, P35G-1.5-14-CGRD). At the respective time points they were chemically fixed with freshly prepared 4%

formaldehyde (FA) (Electron Microscopy Sciences, 15710) and 0.1% glutaraldehyde (GA) (Electron Microscopy Sciences, 16020) in 0.1M PHEM buffer (60mM PIPES; 25mM HEPES; 10mM EGTA: 2mM Magnesium chloride: pH 6.9). 2X fixative was added directly to the dish in a 1:1 ratio with culture medium and replaced after 5 minutes with 1x fixative. Prior to light microscopy, quenching of excess fixative was performed with 0.15 M glycine in 0.1M PHEM.

Light microscopy was carried out with cells covered with 0.1M PHEM using a FV 1200 confocal microscope (Olympus) or Axio Observer.Z1 widefield microscope with a side mounted Axio MRm camera (Zeiss). Care was taken that the MatTek dish coordinates were clearly visible in images of interest.

After imaging, samples were fixed with 2.5% GA and 4% FA in 0.1 M cacodylate buffer, followed by rinsing with 0.1 M cacodylate and post-fixation with 1% osmium tetroxide (OsO4) and 0.8% potassium ferrocyanide (K3Fe(CN)6) in water. Samples were then further rinsed with 0.1 M cacodylate buffer and stained with 1% tannic acid for 20 min on ice. The tannic acid was removed and samples rinsed with water, before staining with 1% uranyl acetate (UA) (in water), and rinsed with water. Samples were then taken through a series of dehydration steps with ethanol (EtOH) (25%, 50%, 75%, 90%, 95% and 2x100%). Finally, they were infiltrated with EPON (Serva) resin and polymerized in a 60°C oven for 48 h. All processing steps were performed using a microwave as described below, except for tannic acid incubation.

Polymerized samples were removed from the MatTek dish and the coordinate system was used to trim the resin block around the region of interest (ROI). For this an EM UC7 ultramicrotome (Leica) with an ultra 45° diamond knife (Diatome) was used to cut 70 nm sections that were placed on slot grids (Plano, G2500C). Post section contrasting was performed with 2% UA in water for 5 min and Reynolds lead citrate for 30 sec. Electron microscopy was carried out on a Biotwin CM120 electron microscope (FEI) and images acquired with a bottom mounted 1K CCD Camera (Keen View, SIS).

5.6.4.2 Zebrafish embryo

4dpf zebrafish embryos *Tg(spi1b:Gal4,UAS:RFP)* were anesthetized (0.01% tricaine) and immersed in fixative (2.5% GA and 4% FA in 0.1M PHEM buffer). Heads were immediately removed and processed in the microwave as detailed below.

Light microscopy was carried out with a FEI Corrsight prototype or 780 NLO two photon microscope (Zeiss). In both cases, a near-infrared laser was used to create artificial landmarks

(circles 20-30 µm in diameter) in the brain surrounding the cell of interest, after which a z-stack of the entire area was recorded.

Serial block-face scanning electron microscopy (SBF-SEM) sample preparation was adapted from Hua and colleagues (Hua et al., 2015). Incubation steps were performed in a microwave as detailed below. Excessive resin was removed and samples polymerized. Samples were mounted on microtome stubs (Agar Scientific, G1092450) using an EPO-TEK adhesive (Electron Microscopy Sciences, #12670-EE) and polymerized for 48 h at 60 °C. X-ray microtomography (µCT) scanning was performed in a Phoenix Nanotom m (GE Sensing & Inspection Technologies, Fairfield, CT) operating under xs control and Phoenix datos|x acquisition software (both GE Sensing & Inspection Technologies).

SBF-SEM was performed with the FEI Teneo VolumeScope (VS) and the VS plugin of the Maps software (FEI). The microscope was operated at 1.78 kV and 0.1 nA, imaging parameters used were 2.5 nanometer pixel size, with a dwell time of 100 nanoseconds and 4 times averaging, and the microtome was set to section 30 nanometer slices. Post-acquisition processing of Teneo images was performed using Fiji. A Gaussian blur, sigma 2.0 was applied for de-noising before xy scaling of 0.5 and the grayscale was inverted.

For electron microscopy on the *blb* mutant no CLEM was required as vacuoles could be detected readily by µCT or at low magnification in the electron microscope.

5.6.4.3 Biowave processing

A PELCO Biowave equipped with a ColdSpot (Ted Pella) was used for all processing steps except where stated otherwise. For the GA/FA fixation and OsO4 post-fixation the microwave was operated at 100W cycling intervals of 2 min under vacuum at room temperature. For Thiocarbohydrazide ((NH2NH)2CS) the same settings were used at 40 °C and for UA and lead aspartate (C4H5NO4Pb) at 50 °C. Quenching, rinses and dehydration were 40 sec long at 250W with no vacuum at room temperature. The resin infiltration was a 5-step-graded series of EtOH/resin followed by 2 changes of 100% resin; these steps were 3 min long at 250W under vacuum at room temperature.

5.7 LIQUID CHROMATOGRAPHY MASS SPECTROMETRY (LC-MS)

To investigate which compounds get accumulated in the *blb* zebrafish head, we performed LC-MS. To this aim, 4 dpf zebrafish embryos were anesthetized with 0.01% tricaine and decapitated with a scalpel. Heads were processed with 500 μL cold methanol and vortexed 5 min vigorously followed by sonication in ice for 10 min. Extracts were centrifuged at 3,500 rpm for 10min at 4°C and supernatant was transferred in a 2ml tube. All samples were centrifuge again at 14,000 rpm for 5 min to remove particulate matter. LC-MS was performed and analysed by the metabolomic core facility at EMBL Heidelberg (Germany).

5.8 STATISTICAL ANALYSIS

Statistical analysis was performed using the scipy.stats library (version 0.19.0) for python 2.7.11 or using Prism 7. All hypothesis tests were performed without parametric assumptions. Unless otherwise specified, conditions were compared using two-tailed Mann-Whitney U tests (scipy.stats.mannwhitneyu). The python scripts were written by Jonas Hartmann.

P Value	*Wording*	*Summary*
< 0.0001	Very highly significant	****
0.0001 to 0.001	Highly significant	***
0.001 to 0.01	Very significant	**
0.01 to 0.05	Significant	*
≥ 0.05	Not significant	ns

5.9 SOFTWARE USED

In the course of my PhD I have taken advantage of the following software:

Software	*Developer*
Fiji	
ImageJ 1.46r	NIH
Imaris 7.6.4	Bitplane
FV-ASW-2.1c	Olympus
ZEN 2012	Zeiss
Photoshop CC 2018	Adobe
Illustrator CC 2017	Adobe
Keynote	Apple
Microsoft Word	Microsoft
Microsoft Excel	Microsoft
Microsoft PowerPoint	Microsoft
Pubmed	NCBI
Ensembl Genome Browser	EMBL-EBI, Wellcome Trust Sanger Institute
Geneious	Biomatters
Papers3 for Mac	MIT
Prism 7	Graphpad

6 APPENDIX:

TOWARDS UNDERSTANDING NEURONAL-MICROGLIAL INTERACTION VIA PURINERGIC SIGNALLING

6.1 INTRODUCTION

Cell signalling is a topic of great interest for both cell and developmental biology. The ability of cells to communicate relies on an exchange of "messages" with the surrounding environment and is key for the proper functioning of tissues and organs. Importantly, individual cells can receive several distinct signals simultaneously and integrate this information into a unified action plan. Often, the same receptor can be activated by multiple ligands and these in turn can stimulate several receptors, adding extra layers of complexity to the system. As an example, in many biological contexts diffusible molecules are employed to provide directionality by forming gradients that guide motile cells towards a given location within tissues.

6.1.1 SOLUBLE CUES AND DIRECTED MIGRATION

Directed migration occurs on multiple scales, from the movement of bacteria towards a source of nutrients to the migration of microglia in the developing brain. A common base in all these mechanisms, is that the cell interprets and responds to an environmental cue to guide its migratory route. Migration of individual cells can be stimulated by a wide variety of different cues including chemicals, light, stiffness, temperature, electric fields and even gravity (Thomas et al., 2018). Most importantly, cells display tactic reaction only in response to temporal or spatial gradients.

Nearly all cells exhibit gradient senses capabilities, however prokaryotes and eukaryotes sense external gradients through different mechanisms. The firsts mainly rely on random tumbling to stochastically reach a region of higher stimulus concentration, at which point they decrease the tumbling rate (Sourjik and Wingreen, 2012). In contrast, eukaryotic cells integrate spatial and temporal information to actively sense gradients, exploiting cell surface receptors and

complex intracellular signalling pathways to measure the stimulant ligand (Devreotes and Janetopoulos, 2003; Swaney et al., 2010). In particular, the directed migration of cells in response to a chemical stimulus is known as chemotaxis, a crucial mechanism in several biological processes such as immune-cell migration, angiogenesis, haematopoiesis, neuronal development and migration of germ cells.

To date, several molecules have been shown to have chemotactic properties for eukaryotic cells, including lipids (e.g. platelet-activating factor (PAF) (Carolan and Casale, 1990)), protein fragments (e.g. C5a (Ehrengruber et al., 1994)), peptides (e.g. fMLP (Dorward et al., 2015)) and proteins (e.g. chemokines (de Oliveira et al., 2016; McDonald and Kubes, 2011)). Interestingly, chemoattractant messages are primarily transmitted through G-protein coupled receptors (GPCRs) (Murphy et al., 2000). The members of this superfamily share a seven transmembrane (7TM) architecture with an extracellular N-terminal and an intracellular C-terminus (Tuteja, 2009). The TM and extracellular protein domains are involved in ligand binding and activation of the receptor, while the intracellular loops and the C-terminus domain are involved in receptor trafficking, subcellular localization and selective coupling to heterotrimeric G-proteins (Erb and Weisman, 2012). Binding of GPCR agonists classically results in the activation of the G-protein, which consists of 3 subunits, G_α, G_β and G_γ . Upon activation, exchange of GDP to GTP is mediated by G_α and the heterotrimer dissociates into G_α-GTP and $G_{\beta\gamma}$ which will subsequentially activate a number of distinct intracellular pathways. On top of this, three main GPCR-coupled pathways can be distinguished, i.e. $G_{i/o}$, G_q and G_s. In particular, the $G_{i/o}$ modulates ion channel conductances, the G_q mediates Ca^{2+} release from intracellular stores and activates ion conductances, while the G_s pathway uses cAMP as its second messenger (Tuteja, 2009).

Among the different soluble cues identified, the class of protein-chemoattractant is surely the best characterized. One such examples, are chemokines, small vertebrate-specific proteins (~8-10 kDa), usually secreted in the extracellular space and able to trigger cellular response upon binding with a receptor. Chemokines are divided in four classes (C, CC, CXC and CX3C), based on the position of the cysteine residue within their amino acidic sequence (Zlotnik and Yoshie, 2000). Those proteins are among the most studied chemoattractant and can function both as gradients leading to directed cell migration or in a non-graded manner, as for example during the extravasation of leukocytes from the blood vessels (Girard et al., 2012).

In addition to chemokines, more recently, nucleotides have been identified as signalling molecules with very potent chemotactic properties. These molecules, behind their mostly known role for nucleic acids building blocks and energy carriers, also cover a variety of additional functions ranging from extracellular messengers to regulators of cell behaviours. In the following section, I will summarize the main aspects of nucleotides signalling, with particular attention to their receptors.

6.1.2 NUCLEOTIDE SIGNALLING AND PURINERGIC RECEPTORS

Nucleotides, in particular ATP, are well known for their function as intracellular energy source. Interestingly, those have a completely different role in the extracellular compartment, where they function as highly potent signalling molecules. The first evidence for nucleotides working as extracellular transmitters, dates back to the late '50s when sensory nerves were observed to release ATP upon stimulation (Holton, 1959). Since then, extracellular ATP has been described in several processes such as activation of ion channels (Kolb and Wakelam, 1983), neuron depolarization (Krishtal et al., 1983) and synaptic transmission (Edwards et al., 1992; Evans et al., 1992). To date, it is well known that besides serving as energy carriers for virtually all cell functions, nucleotides are also very powerful chemoattractant. Although some studies claim that ATP is not directly involved in inflammatory cell chemotaxis, but rather mediates the release of additional chemoattractants (Kronlage et al., 2010; McDonald et al., 2010), other show clear evidence for ATP and ADP functioning as true chemotactic signals (Davalos et al., 2005; Haynes et al., 2006; Honda et al., 2001). In this context, pannexins might be involved in the release of ATP from apoptotic cells (Chekeni et al., 2010). Moreover, Idzko and colleagues showed that neutrophils and mast cells migrate in response to UTP (Idzko et al., 2001).
To date, many reports showed in particular that in immune cells extracellular nucleotides signal via the activation of nucleotide receptors, referred to as purinergic P2 receptors. In contrast to the purinergic P1 receptors, which are activated by the ATP metabolite adenosine, the P2 receptors are activated by ATP and/or other nucleotides (such as UTP). P2 are further divided in two subfamilies: the metabotropic P2Y (GPCRs) and the ionotropic P2X (cation channels) receptors, which are described in the following sub-sections.

6.1.2.1 Metabotropic P2Y receptors

Among the P2R, the group of metabotropic receptors (P2YRs) consists of eight subtypes, a family of P2Y1, P2Y2, P2Y4, P2Y6, P2Y11, P2Y12, P2Y13 and P2Y14. The missing numbers represent either non-mammalian receptors (P2Y3 is the chicken orthologue of human P2Y6) or other GPCRs that share some sequence homology with P2YRs, but cannot be activated by nucleotides. Moreover, depending on the sequence and phylogenic divergence, two distinct subgroups have been proposed for P2Ys. The first group includes P2Y1/2/4/11 receptors which are characterized by a 35-52% of amino acids sequence homology and the presence of a

specific motif in the TM alpha helix 7, thus affecting ligand-binding characteristics. The second group includes P2Y12/13/14 receptors, with members sharing a sequence homology of 47-48% and, once again, the presence of a conserved motif in the TM alpha helix 7. The two groups also differ in their primary coupling to G proteins; while the first group is paired to G_q/G_{11} (leading to Ca^{2+} release), the second group binds to $G_{i/o}$ proteins (which inhibit adenylate cyclase and modulate flow through channels) (Burnstock, 2009; King and Burnstock, 2002).

The most abundant and best characterized endogenous ligand for P2YRs is ATP, which binds to all P2YRs except P2Y6 and P2Y14. At low concentrations, ATP is the only native agonist for P2Y11, but at higher concentrations it functions as partial agonist for P2Y1 and P2Y13. Other nucleotides such as ADP, UTP, UDP and UDP-sugars are more specific for individual P2Ys. For example, ADP activates P2Y1, P2Y12 and P2Y13, while UTP primarily binds P2Y2 and P2Y4 and to a lower extent to P2Y6, for which UDP is the preferred endogenous ligand. Only P2Y14 is predominantly activated by UTP-glucose (or other UTP-sugars). Thus, the ability of different nucleotides to bind specifically to individual P2YRs (Table 6.1) highlights the complexity of P2YRs signalling and suggests non-redundant signalling pathways.

On the other hand, studies on mice carrying large P2YRs deletions indicate the likelihood for some partial redundancy in the signalling system, or at least the existence of compensatory mechanisms among the different P2YRs. In fact, despite the widespread expression of these receptors, mice lacking individual P2YRs only display mild phenotypes (when maintained unchallenged in a germ-free environment).

RECEPTOR	AGONIST	G PROTEIN	MAIN EFFECTOR MOLECULES
P2Y1	ADP	$G_{q/11}$	PLC (+), Ca^{2+} release
P2Y2	ATP, UTP	$G_{q/11}$	PLC (+), Ca^{2+} release
	ATP, UTP	G_o	PLC (+), Ca^{2+} release, Rac (+)
	ATP, UTP	G_{12}	RhoA (+)
P2Y4	UTP	$G_{q/11}$	PLC (+), Ca^{2+} release
	UTP	G_o	PLC (+), Ca^{2+} release
P2Y6	UDP	$G_{q/11}$	PLC (+), Ca^{2+} release
P2Y11	ATP	$G_{q/11}$	PLC (+), Ca^{2+} release
	ATP	G_s	AC (+), increased cAMP
	UTP	G_o	PLC-independent Ca^{2+} release

P2Y12	ADP	G_i	AC (-), decreased cAMP
	ADP	$G_{12/13}$?	RhoA (+)
P2Y13	ADP	$G_{i/o}$	AC (-), decreased cAMP PLC(+),Ca^{2+} release
P2Y14	UDP-glucose	$G_{i/o}$	PLC(+),Ca^{2+} release

Table 6.1. P2Y receptor subtypes and G-protein coupling.

List of P2Y receptors and their ligand(s), associated G protein and downstream pathway. Modified from (Erb et al., 2006).

6.1.2.2 Ionotropic P2X receptors

P2XR are plasma membrane channels selective for monovalent and divalent cations (Na^+, Ca^{2+} and K^+) which are directly activated by extracellular ATP. P2XR have seven subunits that may form six homomeric (P2X1-P2X5Rs and P2X7R), and at least seven heterotrimeric (P2X1/2, P2X1/4, P2X1/5, P2X2/3, P2X2/5, P2X2/6 and P2X4/6Rs) receptors (Burnstock, 2009; King and Burnstock, 2002). Contrary to the P2YRs, the primary sequence of P2XRs has no important sequence homology with any other proteins, and among the family they share a common topology with two TM domains (TM1 and TM2), a large extracellular loop responsible for ligand binding and an intracellular N and a longer C terminus.

In contrast to P2YRs signalling, all human P2XRs have ATP as their main endogenous agonist. However, despite the shared agonist and the significant sequence homology they have little redundancy due to the fact that they come together forming homomeric and heterotrimeric receptors (Idzko et al., 2014).

In line with this, although single P2XRs knockout mice are viable and survive to adulthood, some of them reveal unexpected phenotypes, suggesting that functional roles of individual receptors subunits that can't be compensated by others. Several evidences implicate P2XRs in particular during inflammation and immune response against microbes (Coutinho-Silva and Ojcius, 2012; North and Jarvis, 2013).

6.1.3 NUCLEOTIDES AND PURINERGIC SIGNALLING IN APOPTOTIC CELL CLEARANCE: A LESSON FROM MICROGLIA

Of particular interest for this thesis, is the role of purinergic signalling in the clearance of apoptotic cells. Apoptotic engulfment is characterized by the migration of the phagocyte toward the dying cell, followed by recognition and degradation. During this process, signalling exchange between the dying cell and the phagocyte is key to ensure efficient clearance (Medina and Ravichandran, 2016). In particular, it has been shown that apoptotic cells are likely to release "long-range attraction" and "short-range interaction-protrusion" signals that allow the phagocyte to sense the damage and selectively recognize and remove the dying cells from the living-healthy tissue. Many key molecules and several pathways have been identified to orchestrate the safe disposal of apoptotic cells. Those are generally referred to as "find-me" and "eat-me" signals, and a detailed description of those, together with references, can be found in the main introduction of this thesis. Here, I would like to focus in particular on nucleotides and purinergic signalling in the context of apoptotic cell clearance (a process referred to as efferocytosis).

The release of nucleotides from dying cells and subsequent purinergic signalling play a pivotal role in efferocytosis (Elliott et al., 2009; Ravichandran, 2010; Sieger et al., 2012). During the last decade, several studies showed the fundamental role for P2YRs in this process. ATP release and concomitant P2Y2 signalling has been identified as a "find-me" signal for leukocytes, promoting phagocytic clearance of apoptotic bodies or bacteria by macrophages (Elliott et al., 2009) and neutrophils (Chen et al., 2006; 2010b), therefore contributing to the resolution of inflammation. The study from Elliot et al. showed that "small" amounts of ATP and UTP are released during early apoptosis to establish a gradient for macrophages attraction through binding with P2Y2 receptor (Elliott et al., 2009). Several other studies also confirm that binding of nucleotides to P2Y2R promotes monocyte migration by regulating adhesion molecule/chemokine expression in vascular endothelial cells (Goepfert et al., 2001; Seye et al., 2003). It has also been proposed that macrophages navigate in a gradient of the chemoattractant C5a through the release of ATP and autocrine "purinergic feedback loops" involving P2Y2 and P2Y12 receptors (Kronlage et al., 2010).

A great advance in our understanding of purinergic signalling in the removal of apoptotic cells comes from studies on microglia, the tissue resident macrophages of the brain (a detailed

description of these cell can be found in the main introduction of this thesis). Those studies showed that ATP induces chemotaxis as well as phagocytosis through P2Y12 and P2Y13 receptors and P2Y6 receptor, respectively (Davalos et al., 2005; Haynes et al., 2006; Honda et al., 2001; Koizumi et al., 2007; Sieger et al., 2012). In particular, the first study linking extracellular ATP and ADP and microglia chemotaxis with P2YRs dates back to 2001. Here, Honda and colleagues showed that membrane ruffling induced by these extracellular nucleotides and the subsequent cell migration is most likely mediated by $G_{i/o}$-coupled P2YRs, such as P2Y12 and P2Y13. Interestingly, this first study showed that although UTP induced obvious morphological changes, ruffle formation was not significant. On the other hand, adenosine (the endogenous ligand for P1 receptors) induced neither morphological change nor ruffle formation (Honda et al., 2001). Only few years later, *in vivo* studies showed that within minutes of brain damage microglial processes rapidly extend toward the injured site (Davalos et al., 2005). In particular, the chemotactic response is triggered by ATP which is released at the site of injury and the consequent activation of P2Y12 receptor on microglia (Davalos et al., 2005; Haynes et al., 2006). More recently, work from our lab has shed light on the mechanism behind nucleotide release upon laser injury, illustrating how extracellular nucleotides sensed by P2Y12 receptors induce a redistribution of microglia. By using zebrafish as a model system (see main introduction for a detailed description), we showed that, upon tissue damage, glutamate released from injured neurons induces the formation of Ca^{2+} waves via activation of N-methyl-D-aspartate (NMDA) receptors on neighbouring cells. This in turn leads to ATP release which provides a guidance for microglia in their migration towards the injury site (Figure 6.1) (Sieger et al., 2012).

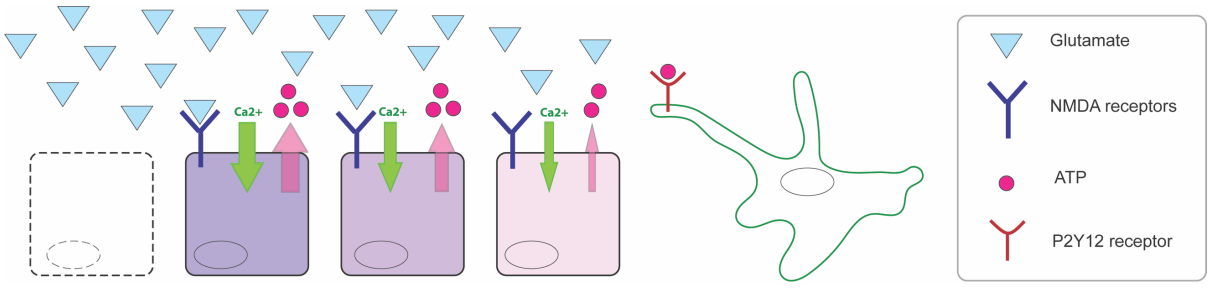

Figure 6.1. Schematic overview of the microglial response to injury.

The injured dying cells release glutamate. This, through binding to NMDA receptor on the neighbouring cells leads to an influx of Ca^{2+}, which in turn leads to release of ATP that is sensed by microglia via their P2Y12 receptor. Reproduced from (Sieger et al., 2012).

Interestingly, all these studies showed that lack of P2Y12 significantly delays but does not abolish the ability of microglia to respond to local tissue damage (Haynes et al., 2006; Koizumi et al., 2013; Sieger et al., 2012), without affecting the baseline motility (Madry and Attwell, 2015). In line with this, *in vitro* studies have shown that P2Y13 receptors might fulfil similar functions as P2Y12, suggesting a possible redundancy between those two molecules (Idzko et al., 2014; Zeng et al., 2014).

While ATP and ADP have been shown to be involved in microglia chemotaxis, work *in vitro* points to a role for UDP and its receptor P2Y6 in promoting the actual removal of dying cells. In an elegant study, Koizumi and colleagues showed that injured neurons release UTP and UDP, causing the upregulation of P2Y6R expression on microglia, and simultaneous enhancement of their phagocytic capacity for dying cells (Koizumi et al., 2007).

Specifically, microglia are reported to express several P2 receptors; P2X4 and P2X7 receptors which form ion channels, and the GPCRs P2Y2, P2Y6, P2Y12 and P2Y13. A notable characteristic of microglial P2XRs is calcium entry through the channel which is often associated with cytokine and chemokine release in the context of inflammation and bacterial removal (Burnstock, 2016; Inoue et al., 1998; Lister et al., 2007). On the other hand, as described above, microglial P2YRs have been shown to mediate efferocytosis, making those cells an interesting model to study purinergic signalling in apoptotic cell clearance. Although many studies have already established a requirement for P2YRs in this context, not much is known about their regulation in both space and time and how they induce distinct cellular activities and behaviours in microglia. Interestingly, it has been suggested that the expression of purinergic receptors is temporally regulated, i.e. upon microglial binding to ATP/ADP, P2Y12 receptors are down-regulated, while P2Y6 expression is up- regulated (Koizumi et al., 2013). Thus, while P2Y12 is involved in sensing the “long range- attraction” signal, P2Y6 might be important for subsequent steps of phagocytosis. These data suggest that distinct P2Y receptors might have different roles in engulfment of dying cells. Importantly, the functional activity and specificity of these receptors have been mainly studied by using agonist/antagonist approaches -such as ATP, Suramin, Reactive Blue-2, etc.- and generating single *knock out* mice. These approaches allowed to study end point phenotypes, however to date we still lack a mechanistic understanding of how nucleotides can elicit distinct microglial functions (Kügelgen and Hoffmann, 2015; Madry and Attwell, 2015). The ultimate goal is to understand how these receptors are controlled with spatial and temporal precision to mediate and orchestrate

microglial activities. A proper understanding of P2Ys coordination could clarify how microglia are able to communicate with each other to coordinate their activities.

6.1.4 METHODS AND TOOLS FOR THE STUDY OF GPCRS

Purinergic signalling has been shown to be involved in several pathways and therefore altered in different diseases, ranging from Cystic Fibrosis (Burnstock et al., 2012) to chronic obstructive pulmonary disease (COPD) (Lommatzsch et al., 2010) to neurodegenerative disorders, such Alzheimer's disease (AD) (Kim et al., 2012). In general, P2YRs have crucial roles in regulating immune response, becoming an obvious pharmacological target for the treatment of infectious or inflammatory diseases. Owing to their diverse modulatory functions, in general GPCRs represent one of the major drug targets in the pharmaceutical industry.

The first methods that have been developed for the control of GPCRs relied on chemical compounds, which either activate or inhibit GPCRs pathways, albeit with limited specificity. One such examples are RASSLs (Receptors Activated Solely by Synthetic Ligands), engineered receptors which lack the ability to respond to their endogenous ligand and are exclusively activated by synthetic compounds (Strader et al., 1991). Here, replacement of amino acids in the neuronal β adrenergic receptor (βAR) successfully modified its specificity. This system surely introduced a great innovation in the study of GPCRs, however still had some limitations. In particular, due to the much lower binding affinity of RASSLs compared to the native ligands, it is not clear whether the synthetic ligands might influence other proteins in the same neuronal circuit. The second generation of RASSLs has been termed DREADDS (Designer Receptors Exclusively Activated by Designer Drugs), which are GPCRs engineered to be activated exclusively by synthetic, biologically inert drugs (Armbruster et al., 2007). Those constitutes powerful tools in probing GPCRs signalling by triggering selectively individual GPCR subtypes without side effects. However, the spatiotemporal resolution *in vivo* is very low with these methods because of the slow application kinetics, washout and ligand degradation.

More recently, new approaches have been developed for controlling signalling cascades. Those allow the targeting of specific receptors and cell types and the control of GPCRs with high spatio-temporal resolution. In particular, different tools have been developed to activate GPCRs via a light stimulus that is able to penetrate tissues and cells. This method is generally referred to as optogenetics.

The first optogenetic approach to control GPCRs pathways was the chARGe system developed by Zemelman and colleagues in the early 2000 (Zemelman et al., 2002). This was based on the co-expression of three genes belonging to the Drosophila visual phototransduction cascade:

Arrestin-2, Rhodopsin and the α subunit of the cognate heterotrimeric G protein (hence the name chARGe). Here the authors reported that illumination of a mixed population of neurons elicits a response selectively in the genetically chARGed members (Zemelman et al., 2002).

Only few years later, vertebrate rhodopsin (vRh) and the green algae channelrhodopsin 2 (ChR2) have successfully been used to control neuronal excitability and modulate synaptic transmission *in vitro* and *in vivo* (Li et al., 2005). vRh has been engineered also for the study of the serotonergic (5-HT) signalling by the generation of a light-activatable GPCR that targets into 5-HT receptor domains and substitutes for endogenous receptors (Oh et al., 2010).

Moreover, the Khorana's group has demonstrated that similar goals can be achieved by the generation of chimeric receptors (Kim et al., 2005). In this study, the authors replaced the cytoplasmic loops of rhodopsin with those of the β_2-adrenergic receptor (β_2-AR) to specifically activate the signalling mediated by β_2-AR by light. Similarly, other GPCRs, such as the a1a-adrenergic receptor, have been engineered to chimeric receptors with rhodopsin (Airan et al., 2009).

More recently, Karunarathne and colleagues developed a set of optical triggers based on non-rhodopsin opsins capable of selectively modulating the activity of all three major heterotrimeric G proteins ($G_{i/o}$, G_q and G_s) in selected regions of the cell in a fast and reversible manner (Karunarathne et al., 2013).

To date, there are no reports of opto-P2YRs. However, taking an optogenetic approach to investigate P2Ys would allow testing of several key unknowns, namely if the activation of these receptors is sufficient to trigger specific cellular events such as migration and phagocytosis, if these receptors work in concert or sequentially and if their behavioural outputs depend on signalling duration and strength. In particular, the use of zebrafish as a model system, thanks to its transparency, small size and genetic accessibility, would allow the investigation of these systems *in vivo*, in a physiological-unperturbed context.

6.2 AIM OF THE PROJECT

There is no doubt that phagocytes, such as microglia, have the ability to recognize and remove apoptotic cells with great precision and that nucleotides and purinergic receptors are needed to mediate these interactions. The aim of this project is to understand how the activation of these receptors is controlled in space and time to mediate and orchestrate different microglial responses. The immediate goal is to create knock-outs for purinergic receptors such as P2Y6, P2Y12 and P2Y13 to determine their functional requirement in microglia. The second goal is to generate knock-ins for real-time visualization of receptor activity and light-mediated manipulation *in vivo*.

During my PhD, in parallel to my main thesis project (described before), I worked on these aims and I followed a combined approach to simultaneously knock out these receptors in zebrafish and introduce "landing sites" for targeted site-specific insertion at endogenous loci. These acceptor lines will be used to define loss of function phenotypes, to express novel live reporters for signal activity and to perform optical perturbations *in vivo*.
In the following sections I will describe the state of this project, including preliminary data.

6.3 RESULTS

The Peri lab has developed a system aimed at studying the removal of dying neurons by microglia in the transparent zebrafish larva. This involved the generation of transgenic lines to visualize microglia, macrophages, neurons, apoptotic neurons and the signalling systems that allow them to communicate (Casano et al., 2016; Mazaheri et al., 2014; Peri and Nüsslein-Volhard, 2008; Sieger et al., 2012). With its small dimension (400 µm wide), the zebrafish brain is a powerful model system which allows unprecedented imaging of the entire microglia network. In this context, reverse genetics to remove specific receptors of the phagocytic pathway has been essential for establishing the role of these factors in apoptotic cell clearance. For example, a previous study from our lab revealed novel and distinct functions for the surface receptors TIM4 and BAI1, previously described as general dying cell "recognition receptors" (Miyanishi et al., 2007; Park et al., 2007a). Using live imaging and reverse genetic to knock-down these two phagocytic receptors simultaneously or separately, Mazaheri and colleagues showed that while BAI1 is required for phagosome formation, TIM4 is involved in phagosome stabilization (Mazaheri et al., 2014). I intend to use a similar combination of live imaging and targeted perturbations to uncover the function of P2YRs in neuronal recognition and removal. The first aim of this project is to quantitatively define the morphology and behaviour of microglia in absence of P2YRs signalling, via the analysis and comparison of mutant phenotypes using live imaging approaches. To this aim, I followed a combined approach to simultaneously knock-out these receptors and to introduce "landing sites" for the targeted site-specific insertion at the endogenous genes. These acceptor lines will be used to determine loss of function phenotypes and to express novel live reporters of P2YRs signalling and optical perturbation tools under the endogenous transcriptional regulation.

In the following paragraphs I will present the state of this project and the preliminary results obtained so far.

6.3.1 GENERATION OF P2Y6, P2Y12 AND P2Y13 ATTB/STOP LINES

To investigate the role of purinergic receptors in the removal of dead neurons, I combined CRISPR-Cas9 genome editing and PhiC31 Integrase recombination to allow one-step generation of knock-outs and insertion of a landing site for subsequent integration in the endogenous loci. In particular, I used CRISPR-Cas9 technology to introduce a double strand break (DSB) at the beginning of the genes and to promote homology directed repair (HDR) to introduce a cassette containing STOP codons and an attB site (attB/STOP). By using the software CHOPCHOP I designed three different sgRNAs/gene directed to the sequences of interest. To test the efficiency of each sgRNA *in vivo* and select the best working one, I co-injected those in one cell stage wild type embryos together with Cas9 protein. The efficiency of the sgRNAs in introducing DSB was tested by extracting the genomic DNA of 20 randomly selected injected embryos per condition and running on an agarose gel a 100 bp PCR amplificate of the targeted region next to the same amplificate from un-injected controls. DSBs are repaired by non-homologous end joining (NHEJ) which introduces insertion and/or deletions. Those can be visualized by gel as smeared bands due to the mosaic expression of different mutations in the injected embryo. Thus, depending on the number of embryos out of the 20 randomly selected presenting a smear and therefore a DSB, I selected for each gene the most efficient sgRNA. The chosen sgRNA was co-injected with the Cas9 protein and the attB/STOP cassette containing 30bp homology arms at both sides (Figure 6.2 B). In this way, insertion of the STOP cassette will introduce stop codons regardless of the reading frame allowing the generation of knock-out lines, while the attB sequence will be used to mediate the subsequent PhiC31 integrase-mediated integration (Figure 6.2 A). Following this strategy, I obtained fish carrying the cassette -in homozygosis- in the P2Y6, P2Y12 and P2Y13 locus, respectively (Figure 6.2 C-E). Importantly, to limit as much as possible the presence of Cas9 off targets, it has been crucial to do multiple outcrossing rounds and select only the genotype of interest.

To investigate the role of different P2YRs in phagocytic microglia, these engineered lines have also been crossed into the background of several apoptotic and/or microglial reporters. Trans-heterozygotes for these mutations have also been generated and will be used to obtain double knock-outs. The current status of this project is summarized in Table 6.2.

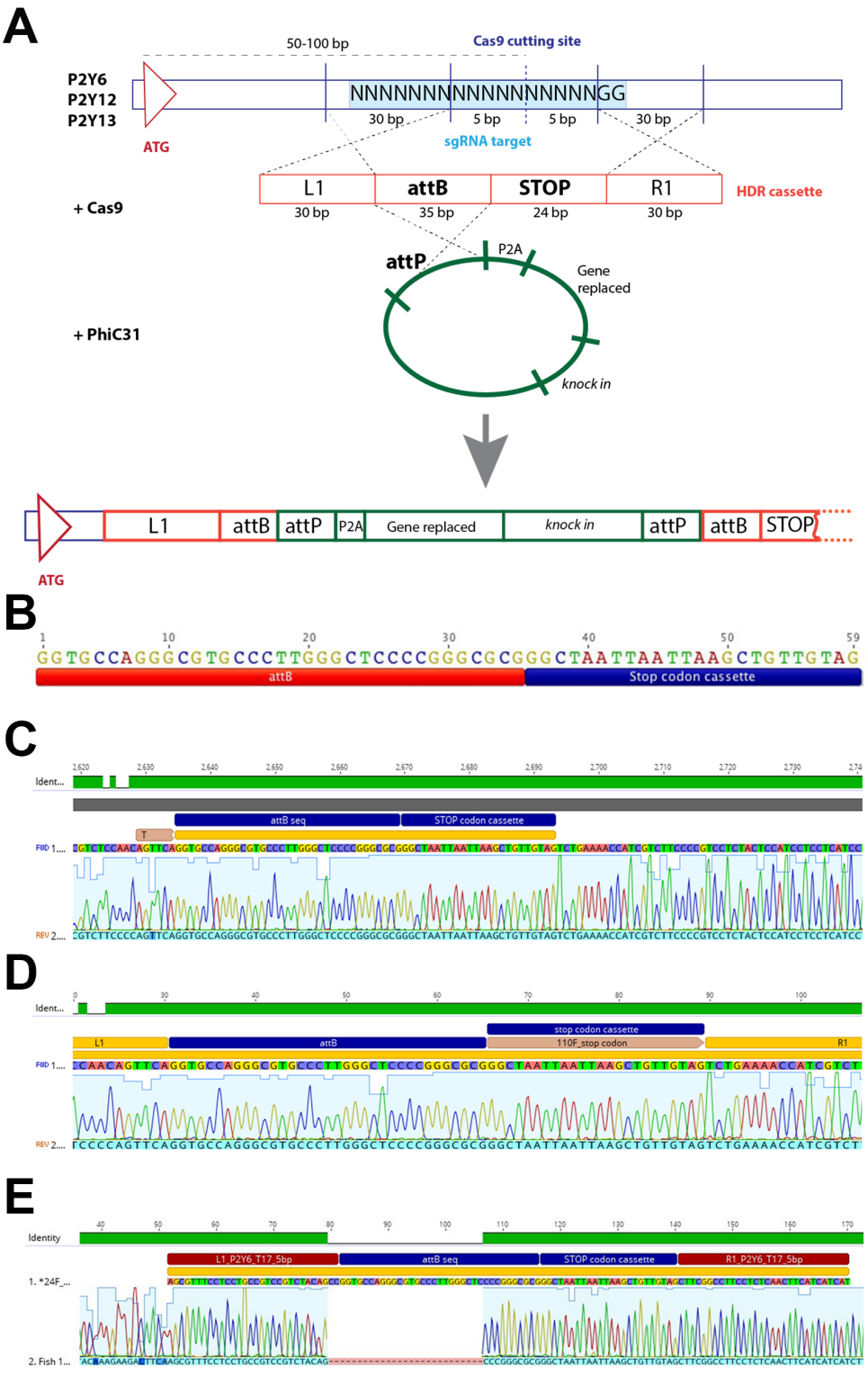

Figure 6.2. Generation of P2Ys knock-out lines containing the landing site for knock-in generation.

(**A**) CRISPR-Cas9 technology has been used for the insertion of the attB/STOP cassette in the locus of interest (50-100 bp from endogenous ATG of P2Y6, P2Y12 or P2Y13 genes). The schematic shows the strategy for the generation of knock-outs and knock-ins by the use of CRISPR-Cas9 and PhiC31 technologies.
(**B**) Sequence of the attB/STOP cassette.
(**C-E**) Alignment of homozygous P2Y12 (C), P2Y13 (D) and P2Y6 (E) to the cassette sequence (homozygous insertion of the cassette).

Genotypes obtained	*Reporters crossed with each genotype*
P2Y12 attB/STOP – homoz.	*Tg(mpeg1:eGFP)*
P2Y12 38 bp del (several stops) – heteroz.	*Tg(mpeg1:eGFP-caax)*
P2Y12 135 bp deletion – heteroz.	*Tg(NBT:secA5-BFP/RFP)*
P2Y13 attB/STOP – homoz.	*Tg(mpeg1:eGFP-caax);Tg(NBT:secA5-BFP)*
P2Y6 attb/STOP – homoz.	*Tg(NBT:dsRed)*
P2Y12 attB/STOP; P2Y6 attB/STOP	*Tg(NBT:NTR-mCherry)*
P2Y12 attB/STOP; P2Y13 attB/STOP	*Tg(mpeg1:Gal4,UAS:Kaede)*
P2Y6 attB/STOP; P2Y13 attB/STOP	*Tg(mpeg1:eGFP-caax);Tg(sp1b:Gal4,UAS:nls-Crimson)*

Table 6.2. List of the lines currently available.

On the left is a list of the available genotypes. On the right is a list of the transgenic lines which have been already crossed with each of the genotypes listed on the left.

The generation of knock-outs for these receptors allows us to investigate the role of purinergic signalling in establishing key features of microglia such as their number in the brain, phagocytic activity, rate of apoptosis and response to injury.

6.3.2 MICROGLIAL NUMBER DURING DEVELOPMENT IS AFFECTED IN PURINERGIC RECEPTORS MUTANTS

Previous work in the lab has shown that pharmacological inhibition of purinergic receptors by suramin, a broad purinergic receptors inhibitor, significantly reduces the number of microglia in the brain without affecting the level of neuronal cell death or basal motility of macrophages that are outside the brain (Casano et al., 2016). Thus, to test if P2Y6, P2Y12 or P2Y13 are directly involved in promoting microglia brain colonization, I first determined the number of microglia in the optic tectum throughout development. This was assessed in individual P2Ys mutants and wild type (from 2 to 5 dpf) by staining with Neutral red, a pH indicator which labels microglia in the brain. This experiment showed that in P2Y12 KO microglial brain colonization is delayed (Figure 6.3). Further experiments will determine whether this is a microglia specific phenotype or a secondary consequence of a delay in macrophages production and development. Surprisingly, P2Y13 KO brains are populated by a significantly higher number of microglia at 4 dpf (Figure 6.3 C). This result shines new light on the importance of P2Y13 receptor, as it is mostly considered redundant to P2Y12. On the other hand, lack of P2Y6 receptor results in a drastic reduction in number of microglia (Figure 6.3 B and C). Moreover, also in this case at 5 dpf there is a partial rescue of the phenotype (Figure 6.3 C).

Preliminary results show that the number of microglia during development is affected in the lines generated. Further experiments will be necessary to confirm these data and investigate in depth the cause of those phenotypes.

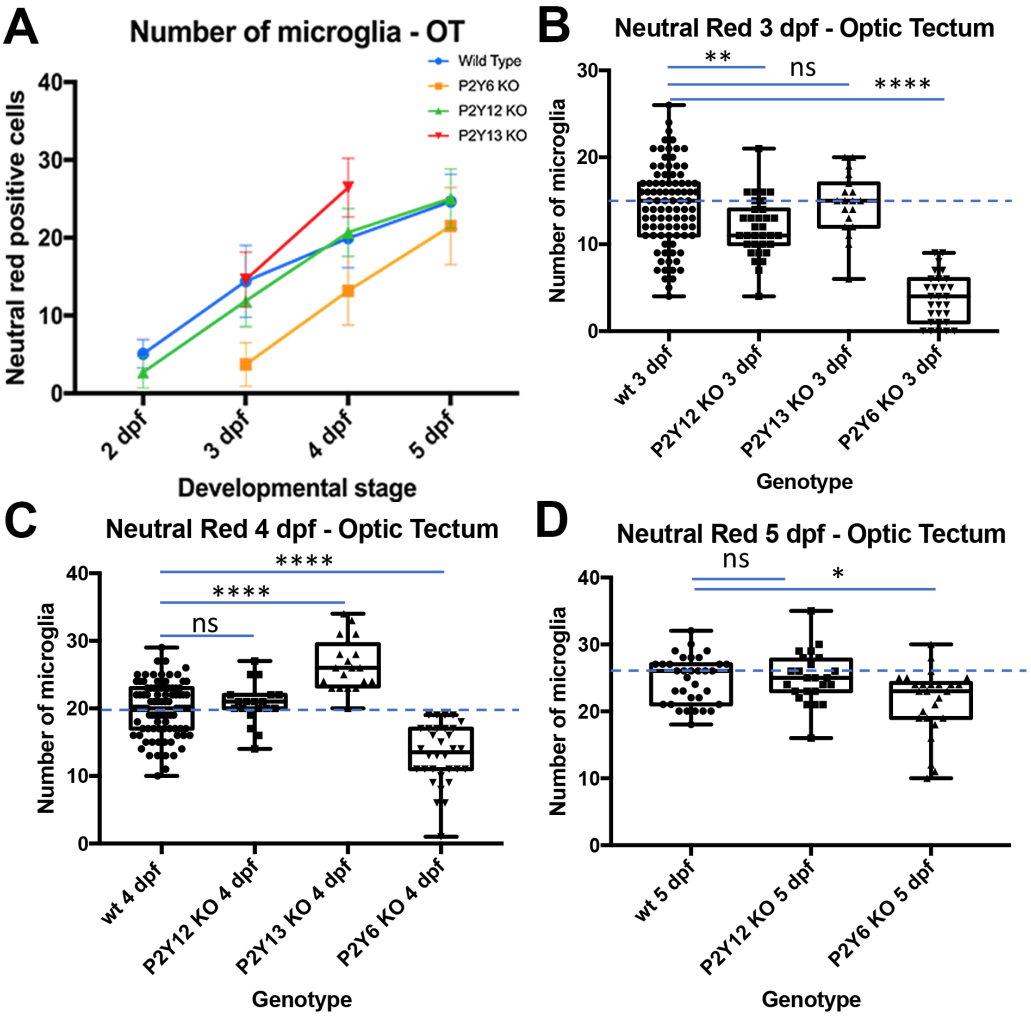

Figure 6.3. Number of microglia during development in P2Ys knock-outs and wild type.

(A-D) Number of microglia quantified by Neutral red positive staining in P2Ys knock outs and wild type during development. (A) Number of microglia throughout development in wild type (blue line), P2Y6KO (orange line), P2Y12KO (green line) and P2Y13KO (red line). (B) Wild type, P2Y12 KO, P2Y13 KO and P2Y6 KO 3 dpf. (C) Wild type, P2Y12 KO, P2Y13 KO and P2Y6 KO 4 dpf. (D) Wild type, P2Y12 KO and P2Y6 KO 5 dpf. * P value < 0.01; ** P value < 0.01; *** P value < 0.001; **** P value < 0.0001.

6.3.3 THE NUMBER OF UNCOLLECTED APOPTOTIC NUCLEI IN P2YS MUTANT REFLECTS THE NUMBER OF MICROGLIA

In the brain, quantification of uncollected apoptotic nuclei visualized by using Acridine Orange (AO) staining, can be used to determine the rate of phagocytosis in microglia. The number of dying neurons was quantified at 3 and 4 dpf in P2Y6, P2Y12, P2Y13 knock-outs and wild type. While at day 3 wild type and mutant embryos are comparable (Figure 6.4 A), at 4 dpf P2Y12 KO and P2Y6 KO have a significantly higher number of uncollected apoptotic cells (Figure 6.4 B). As I have shown that in these mutants there are also fewer microglia, simply it is possible that these defects are due to low microglia number. Further experiments are needed to determine the phagocytic rate of single microglia.

NR and AO experiments have been performed also on heterozygous mutants. The data have been analysed in an unbiased way, as genotypes were assigned only after quantification. This showed that, interestingly, heterozygous KO reflect the same tendencies as the homozygous KO for both number of microglia and level of apoptosis at the different developmental stages.

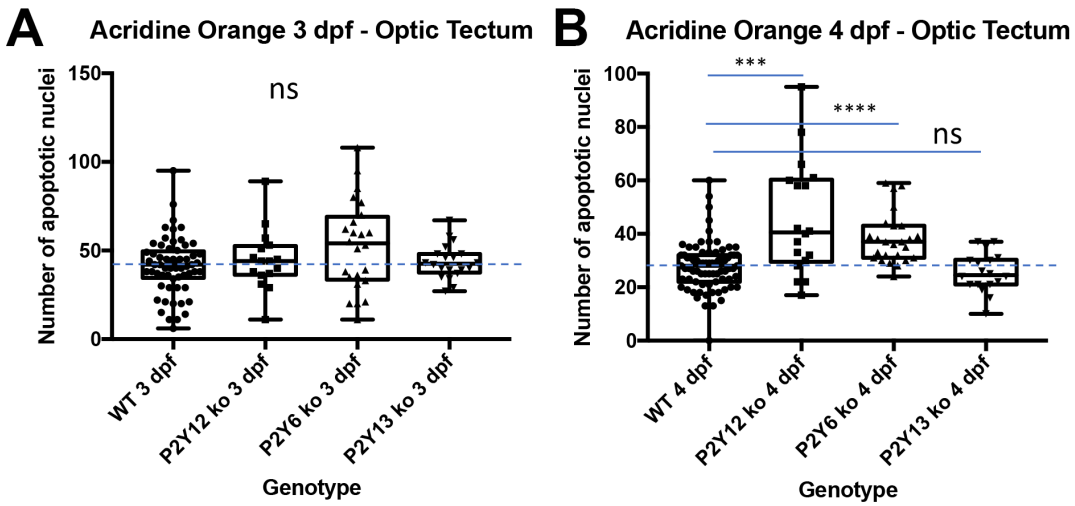

Figure 6.4. Number of apoptotic nuclei during development in P2Ys knock outs and wild type.

(**A-B**) Number of apoptotic nuclei quantified by Acridine Orange (AO) staining in P2Ys knock outs and wild type during development. (A) AO Quantification in the optic tectum, 3 dpf. (B) AO Quantification in the optic tectum, 4 dpf. * P value < 0.01; ** P value < 0.01; *** P value < 0.001; **** P value < 0.0001.

6.3.4 *P2Y12 KO MICROGLIA SHOW A DEFECT IN INJURY REACTION*

A method commonly used to study microglia migration and positioning is by ablating neurons using a pulsed laser (Davalos et al., 2005; Haynes et al., 2006; Sieger et al., 2012). Upon neuronal ablations in the living zebrafish brain microglia respond, first by polarizing their cellular branches, then by migrating toward the site of injury (Sieger et al., 2012). ATP is a key signal for promoting microglial migration. Perturbing ATP distribution (Davalos et al., 2005) or its receptor P2Y12 (Haynes et al., 2006; Sieger et al., 2012) causes a significant delay in microglial response to photo ablation.

A preliminary experiment has been performed to investigate the contribution of P2Y12 receptor in injury response. To this aim, I started with crossing heterozygote P2Y12 fish that carry the attB/STOP cassette and using a UV pulsed laser I injured the brain of their progeny (35 embryos in total). All embryos were injured at the midline and imaged after 2 hours to visualize microglial migration to the site of injury. After imaging, genomic DNA was extracted for genotyping. To analyse microglial reaction to the injury, I defined three classes (1-3) depending on the phenotype:

1. Less than two microglia reacted to the injury
2. At least two microglia reacted to the injury, but in an unorganized way
3. More than 3 microglia reacted to the injury, creating a circumference around the damaged tissue

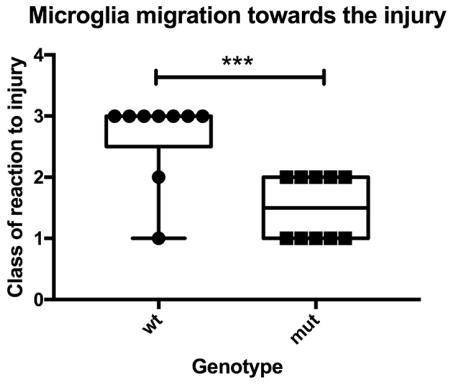

Figure 6.5. Classification of the reaction to injury in P2Y12 knock-out compared to wild type.

Microglia migration towards UV laser ablation in the middle of the brain is impaired in P2Y12 KO embryos.

Interestingly, microglia of knock-outs have a significant reduced reaction to injury when compared to wild type embryos (Figure 6.5). This encouraging preliminary result confirmed the role of P2Y12 in mediating microglial responses to injury.

Further experiments will investigate the contribution of different purinergic receptors in response to an injury. Quantification of the percentage of microglia reacting to the neuronal ablation and of the time and space covered during microglia migration will determine the role of each P2YR in this process.

6.4 OUTLOOK

In recent years microglia have emerged as multitasking specialist of the brain that interact with the local neuronal environment to promote its development and connectivity. A key function of microglia is the removal of dying neurons, both in response to brain damage, when they promote repair and during development, when they contribute to shaping neuronal activity (Loane and Kumar, 2016; Neumann, 2013). Lack of microglia has been shown to severely compromise proper brain functionality, particularly affecting individual behaviour and learning skills (Chen et al., 2010a; Loane and Kumar, 2016), further highlighting how presence and proper activity of those cells are essential for guaranteeing brain homeostasis.

A proper understanding of how microglia are able to recognize their target and distinguish it from healthy tissue is key to be able to manipulate their activity.

Purinergic receptors expressed on microglia bind nucleotides released by apoptotic and damaged cells guiding the phagocyte in the site of death. Release of different nucleotides activate other purinergic receptors which mediate the actual engulfment of the target. Given that directed migration and target engulfment both involve similar changes in cell morphology and cytoskeletal organization (Erb and Weisman, 2012), and engage an overlapping set of effectors, it is clear that these processes must be coordinated via cellular feedback mechanisms. The finding that these behaviours in microglia appear to be controlled by distinct GPCRs offers a unique opportunity to investigate this interplay by developing robust reporters for monitoring the activity of P2Y receptors *in vivo*.

The generation of knock outs for P2Y6, P2Y12 and P2Y13 (P2YRs that are known to be expressed on microglia) allows the study first of all their loss-of-function phenotypes alone and in combination. The results obtained so far show that all individual knock-outs have phenotypes in terms of microglial numbers and phagocytic activity in the developing brain. Interestingly, preliminary observations showed that P2Y12 mutant embryos have microglia with normal morphology that however fail to respond to neuronal injuries induced by using a UV-pulsed laser. On the other hand, microglia lacking P2Y6 have an aberrant round morphology that is often indicative of phagocytic defects (Figure 6.6). Further experiments are needed to characterize in more depth these phenotypes focusing in particular on basal surveillance of microglia, phagocytic activity and ability to respond to injury.

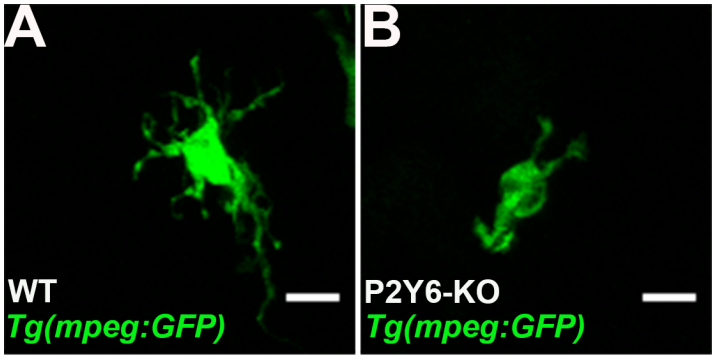

Figure 6.6. Microglia morphology is affected in P2Y6 knock-outs.

(**A and B**) Microglia cells labelled with *Tg(mpeg1:eGFP)* in 3 dpf wild type (A) and P2Y6 KO (B) embryos. Scale bar 10 µm.

One key question is whether the controlled activation of these receptors is sufficient to trigger microglial key behaviours -such as directed migration and engulfment- "at will". The homozygous knock-out lines contain the attB site that can be used to generate knock-ins. These acceptor lines will be used to express live reporter of P2Y signalling and optical perturbation tools under endogenous transcriptional regulation.

6.4.1 SPATIOTEMPORAL DISSECTION OF P2Y SIGNALLING IN MICROGLIA

One key aim of this project is the development of robust *in vivo* reporters for P2Y signalling. A direct readout for GPCRs activity takes advantage of the fact that those receptors undergo internalization and recycling upon ligand binding. For example, by labelling the platelet P2Y12 receptor Nisar and colleagues showed that the C-terminus of this receptor is essential to ensure its correct traffic, internalization and recycling necessary to maintain its responsiveness *in vitro* (Nisar et al., 2011). Similarly, live imaging of P2YRs tagged with fluorescent proteins through PhiC31 integration can provide a live reporter for studying P2YRs dynamics during microglial phagocytosis and migration. The introduction of fluorescent reporters in the endogenous locus will allow us to investigate the localization, expression and turnover of distinct P2YRs *in vivo*.

Furthermore, a reliable readout for GPCRs signalling and dynamics is the use of the recently developed tandem fluorescent protein timers (tFTs) (Barry et al., 2016; Donà et al., 2013). Here, tandem fusions of two fluorescent proteins with different maturation kinetics provide a ratiometric visualization of protein synthesis and turnover in living animals. In the case of GPCRs, ligand-triggered receptor internalization results in low red/green ratios due to high receptor turnover. This approach was successfully used to monitor chemokine signalling during the migration of the zebrafish lateral line (Donà et al., 2013). Tagging the microglial purinergic receptors with optimized tFTs will allow signalling-triggered receptor turnover to be monitored *in vivo*. By taking advantage of these approaches we will correlate the activation of the receptor with distinct cellular responses and activities in response to neuronal cell death.

6.4.2 OPTOGENETIC APPROACHES TO INVESTIGATE P2YRS FUNCTIONS IN MICROGLIA

The development of methods to precisely control cellular processes using light has the potential to revolutionize the way we address complex biological problems. Indeed, whereas previously we mainly relied on loss-of-function phenotypes to study gene function, now we can use light to switch on and off molecules in a spatial and temporal controlled manner. Taking an optogenetic approach (Idevall-Hagren et al., 2012; Karunarathne et al., 2013) to investigate P2YRs will allow testing of several key unknowns, namely if the activation of these receptors is sufficient to trigger specific cellular events such as migration and phagocytosis, if these receptors work in concert or sequentially and if their behavioural outputs depend on signalling duration and strength. In particular, we will pursue several overlapping approaches to place P2YRs signalling under light-regulated control, such as the use of rhodopsin to engineer P2YRs or for the generation of chimeric receptors (Airan et al., 2009; Kim et al., 2005; Li et al., 2005; Oh et al., 2010). An alternative optogenetic approach uses members of the opsin family of GPCR light-sensors to activate the same downstream G-proteins as specific receptors of interest (Karunarathne et al., 2013).

The use of optogenetics will allow us to probe how microglia respond to P2YRs activation/de-activation and their mode of action during phagocytosis. Combining optogenetic manipulation of P2Y signalling with the quantitative behavioural assays and live activity reporters described above will significantly advance our understanding microglial-neuronal interactions.

7 REFERENCES

Abrams, J.M., White, K., Fessler, L.I., and Steller, H. (1993). Programmed cell death during Drosophila embryogenesis. Development 117, 29–43.

Airan, R.D., Thompson, K.R., Fenno, L.E., Bernstein, H., and Deisseroth, K. (2009). Temporally precise in vivo control of intracellular signalling. Nature 458, 1025–1029.

Amatruda, J.F., Shepard, J.L., Stern, H.M., and Zon, L.I. (2002). Zebrafish as a cancer model system. Cancer Cell 1, 229–231.

Armbruster, B.N., Li, X., Pausch, M.H., Herlitze, S., and Roth, B.L. (2007). Evolving the lock to fit the key to create a family of G protein-coupled receptors potently activated by an inert ligand. PNAS 104, 5163–5168.

Arnò, B., Grassivaro, F., Rossi, C., Bergamaschi, A., Castiglioni, V., Furlan, R., Greter, M., Favaro, R., Comi, G., Becher, B., et al. (1AD). Neural progenitor cells orchestrate microglia migration and positioning into the developing cortex. Nature Communications 5, 1–13.

Arur, S., Uche, U.E., Rezaul, K., Fong, M., Scranton, V., Cowan, A.E., Mohler, W., and Han, D.K. (2003). Annexin I Is an Endogenous Ligand that Mediates Apoptotic Cell Engulfment. Developmental Cell 4, 587–598.

Ashwell, K. (1990). Microglia and cell death in the developing mouse cerebellum. Developmental Brain Research 55, 219–230.

Barkal, A.A., Weiskopf, K., Kao, K.S., Gordon, S.R., Rosental, B., Yiu, Y.Y., George, B.M., Markovic, M., Ring, N.G., Tsai, J.M., et al. (2018). Engagement of MHC class I by the inhibitory receptor LILRB1 suppresses macrophages and is a target of cancer immunotherapy. Nat Immunol 19, 76–84.

Barres, B.A., Hart, I.K., Coles, H.S.R., Burne, J.F., Voyvodic, J.T., Richardson, W.D., and Raff, M.C. (1992). Cell Death in the Oligodendrocyte Lineage. Journal of Neurobiology 23, 1221–1230.

Barry, J.D., Donà, E., Gilmour, D., and Huber, W. (2016). TimerQuant: a modelling approach to tandem fluorescent timer design and data interpretation for measuring protein turnover in embryos. Development 143, 174–179.

Bartoloni, L., and Antonarakis, S.E. (2004). The human sugar-phosphate/phosphate exchanger family SLC37. Pflugers Arch. 447, 780–783.

Bedell, V.M., Westcot, S.E., and Ekker, S.C. (2011). Lessons from morpholino-based screening in zebrafish. Briefings in Functional Genomics 10, 181–188.

Beers, D.R., Henkel, J.S., Xiao, Q., Zhao, W., Wang, J., Yen, A.A., Siklos, L., McKercher, S.R., and Appel, S.H. (2006). Wild-type microglia extend survival in PU.1 knockout mice with familial amyotrophic lateral sclerosis. PNAS 103, 16021–16026.

Bennett, M.L., Bennett, F.C., Liddelow, S.A., Ajami, B., Zamanian, J.L., Fernhoff, N.B., Mulinyawe, S.B., Bohlen, C.J., Adil, A., Tucker, A., et al. (2016). New tools for studying microglia in the mouse and human CNS. PNAS 113, E1738–E1746.

Berg, R.D., Levitte, S., O'Sullivan, M.P., O'Leary, S.M., Cambier, C.J., Cameron, J., Takaki, K.K., Moens, C.B., Tobin, D.M., Keane, J., et al. (2016). Lysosomal Disorders Drive Susceptibility to Tuberculosis by Compromising Macrophage Migration. Cell 165, 139–152.

Bin He, Yu, X., Margolis, M., Liu, X., Leng, X., Etzion, Y., Zheng, F., Lu, N., Quiocho, F.A., Danino, D., et al. (2010). Live-Cell Imaging in Caenorhabditis elegans Reveals the Distinct Roles of Dynamin Self-Assembly and Guanosine Triphosphate Hydrolysis in the Removal of Apoptotic Cells. Molecular Biology of the Cell 21, 610–629.

Bissa, B., Beedle, A.M., and Govindarajan, R. (2016). Lysosomal solute carrier transporters gain momentum in research. Clin. Pharmacol. Ther. 100, 431–436.

Bohlen, C.J., Bennett, F.C., Tucker, A.F., Collins, H.Y., Mulinyawe, S.B., and Barres, B.A. (2017). Diverse Requirements for Microglial Survival, Specification, and Function Revealed by Defined-Medium Cultures. Neuron 94, 759–773.

Boulais, J., Trost, M., Landry, C.R., Dieckmann, R.E.G., Levy, E.D., Soldati, T., Michnick, S.W., Thibault, P., and Desjardins, M. (2010). Molecular characterization of the evolution of phagosomes. Molecular Systems Biology 6, 1–14.

Boyden, E.S., Zhang, F., Bamberg, E., Nagel, G., and Deisseroth, K. (2005). Millisecond-timescale, genetically targeted optical control of neural activity. Nat Neurosci 8, 1263–1268.

Bray, D. (2001). Cell Movements: From Molecules to Motility (Garland Pub.).

Brightwell, R.M., Grzankowski, K.S., Lele, S., Eng, K., Arshad, M., Chen, H., and Odunsi, K. (2016). The CD47 "don't eat me signal" is highly expressed in human ovarian cancer. Gynecologic Oncology 1–5.

Brown, S., Heinisch, I., Ross, E., Shaw, K., Buckley, C.D., and Savill, J. (2002). Apoptosis disables CD31-mediated cell detachment from phagocytes promoting binding and engulfment. Nature 418, 200–203.

Burnstock, G. (2009). Purinergic signalling: past, present and future. Brazilian Journal of Medical and Biological Research 42, 3–8.

Burnstock, G. (2016). P2X ion channel receptors and inflammation. Purinergic Signalling 12, 59–67.

Burnstock, G., Brouns, I., Adriaensen, D., and Timmermans, J.-P. (2012). Purinergic signaling in the airways. Pharmacol. Rev. 64, 834–868.

Campbell-Valois, F.-X., Trost, M., Chemali, M., Dill, B.D., Laplante, A., Duclos, S., Sadeghi, S., Rondeau, C., Morrow, I.C., Bell, C., et al. (2012). Quantitative Proteomics Reveals That Only a Subset of the Endoplasmic Reticulum Contributes to the Phagosome. Mol Cell Proteomics 11, M111.016378–13.

Cardoso, C.M.P., Jordao, L., and Vieira, O.V. (2010). Rab10 Regulates Phagosome Maturation and Its Overexpression Rescues Mycobacterium-Containing Phagosomes Maturation. Traffic 11, 221–235.

Carolan, E.J., and Casale, T.B. (1990). Degree of platelet activating factor-induced neutrophil migration is dependent upon the molecular species. The Journal of Immunology 145, 2561–2565.

Casano, A.M., and Peri, F. (2015). Microglia: Multitasking Specialists of the Brain. Developmental Cell 32, 469–477.

Casano, A.M., Albert, M., and Peri, F. (2016). Developmental Apoptosis Mediates Entry and Positioning of Microglia in the Zebrafish Brain. CellReports 16, 897–906.

César-Razquin, A., Snijder, B., Frappier-Brinton, T., Isserlin, R., Gyimesi, G., Bai, X., Reithmeier, R.A., Hepworth, D., Hediger, M.A., Edwards, A.M., et al. (2015). A Call for Systematic Research on Solute Carriers. Cell 162, 478–487.

Chekeni, F.B., Elliott, M.R., Sandilos, J.K., Walk, S.F., Kinchen, J.M., Lazarowski, E.R., Armstrong, A.J., Penuela, S., Laird, D.W., Salvesen, G.S., et al. (2010). Pannexin 1 channels mediate "find-me" signal release and membrane permeability during apoptosis. Nature 467, 863–867.

Chen, S.-K., Tvrdik, P., Peden, E., Cho, S., Wu, S., Spangrude, G., and Capecchi, M.R. (2010a). Hematopoietic Origin of Pathological Grooming in Hoxb8 Mutant Mice. Cell 141, 775–785.

Chen, Y., and Zhao, X. (1998). Shaping Limbs by Apoptosis. The Journal of Experimental Zoology 282, 691–702.

Chen, Y., Corriden, R., Inoue, Y., Yip, L., Hashiguchi, N., Zinkernagel, A., Nizet, V., Insel, P.A., and Junger, W.G. (2006). ATP release guides neutrophil chemotaxis via P2Y2 and A3 receptors. Science 314, 1792–1795.

Chen, Y., Yao, Y., Sumi, Y., Li, A., To, U.K., Elkhal, A., Inoue, Y., Woehrle, T., Zhang, Q., Hauser, C., et al. (2010b). Purinergic signaling: a fundamental mechanism in neutrophil activation. Sci Signal 3, ra45–ra45.

Chou, J.Y., Jun, H.S., and Mansfield, B.C. (2010a). Neutropenia in type Ib glycogen storage disease. Current Opinion in Hematology 17, 36–42.

Chou, J.Y., Jun, H.S., and Mansfield, B.C. (2010b). Glycogen storage disease type I and G6Pase-β deficiency: etiology and therapy. Nat Rev Endocrinol 6, 676–688.

Chou, J.Y., Sik Jun, H., and Mansfield, B.C. (2013). The SLC37 family of phosphate-linked sugar phosphate antiporters. Molecular Aspects of Medicine 34, 601–611.

Claessens, M.M.A.E., Leermakers, F.A.M., Hoekstra, F.A., and Stuart, M.A.C. (2008). Osmotic shrinkage and reswelling of giant vesicles composed of dioleoylphosphatidylglycerol and cholesterol. Biochimica Et Biophysica Acta (BBA) - Biomembranes 1778, 890–895.

Cole, L.K., and Ross, L.S. (2001). Apoptosis in the Developing Zebrafish Embryo. Developmental Biology 240, 123–142.

Coutinho-Silva, R., and Ojcius, D.M. (2012). Role of extracellular nucleotides in the immune response against intracellular bacteria and protozoan parasites. Microbes Infect. 14, 1271–1277.

Cowan, W.M., OLeary, J.W.F.D.D.M., and Stanfield, B.B. (1984). Regressive Events in Neurognesis. Science 225, 1258–1265.

Cox, D., Lee, D.J., Dale, B.M., Calafat, J., and Greenberg, S. (2000). A Rab11-containing rapidly recycling compartment in macrophages that promotes phagocytosis. PNAS 97, 680–685.

Cuadros, M.A., Martin, C., Coltey, P., Almendros, A., and Navascués, J. (1993). First Appearance, Distribution, and Origin of Macrophages in the Early Development of the Avian Central Nervous System. The Journal of Comparative Neurology 330, 113–129.

Cullen, P.J., and Korswagen, H.C. (2012). Sorting nexins provide diversity for retromer-dependent trafficking events. Nat Cell Biol 14, 29–37.

Dalmau, I., Finsen, B., Tønder, N., Zimmer, J., González, B., and Castellano, B. (1997). Development of Microglia in the Prenatal Rat Hippocampus. The Journal of Comparative Neurology 377, 70–84.

Damiani, M.T., Pavarotti, M., Leiva, N., Lindsay, A.J., McCaffrey, M.W., and Colombo, M.I. (2004). Rab Coupling Protein Associates with Phagosomes and Regulates Recycling from the Phagosomal Compartment. Traffic 5, 785–797.

Darland-Ransom, M., Wang, X., Sun, C.-L., Mapes, J., Gengyo-Ando, K., Mitani, S., and Xue, D. (2008). Role of C. elegans TAT-1 Protein in Maintaining Plasma Membrane Phosphatidylserine Asymmetry. Science 320, 528–531.

Davalos, D., Grutzendler, J., Yang, G., Kim, J.V., Zuo, Y., Jung, S., Littman, D.R., Dustin, M.L., and Gan, W.-B. (2005). ATP mediates rapid microglial response to local brain injury in vivo. Nat Neurosci 8, 752–758.

Davies, L.C., Jenkins, S.J., Allen, J.E., and Taylor, P.R. (2013). Tissue-resident macrophages. Nat Immunol 14, 986–995.

de Oliveira, S., Rosowski, E.E., and Huttenlocher, A. (2016). Neutrophil migration in infection and wound repair: going forward in reverse. Nat Rev Immunol 16, 378–391.

De Paepe, M.E., Mao, Q., Embree-Ku, M., Rubin, L.P., and Luks, F.I. (2004). Fas/FasL-mediated apoptosis in perinatal murine lungs. American Journal of Physiology-Lung Cellular and Molecular Physiology 287, L730–L742.

Devitt, A., Moffatt, O.D., Raykundalia, C., Capra, J.D., Simmons, D.L., and Gregory, C.D. (1998). Human CD14 mediates recognition and phagocytosis of apoptotic cells. Nature 392, 505–509.

Devreotes, P., and Janetopoulos, C. (2003). Eukaryotic chemotaxis: distinctions between directional sensing and polarization. J. Biol. Chem. 278, 20445–20448.

Donat, C.K., Scott, G., Gentleman, S.M., and Sastre, M. (2017). Microglial Activation in Traumatic Brain Injury. Front. Aging Neurosci. 9, 149–20.

Donà, E., Barry, J.D., Valentin, G., Quirin, C., Khmelinskii, A., Kunze, A., Durdu, S., Newton, L.R., Fernandez-Minan, A., Huber, W., et al. (2013). Directional tissue migration through a self-generated chemokine gradient. Nature 503, 285–289.

Dooley, K., and Zon, L.I. (2000). Zebrafish: a model system for the study of human disease. Current Opinion in Genetics Development 10, 252–256.

Dorward, D.A., Lucas, C.D., Chapman, G.B., Haslett, C., Dhaliwal, K., and Rossi, A.G. (2015). The role of formylated peptides and formyl peptide receptor 1 in governing neutrophil function during acute inflammation. The American Journal of Pathology 185, 1172–1184.

Doyon, Y., McCammon, J.M., Miller, J.C., Faraji, F., Ngo, C., Katibah, G.E., Amora, R., Hocking, T.D., Zhang, L., Rebar, E.J., et al. (2008). Heritable targeted gene disruption in zebrafish using designed zinc-finger nucleases. Nat Biotechnol 26, 702–708.

Driever, W., Solnica-Krezel, L., Schier, A.F., Neuhauss, S.C.F., Malicki, J., Stemple, D.L., Stainier, D.Y.R., Zwartkruis, F., Abdelilah, S., Rangini, Z., et al. (1996). A genetic screen for mutations affecting embryogenesis in zebrafish. Development 123, 37–46.

Duclos, S., Clavarino, G., Rousserie, G., Goyette, G., Boulais, J., Camossetto, V., Gatti, E., LaBoissière, S., Pierre, P., and Desjardins, M. (2011). The endosomal proteome of macrophage and dendritic cells. Proteomics 11, 854–864.

Edwards, F.A., Gibb, A.J., and Colquhoun, D. (1992). ATP receptor-mediated synaptic currents in the central nervous system. Nature 359, 144–147.

Ehrengruber, M.U., Geiser, T., and Deranleau, D.A. (1994). Activation of human neutrophils by C3a and C5A. Comparison of the effects on shape changes, chemotaxis, secretion, and respiratory burst. FEBS Lett. 346, 181–184.

Eimon, P.M., and Ashkenazi, A. (2010). The zebrafish as a model organism for the study of apoptosis. Apoptosis 15, 331–349.

Ekdahl, C.T., Claasen, J.-H., Bonde, S., Kokaia, Z., and Lindvall, O. (2003). Inflammation is detrimental for neurogenesis in adult brain. PNAS 100, 13632–13637.

Ellett, F., Pase, L., Hayman, J.W., Andrianopoulos, A., and Lieschke, G.J. (2011). mpeg1 promoter transgenes direct macrophage-lineage expression in zebrafish. Blood 117, e49–e56.

Elliott, M.R., and Ravichandran, K.S. (2010). Clearance of apoptotic cells: implications in health and disease. J Cell Biol 189, 1059–1070.

Elliott, M.R., and Ravichandran, K.S. (2016). The Dynamics of Apoptotic Cell Clearance. Developmental Cell 38, 147–160.

Elliott, M.R., Chekeni, F.B., Trampont, P.C., Lazarowski, E.R., Kadl, A., Walk, S.F., Park, D., Woodson, R.I., Ostankovich, M., Sharma, P., et al. (2009). Nucleotides released by apoptotic cells act as a find-me signal to promote phagocytic clearance. Nature 461, 282–286.

Elliott, T., and Shadbolt, N.R. (1998). Competition for Neurotrophic Factors: Ocular Dominance Columns. J. Neurosci. 18, 5850–5858.

Ellis, H.M., and Horvitz, H.R. (1986). Genetic Control of Programmed Cell Death in the Nematode C. elegans. Cell 44, 817–829.

Elmore, S. (2007). Apoptosis: A Review of Programmed Cell Death. Toxicol Pathol. 35, 495–516.

Erb, L., and Weisman, G.A. (2012). Coupling of P2Y receptors to G proteins and other signaling pathways. WIREs Membr Transp Signal 1, 789–803.

Erb, L., Liao, Z., Seye, C.I., and Weisman, G.A. (2006). P2 receptors: intracellular signaling. Pflugers Arch. 452, 552–562.

Erblich, B., Zhu, L., Etgen, A.M., Dobrenis, K., and Pollard, J.W. (2011). Absence of Colony Stimulation Factor-1 Receptor Results in Loss of Microglia, Disrupted Brain Development and Olfactory Deficits. PLoS ONE 6, e26317–13.

Ethell, D.W., and Buhler, L.A. (2003). Fas Ligand-Mediated Apoptosis in Degenerative Disorders of the Brain. Journal of Clinical Immunology 23, 363–370.

Evans, R.J., Derkach, V., and Surprenant, A. (1992). ATP mediates fast synaptic transmission in mammalian neurons. Nature 357, 503–505.

Fadok, V.A., Voelker, D.R., Campbell, P.A., Cohen, J.J., Bratton, D.L., and Henson, P.M. (1992). Exposure of phosphatidylserine on the surface of apoptotic lymphocytes triggers specific recognition and removal by macrophages. The Journal of Immunology 148, 2207–2216.

Fadok, V.A., Bratton, D.L., Frasch, S.C., Warner, M.L., and Henson, P.M. (1998a). The role of phosphatidylserine in recognition of apoptotic cells by phagocytes. Cell Death and Differentiation 5, 551–562.

Fadok, V.A., Bratton, D.L., Konowal, A., Freed, P.W., Westcott, J.Y., and Henson, P.M. (1998). Macrophages That Have Ingested Apoptotic Cells In Vitro Inhibit Proinflammatory Cytokine Production Through Autocrine/Paracrine Mechanisms Involving TGF-B, PGE2, and PAF. J. Clin. Invest. 101, 890–898.

Fairn, G.D., and Grinstein, S. (2012). How nascent phagosomes mature to become phagolysosomes. Trends in Immunology 33, 397–405.

Fiorotto, R., Villani, A., Kourtidis, A., Scirpo, R., Ameduni, M., Geibel, P.J., Cadamuro, M., Spirli, C., Anastasiadis, P.Z., and Strazzabosco, M. (2016). The Cystic Fibrosis Transmembrane

Conductance Regulator Controls Biliary Epithelial Inflammation and Permeability by Regulating Src Tyrosine Kinase Activity. Hepatology 64, 2118–2134.

Flannagan, R.S., Jaumouillé, V., and Grinstein, S. (2012). The Cell Biology of Phagocytosis. Annu. Rev. Pathol. Mech. Dis. 7, 61–98.

Fratti, R.A., Backer, J.M., Gruenberg, J., Corvera, S., and Deretic, V. (2001). Role of phosphatidylinositol 3-kinase and Rab5 effectors in phagosomal biogenesis and mycobacterial phagosome maturation arrest. J Cell Biol 154, 631–644.

Frost, J.L., and Schafer, D.P. (2016). Microglia: Architects of the Developing Nervous System. Trends in Cell Biology 26, 587–597.

Gaipl, U.S., Franz, S., Voll, R.E., Sheriff, A., Kalden, J.R., and Herrmann, M. (2004). Defects in the Disposal of Dying Cells Lead to Autoimmunity. Current Rheumatology Reports 6, 401–407.

Gardai, S.J., McPhillips, K.A., Frasch, S.C., Janssen, W.J., Starefeldt, A., Murphy-Ullrich, J.E., Bratton, D.L., Oldenborg, P.-A., Michalak, M., and Henson, P.M. (2005). Cell-Surface Calreticulin Initiates Clearance of Viable or Apoptotic Cells through trans-Activation of LRP on the Phagocyte. Cell 123, 321–334.

Garin, J., Diez, R., Kieffer, S., Dermine, J.-F., Duclos, S., Gagnon, E., Sadoul, R., Rondeau, C., and Desjardins, M. (2001). The Phagosome Proteome: Insight into Phagosome Functions. J Cell Biol 152, 165–180.

Gerbod-Giannone, M.-C., Li, Y., Holleboom, A., Han, S., Hsu, L.-C., Tabas, I., and Tall, A.R. (2006). TNFα induces ABCA1 through NF-κB in macrophages and in phagocytes ingesting apoptotic cells. PNAS 103, 3112–3117.

Ginhoux, F., Greter, M., Leboeuf, M., Nandi, S., See, P., Gokhan, S., Mehler, M.F., Conway, S.J., Ng, L.G., Stanley, E.R., et al. (2010). Fate Mapping Analysis Reveals That Adult Microglia Derive from Primitive Macrophages. Science 330, 841–845.

Ginhoux, F., Lim, S., Hoeffel, G., Low, D., and Huber, T. (2013). Origin and differentiation of microglia. Front. Cell. Neurosci. 7, 1–14.

Girard, J.-P., Moussion, C., and Förster, R. (2012). HEVs, lymphatics and homeostatic immune cell trafficking in lymph nodes. Nat Rev Immunol 12, 762–773.

Glücksmann, A. (1951). Cell Death in Normal vertebrate Ontogeny. Biol Rev 59–86.

Goepfert, C., Sundberg, C., Sévigny, J., Enjyoji, K., Hoshi, T., Csizmadia, E., and Robson, S. (2001). Disordered cellular migration and angiogenesis in cd39-null mice. Circulation 104, 3109–3115.

Gomez Perdiguero, E., Klapproth, K., Schulz, C., Busch, K., Azzoni, E., Crozet, L., Garner, H., Trouillet, C., de Bruijn, M.F., Geissmann, F., et al. (2014). Tissue-resident macrophages originate from yolk-sac-derived erythro-myeloid progenitors. Nature 518, 547–551.

Gomez-Nicola, D., and Perry, V.H. (2015). Microglial dynamics and role in the healthy and diseased brain: a paradigm of functional plasticity. Neuroscientist 21, 169–184.

Gordon, S. (2008). Elie Metchnikoff: Father of natural immunity. Eur. J. Immunol. 38, 3257–3264.

Gosselin, D., Link, V.M., Romanoski, C.E., Fonseca, G.J., Eichenfield, D.Z., Spann, N.J., Stender, J.D., Chun, H.B., Garner, H., Geissmann, F., et al. (2014). Environment Drives Selection and Function of Enhancers Controlling Tissue-Specific Macrophage Identities. Cell 159, 1327–1340.

Gosselin, D., Skola, D., Coufal, N.G., Holtman, I.R., Schlachetzki, J.C.M., Sajti, E., Jaeger, B.N., O'Connor, C., Fitzpatrick, C., Pasillas, M.P., et al. (2017). An environment-dependent transcriptional network specifies human microglia identity. Science 356, eaal3222–eaal3228.

Grabert, K., Michoel, T., Karavolos, M.H., Clohisey, S., Baillie, J.K., Stevens, M.P., Freeman, T.C., Summers, K.M., and McColl, B.W. (2016). Microglial brain region−dependent diversity and selective regional sensitivities to aging. Nat Neurosci 19, 504–516.

Greenhalgh, D.G. (1998). The role of apoptosis in wound healing. The International Journal of Biochemistry Cell Biology 1019–1030.

Gregory, C. (2009). Sent by the scent of death. Nature 461, 181–182.

Griffiths, G. (1996). On vesicles and membrane compartments. Protoplasma 195, 37–58.

Griffiths, G., and Mayorga, L. (2007). Phagosome proteomes open the way to a better understanding of phagosome function. Genome Biology 8, 207.1–207.4.

Groth, A.C. (2000). A phage integrase directs efficient site-specific integration in human cells. PNAS 97, 5995–6000.

Groth, A.C. (2004). Construction of Transgenic Drosophila by Using the Site-Specific Integrase From Phage PhiC31. Genetics 166, 1–8.

Gude, D.R., Alvarez, S.E., Paugh, S.W., Mitra, P., Yu, J., Griffiths, R., Barbour, S.E., Milstien, S., and Spiegel, S. (2008). Apoptosis induces expression of sphingosine kinase 1 to release sphingosine-1-phosphate as a "come-and-get-me" signal. Faseb J. 22, 2629–2638.

Guo, P., Hu, T., Zhang, J., Jiang, S., and Wang, X. (2010). Sequential action of Caenorhabditis elegans Rab GTPases regulates phagolysosome formation during apoptotic cell degradation. PNAS 107, 18016–18021.

Haffter, P., Granato, M., Brand, M., Mullins, M.C., Matthias Hammerschmidt, Kane, D.A., Odenthal, J., van Eeden, F.J.M., Jiang, Y.-J., Heisenberg, C.-P., et al. (1996). The identification of genes with unique and essential functions in the development of the zebrafish, Danio rerio. Development 123, 1–17.

Han, C.Z., and Ravichandran, K.S. (2011). Metabolic Connections during Apoptotic Cell Engulfment. Cell 147, 1442–1445.

Hanisch, U.-K. (2013). Functional diversity of microglia – how heterogeneous are they to begin with? Front. Cell. Neurosci. 7, 1–18.

Hanisch, U.-K., and Kettenmann, H. (2007). Microglia: active sensor and versatile effector cells in the normal and pathologic brain. Nat Neurosci 10, 1387–1394.

Harrison, R.E., Bucci, C., Vieira, O.V., Schroer, T.A., and Grinstein, S. (2003). Phagosomes Fuse with Late Endosomes and/or Lysosomes by Extension of Membrane Protrusions along Microtubules: Role of Rab7 and RILP. Mol. Cell. Biol. 23, 6494–6506.

Haynes, S.E., Hollopeter, G., Yang, G., Kurpius, D., Dailey, M.E., Gan, W.-B., and Julius, D. (2006). The P2Y12 receptor regulates microglial activation by extracellular nucleotides. Nat Neurosci 9, 1512–1519.

Heinz, S., Benner, C., Spann, N., Bertolino, E., Lin, Y.C., Laslo, P., Cheng, J.X., Murre, C., Singh, H., and Glass, C.K. (2010). Simple Combinations of Lineage-Determining Transcription Factors Prime cis-Regulatory Elements Required for Macrophage and B Cell Identities. Molecular Cell 38, 576–589.

Henke, K. (2011). Microglia in the zebrafish embryo: Isolation and characterization of molecules involved in their function and colonization of the brain.

Henson, P.M., and Bratton, D.L. (2013). Antiinflammatory effects of apoptotic cells. J. Clin. Invest. 123, 2773–2774.

Herbomel, P., Thisse, B., and Thisse, C. (2001). Zebrafish Early Macrophages Colonize Cephalic Mesenchyme and Developing Brain, Retina, and Epidermis through a M-CSF Receptor-Dependent Invasive Process. Developmental Biology 238, 274–288.

Hochreiter-Hufford, A., and Ravichandran, K.S. (2012). Clearing the Dead: Apoptotic Cell Sensing, Recognition, Engulfment, and Digestion. Cold Spring Harbor Laboratory Press 5, 1–21.

Hoeffel, G., Chen, J., Lavin, Y., Low, D., Almeida, F.F., See, P., Beaudin, A.E., Lum, J., Low, I., Forsberg, E.C., et al. (2015). C-Myb+ Erythro-Myeloid Progenitor-Derived Fetal Monocytes Give Rise to Adult Tissue-Resident Macrophages. Immunity 42, 665–678.

Hoeppner, D.J., Hengartner, M.O., and Schnabel, R. (2001). Engulfment genes cooperate with ced-3 to promote cell death in Caenorhabditis elegans. Nature 412, 1–5.

Holstege, J.C., de Graaff, W., Hossaini, M., Cano, S.C., Jaarsma, D., van den Akker, E., and Deschamps, J. (2008). Loss of Hoxb8 alters spinal dorsal laminae and sensory responses in mice. PNAS 105, 6338–6343.

Holton, P. (1959). The liberation of adenosine triphosphate on antidromic stimulation of sensory nerves. J. Physiol. (Lond.) 145, 494–504.

Honda, S., Sasaki, Y., Ohsawa, K., Imai, Y., Nakamura, Y., Inoue, K., and Kohsaka, S. (2001). Extracellular ATP or ADP Induce Chemotaxis of Cultured Microglia through $G_{i/o}$-Coupled P2Y Receptors. J. Neurosci. 21, 1975–1982.

Hong, J.R. (2004). Phosphatidylserine receptor is required for the engulfment of dead apoptotic cells and for normal embryonic development in zebrafish. Development 131, 5417–5427.

Hong, S., Beja-Glasser, V.F., Nfonoyim, B.M., Frouin, A., Li, S., Ramakrishnan, S., Merry, K.M., Shi, Q., Rosenthal, A., Barres, B.A., et al. (2016a). Complement and microglia mediate early synapse loss in Alzheimer mouse models. Science 352, 712–716.

Hong, S., Dissing-Olesen, L., and Stevens, B. (2016b). ScienceDirect New insights on the role of microglia in synaptic pruning in health and disease. Current Opinion in Neurobiology 36, 128–134.

Horvitz, H.R. (1999). Genetic Control of Programmed Cell Death in the Nematode Caenorhabditis elegans. Cancer Research 59, 1701s–1706s.

Hu, G., Goll, M.G., and Fisher, S. (2011). ΦC31 Integrase Mediates Efficient Cassette Exchange in the Zebrafish Germline. Dev. Dyn. 240, 2101–2107.

Hua, Y., Laserstein, P., and Helmstaedter, M. (2015). Large-volume en-bloc staining for electron microscopy-based connectomics. Nature Communications 6, 1-7.

Huang, P., Xiao, A., Zhou, M., Zhu, Z., Lin, S., and Zhang, B. (2011). Heritable gene targeting in zebrafish using customized TALENs. Nature Publishing Group 29, 699–700.

Huang, T., Cui, J., Li, L., Hitchcock, P.F., and Li, Y. (2012). The role of microglia in the neurogenesis of zebrafish retina. Biochemical and Biophysical Research Communications 421, 214–220.

Hwang, W.Y., Fu, Y., Reyon, D., Maeder, M.L., Kaini, P., Sander, J.D., Joung, J.K., Peterson, R.T., and Yeh, J.-R.J. (2013a). Heritable and Precise Zebrafish Genome Editing Using a CRISPR-Cas System. PLoS ONE 8, e68708–e68709.

Hwang, W.Y., Fu, Y., Reyon, D., Maeder, M.L., Tsai, S.Q., Sander, J.D., Peterson, R.T., Yeh, J.-R.J., and Joung, J.K. (2013b). Efficient genome editing in zebrafish using a CRISPR-Cas system. Nat Biotechnol 31, 227–229.

Idevall-Hagren, O., Dickson, E.J., Hille, B., Toomre, D.K., and Pietro De Camilli (2012). Optogenetic control of phosphoinositide metabolism. PNAS E2316–E2323.

Idzko, M., Dichmann, S., Panther, E., Ferrari, D., Herouy, Y., Virchow, C., Luttmann, W., Di Virgilio, F., and Norgauer, J. (2001). Functional characterization of P2Y and P2X receptors in human eosinophils. J. Cell. Physiol. 188, 329–336.

Idzko, M., Ferrari, D., and Eltzschig, H.K. (2014). Nucleotide signalling during inflammation. Nature 509, 310–317.

Inoue, K., Nakajima, K., Morimoto, T., Kikuchi, Y., Koizumi, S., Illes, P., and Kohsaka, S. (1998). ATP stimulation of Ca2+ -dependent plasminogen release from cultured microglia. Br. J. Pharmacol. 123, 1304–1310.

Ishimoto, Y., Ohashi, K., Mizuno, K., and Nakano, T. (2000). Promotion of the Uptake of PS Liposomes and Apoptotic Cells by a Product of Growth Arrest-Specific Gene, gas6. J Biochem 127, 411–417.

Jahraus, A., Storrie, B., Griffiths, G., and Desjardins, M. (1994). Evidence for retrograde traffic between terminal lysosomes and the prelysosomal/late endosome compartment . Journal of Cell Science 107, 145–157.

Jun, H.S., Lee, Y.M., Cheung, Y.Y., McDermott, D.H., Murphy, P.M., De Ravin, S.S., Mansfield, B.C., and Chou, J.Y. (2010). Lack of glucose recycling between endoplasmic reticulum and cytoplasm underlies cellular dysfunction in glucose-6-phosphatase- -deficient neutrophils in a congenital neutropenia syndrome. Blood 116, 2783–2792.

Karunarathne, W.K.A., Lopamudra Giri, V.K., and Gautam, N. (2013). Optically triggering spatiotemporally confined GPCR activity in a cell and programming neurite initiation and extension. PNAS E1565–E1574.

Kawane, K., Fukuyama, H., Kondoh, G., Takeda, J., Ohsawa, Y., Uchiyama, Y., and Nagata, S. (2001). Requirement of DNase II for Definitive Erythropoiesis in the Mouse Fetal Liver. Science 292, 1546–1549.

Kawane, K., Fukuyama, H., Yoshida, H., Nagase, H., Ohsawa, Y., Uchiyama, Y., Okada, K., Iida, T., and Nagata, S. (2003). Impaired thymic development in mouse embryos deficient in apoptotic DNA degradation. Nat Immunol 4, 138–144.

Keller, S., Berghoff, K., and Kress, H. (2017). Phagosomal transport depends strongly on phagosome size. Sci. Rep. 7, 1–15.

Kerr, J.F.R., Wyllie, A.H., and Currie, A.R. (1972). Apoptosis: a Basic Biological Phenomenon with Wide- Ranging Implications in Tissue Kinetics. Br. J. Cancer 26, 239–257.

Kerr, J.F.R., Winterford, C.M., and Harmon, B.V. (1994). Apoptosis. Its significance in Cancer and Cancer Therapy. Cancer 73, 2013–2026.

Kettenmann, H., Hanisch, U.K., Noda, M., and Verkhratsky, A. (2011). Physiology of Microglia. Physiological Reviews 91, 461–553.

Kim, H.J., Ajit, D., Peterson, T.S., Wang, Y., Camden, J.M., Gibson Wood, W., Sun, G.Y., Erb, L., Petris, M., and Weisman, G.A. (2012). Nucleotides released from $A\beta_{1\text{-}42}$-treated microglial cells increase cell migration and $A\beta_{1\text{-}42}$ uptake through $P2Y_2$ receptor activation. J. Neurochem. 121, 228–238.

Kim, J.Y., Tillison, K., Zhou, S., Wu, Y., and Smas, C.M. (2007). The major facilitator superfamily member Slc37a2 is a novel macrophage- specific gene selectively expressed in obese white adipose tissue. Am. J. Physiol. Endocrinol. Metab. 293, E110–E120.

Kim, J.-M., Hwa, J., Garriga, P., Reeves, P.J., RajBhandary, U.L., and Khorana, H.G. (2005). Light-Driven Activation of β 2-Adrenergic Receptor Signaling by a Chimeric Rhodopsin Containing the β 2-Adrenergic Receptor Cytoplasmic Loops †. Biochemistry 44, 2284–2292.

Kimmel, C.B., Ballard, W.W., Kimmel, S.R., Ullmann, B., and Schilling, T.F. (1995). Stages of embryonic development of the zebrafish. Dev. Dyn. 203, 253–310.

Kinchen, J.M., and Ravichandran, K.S. (2008). Phagosome maturation: going through the acid test. Nat Rev Mol Cell Biol 9, 781–795.

Kinchen, J.M., Doukoumetzidis, K., Almendinger, J., Stergiou, L., Tosello-Trampont, A., Sifri, C.D., Hengartner, M.O., and Ravichandran, K.S. (2008). A pathway for phagosome maturation during engulfment of apoptotic cells. Nat Cell Biol 10, 556–566.

King, B.F., and Burnstock, G. (2002). Purinergic receptors. pp. 422–438.

Kiss, R.S., Elliott, M.R., Ma, Z., Marcel, Y.L., and Ravichandran, K.S. (2006). Apoptotic Cells Induce a Phosphatidylserine-Dependent Homeostatic Response from Phagocytes. Current Biology 16, 2252–2258.

Knapp, P.E., Skoff, F.P., and Redstone, D.W. (1986). Oligodendroglial Cell Death in Jimpy Mice: An Explanation for the Myelin Deficit. J. Neurosci. 6, 2813–2822.

Kobayashi, T., Beuchat, M.H., Lindsay, M., Frias, S., Palmiter, R.D., Sakuraba, H., Parton, R.G., and Gruenberg, J. (1999). Late endosomal membranes rich in lysobisphosphatidic acid regulate cholesterol transport. Nat Cell Biol 1, 113–118.

Kohyama, M., Ise, W., Edelson, B.T., Wilker, P.R., Hildner, K., Mejia, C., Frazier, W.A., Murphy, T.L., and Murphy, K.M. (2012). Critical role for Spi-C in the development of red pulp macrophages and splenic iron homeostasis. Nature 457, 318–321.

Koizumi, S., Ohsawa, K., Inoue, K., and Kohsaka, S. (2013). Purinergic receptors in microglia: Functional modal shifts of microglia mediated by P2 and P1 receptors. Glia 61, 47–54.

Koizumi, S., Shigemoto-Mogami, Y., Nasu-Tada, K., Shinozaki, Y., Ohsawa, K., Tsuda, M., Joshi, B.V., Jacobson, K.A., Kohsaka, S., and Inoue, K. (2007). UDP acting at $P2Y_6$ receptors is a mediator of microglial phagocytosis. Nature 446, 1091–1095.

Kolb, H.A., and Wakelam, M.J. (1983). Transmitter-like action of ATP on patched membranes of cultured myoblasts and myotubes. Nature 303, 621–623.

Kolter, T., and Sandhoff, K. (2010). Lysosomal degradation of membrane lipids. FEBS Lett. 584, 1700–1712.

Kornfeld, S., and Mellman, I. (1989). The biogenesis of lysosomes. Annu. Rev. Cell Biol. 5, 483–525.

Krajcovic, M., Krishna, S., Akkari, L., Joyce, J.A., and Overholtzer, M. (2013). mTOR regulates phagosome and entotic vacuole fssion. 24, 3736–3745.

Krieser, R.J., MacLea, K.S., Longnecker, D.S., Fields, J.L., Fiering, S., and Eastman, A. (2002). Deoxyribonuclease IIa is required during the phagocytic phase of apoptosis and its loss causes perinatal lethality. Cell Death and Differentiation 9, 956–962.

Krishna, S., Palm, W., Lee, Y., Yang, W., Bandyopadhyay, U., Xu, H., Florey, O., Thompson, C.B., and Overholtzer, M. (2016). PIKfyve Regulates Vacuole Maturation and Nutrient Recovery following Engulfment. Developmental Cell 38, 536–547.

Krishtal, O.A., Marchenko, S.M., and Pidoplichko, V.I. (1983). Receptor for ATP in the membrane of mammalian sensory neurones. Neuroscience Letters 35, 41–45.

Kronlage, M., Song, J., Sorokin, L., Isfort, K., Schwerdtle, T., Leipziger, J., Robaye, B., Conley, P.B., Kim, H.-C., Sargin, S., et al. (2010). Autocrine purinergic receptor signaling is essential for macrophage chemotaxis. Sci Signal 3, ra55–ra55.

Kügelgen, von, I., and Hoffmann, K. (2015). Pharmacology and structure of P2Y receptors. Neuropharmacology 1–12.

Lauber, K., Bohn, E., Kröber, S.M., Xiao, Y.-J., Blumenthal, S.G., Lindemann, R.K., Marini, P., Wiedig, C., Zobywalski, A., Baksh, S., et al. (2003). Apoptotic Cells Induce Migration of Phagocytes via Caspase-3-Mediated Release of a Lipid Attraction Signal. Cell 113, 717–730.

Lavin, Y., Winter, D., Blecher-Gonen, R., David, E., Keren-Shaul, H., Merad, M., Jung, S., and Amit, I. (2014). Tissue-Resident Macrophage Enhancer Landscapes Are Shaped by the Local Microenvironment. Cell 159, 1312–1326.

Lawson, L.J., Perry, V.H., Dri, P., and Gordon, S. (1990). Heterogeneity in the distribution and morphology of microglia in the normal adult mouse brain. Neuroscience 39, 151–170.

Lee, C.S., Penberthy, K.K., Wheeler, K.M., Juncadella, I.J., Vandenabeele, P., Lysiak, J.J., and Ravichandran, K.S. (2016). Boosting Apoptotic Cell Clearance by Colonic Epithelial Cells Attenuates Inflammation In Vivo. Immunity 44, 807–820.

Lele, Z., and Krone, P.H. (1996). The Zebrafish as a model system in developmental, toxicological and transgenic research. Biotechnology Advances 14, 57–72.

Lelli, A., Gervais, A., Colin, C., Chéret, C., de Almodovar, C.R., Carmeliet, P., Krause, K.-H., Boillée, S., and Mallat, M. (2013). The NADPH oxidase Nox2 regulates VEGFR1/CSF-1R-mediated microglial chemotaxis and promotes early postnatal infiltration of phagocytes in the subventricular zone of the mouse cerebral cortex. Glia 61, 1542–1555.

Lenz, K.M., and Nelson, L.H. (2018). Microglia and Beyond: Innate Immune Cells As Regulators of Brain Development and Behavioral Function. Front. Immunol. 9, 13–13.

Lettre, G., and Hengartner, M.O. (2006). Developmental apoptosis in C. elegans: a complex CEDnario. Nat Rev Mol Cell Biol 7, 97–108.

Levi-Montalcini, R. (2005). The Nerve Growth Factor 35 Years Later. Science 237, 1154–1162.

Levin, R., Grinstein, S., and Canton, J. (2016). The life cycle of phagosomes: formation, maturation, and resolution. Immunological Reviews 273, 156–179.

Li, F., Jiang, T., Li, Q., and Ling, X. (2017). Camptothecin (CPT) and its derivatives are known to target topoisomerase I (Top1) as their mechanism of action: did we miss something in CPT

analogue molecular targets for treating human disease such as cancer? Am J Cancer Res 7, 2350–2394.

Li, X., Gutierrez, D.V., Hanson, M.G., Han, J., Mark, M.D., Chiel, H., Hegemann, P., Landmesser, L.T., and Herlitze, S. (2005). Fast noninvasive activation and inhibition of neural and network activity by vertebrate rhodopsin and green algae channelrhodopsin. PNAS 102, 17816–17821.

Linke, T., Wilkening, G., Lansmann, S., Moczall, H., Bartelsen, O., Weisgerber, J., and Sandhoff, K. (2001). Stimulation of acid sphingomyelinase activity by lysosomal lipids and sphingolipid activator proteins. Biol. Chem. 382, 283–290.

Lister, J.A. (2010). Transgene excision in zebrafish using the phiC31 integrase. Genesis 48, 137–143.

Lister, J.A. (2011). Use of Phage PhiC31 Integrase as a Tool for Zebrafish Genome Manipulation. Methods Cell Biol 104, 195–208.

Lister, M.F., Sharkey, J., Sawatzky, D.A., Hodgkiss, J.P., Davidson, D.J., Rossi, A.G., and Finlayson, K. (2007). The role of the purinergic P2X7 receptor in inflammation. J Inflamm (Lond) 4, 1-14.

Lloyd-Evans, E., Morgan, A.J., He, X., Smith, D.A., Elliot-Smith, E., Sillence, D.J., Churchill, G.C., Schuchman, E.H., Galione, A., and Platt, F.M. (2008). Niemann-Pick disease type C1 is a sphingosine storage disease that causes deregulation of lysosomal calcium. Nat Med 14, 1247–1255.

Loane, D.J., and Kumar, A. (2016). Microglia in the TBI brain: The good, the bad, and the dysregulated. Experimental Neurology 275, 316–327.

Lommatzsch, M., Cicko, S., Müller, T., Lucattelli, M., Bratke, K., Stoll, P., Grimm, M., Dürk, T., Zissel, G., Ferrari, D., et al. (2010). Extracellular adenosine triphosphate and chronic obstructive pulmonary disease. Am. J. Respir. Crit. Care Med. 181, 928–934.

Lord, C.E.N., and Gunawardena, A.H.L.A.N. (2012). Programmed cell death in C. elegans, mammals and plants. European Journal of Cell Biology 91, 603–613.

Lu, J., Maddison, L.A., and Chen, W. (2010). PhiC31 integrase induces efficient site-specific excision in zebrafish. Transgenic Res 20, 183–189.

Lu, N., and Zhou, Z. (2012). Membrane Trafficking and Phagosome Maturation During the Clearance of Apoptotic Cells. Int Rev Cell Mol Biol 293, 269–309.

Lund, L.R., Rømer, J., Thomasset, N., Solberg, H., Pyke, C., Bissell, M.J., Danø, K., and Werb, Z. (1996). Two distinct phases of apoptosis in mammary gland involution: proteinase-independent and -dependent pathways. Development 122, 181–193.

Madry, C., and Attwell, D. (2015). Receptors, ion channels, and signaling mechanisms underlying microglial dynamics. J. Biol. Chem. 290, 12443–12450.

Mangahas, P.M., Yu, X., Miller, K.G., and Zhou, Z. (2008). The small GTPase Rab2 functions in the removal of apoptotic cells in Caenorhabditis elegans. J Cell Biol 180, 357–373.

Marin-Teva, J.L., Dusart, I., Colin, C., Gervais, A., van Rooijen, N., and Mallat, M. (2004). Microglia Promote the Death of Developing Purkinje Cells. Neuron 41, 535–547.

Matcovitch-Natan, O., Winter, D.R., Giladi, A., Vargas Aguilar, S., Spinrad, A., Sarrazin, S., Ben-Yehuda, H., David, E., Zelada Gonzalez, F., Perrin, P., et al. (2016). Microglia development follows a stepwise program to regulate brain homeostasis. Science 353, aad8670–aad8670.

Matsuo, H., Chevallier, J., Mayran, N., Le Blanc, I., Ferguson, C., Fauré, J., Blanc, N.S., Matile, S., Dubochet, J., Sadoul, R., et al. (2004). Role of LBPA and Alix in multivesicular liposome formation and endosome organization. Science 303, 531–534.

Mazaheri, F., Breus, O., Durdu, S., Haas, P., Wittbrodt, J., Gilmour, D., and Peri, F. (2014). Distinct roles for BAI1 and TIM-4 in the engulfment of dying neurons by microglia. Nature Communications 5, 1–11.

McDonald, B., and Kubes, P. (2011). Cellular and molecular choreography of neutrophil recruitment to sites of sterile inflammation. J. Mol. Med. 89, 1079–1088.

McDonald, B., Pittman, K., Menezes, G.B., Hirota, S.A., Slaba, I., Waterhouse, C.C.M., Beck, P.L., Muruve, D.A., and Kubes, P. (2010). Intravascular danger signals guide neutrophils to sites of sterile inflammation. Science 330, 362–366.

Medina, C.B., and Ravichandran, K.S. (2016). Do not let death do us part: “find-me” signals in communication between dying cells and the phagocytes. Cell Death and Differentiation 1–11.

Meehan, T.L., Joudi, T.F., Timmons, A.K., Taylor, J.D., Habib, C.S., Peterson, J.S., Emmanuel, S., Franc, N.C., and McCall, K. (2016). Components of the Engulfment Machinery Have Distinct Roles in Corpse Processing. PLoS ONE 11, e0158217–e0158222.

Meier, P., Finch, A., and Evan, G. (2000). Apoptosis in development. Nature 407, 796–801.

Meireles, A.M., Shiau, C.E., Guenther, C.A., Sidik, H., Kingsley, D.M., and Talbot, W.S. (2014). The Phosphate Exporter xpr1b Is Required for Differentiation of Tissue-Resident Macrophages. Cell Reports 8, 1659–1667.

Meng, X., Noyes, M.B., Zhu, L.J., Lawson, N.D., and Wolfe, S.A. (2008). Targeted gene inactivation in zebrafish using engineered zinc finger nucleases. Nat Biotechnol 26, 695–701.

Miyanishi, M., Tada, K., Koike, M., Uchiyama, Y., Kitamura, T., and Nagata, S. (2007). Identification of Tim4 as a phosphatidylserine receptor. Nature 450, 435–439.

Miyashita, T., and Reed, J.C. (1995). Tumor Suppressor p53 Is a Direct Transcriptional Activator of the Human bax gene. Cell 80, 293–299.

Monje, M.L., Toda, H., and Palmer, T.D. (2003). Inflammatory Blockade Restores Adult Hippocampal Neurogenesis. Science 302, 1760–1765.

Moritz, C. (2014). Studying microglial responses to neuronal cell death in the living zebrafish brain.

Morsch, M., Radford, R., Lee, A., Don, E.K., Badrock, A.P., Hall, T.E., Cole, N.J., and Chung, R. (2015). In vivo characterization of microglial engulfment of dying neurons in the zebrafish spinal cord. Front. Cell. Neurosci. 9, e90572–11.

Mosher, K.I., Andres, R.H., Fukuhara, T., Bieri, G., Hasegawa-Moriyama, M., He, Y., Guzman, R., and Wyss-Coray, T. (2012). Neural progenitor cells regulate microglia functions and activity. Nat Neurosci 15, 1485–1487.

Mosimann, C., Puller, A.-C., Lawson, K.L., Tschopp, P., Amsterdam, A., and Zon, L.I. (2013). Site-directed zebrafish transgenesis into single landing sites with the phiC31 integrase system. Dev. Dyn. 242, 949–963.

Mukae, N., Yokoyama, H., Yokokura, T., Sakoyama, Y., and Nagata, S. (2002). Activation of the innate immunity in Drosophila by endogenous chromosomal DNA that escaped apoptotic degradation. Genes Development 16, 2662–2671.

Mullins, M.C., Matthias Hammerschmidt, Haffter, P., and Niisslein-Volhard, C. (1994). Large scale mutagenesis in the zebrafish: in search of genes controlling development in vertebrate. Current Biology 4, 189–202.

Murphy, P.M., Baggiolini, M., Charo, I.F., Hébert, C.A., Horuk, R., Matsushima, K., Miller, L.H., Oppenheim, J.J., and Power, C.A. (2000). International union of pharmacology. XXII. Nomenclature for chemokine receptors. Pharmacol. Rev. 52, 145–176.

Nagata, S., Hanayama, R., and Kawane, K. (2010). Autoimmunity and the Clearance of Dead Cells. Cell 140, 619–630.

Navascués, J., Moujahid, A., Almendros, A., Marin-Teva, J.L., and Cuadros, M.A. (1995). Origin of Microglia in the Quail Retina: Central-to-Peripheraland Vitreal-to-Scleral Migration of Microglial Precursors During Development. The Journal of Comparative Neurology 354, 209–228.

Niethammer, P., Grabher, C., Look, A.T., and Mitchison, T.J. (2009). A tissue-scale gradient of hydrogen peroxide mediates rapid wound detection in zebrafish. Nature 459, 996–999.

Nimmerjahn, A., Kirchhoff, F., and Helmchen, F. (2005). Resting Microglial Cells Are Highly Dynamic Surveillants of Brain Parenchyma in Vivo. Science 308, 1310–1314.

Nisar, S., Daly, M.E., Federici, A.B., Artoni, A., Mumford, A.D., Watson, S.P., and Mundell, S.J. (2011). An intact PDZ motif is essential for correct P2Y12 purinoceptor traffic in human platelets. Blood 118, 5641–5651.

Nordmann, M., Cabrera, M., Perz, A., Bröcker, C., Ostrowicz, C., Engelbrecht-Vandré, S., and Ungermann, C. (2010). The Mon1-Ccz1 Complex Is the GEF of the Late Endosomal Rab7 Homolog Ypt7. Current Biology 20, 1654–1659.

North, R.A., and Jarvis, M.F. (2013). P2X receptors as drug targets. Mol. Pharmacol. 83, 759–769.

Nüsslein-Volhard, C., and Dahm, R. (2002). Zebrafish: a practical approach (Oxford University Press).

Oh, E., Maejima, T., Liu, C., Deneris, E., and Herlitze, S. (2010). Substitution of 5-HT1A receptor signaling by a light-activated G protein-coupled receptor. J. Biol. Chem. 285, 30825–30836.

Oppenheim, R.W. (1991). CELL DEATH DURING DEVELOPMENT OF THE NERVOUS SYSTEM. Annu. Rev. Neurosci. 26, 453–501.

Oram, J.F., and Heinecke, J.W. (2005). ATP-Binding Cassette Transporter A1: A Cell Cholesterol Exporter That Protects Against Cardiovascular Disease. Physiological Reviews 85, 1343–1372.

Osborne, B.A. (1996). Apoptosis and the maintenance of homoeostasis in the immune system Barbara A Osborne. Current Opinion in Immunology 8, 245–254.

Pan, C.-J., Chen, S.-Y., Jun, H.S., Lin, S.R., Mansfield, B.C., and Chou, J.Y. (2011). SLC37A1 and SLC37A2 Are Phosphate-Linked, Glucose-6-Phosphate Antiporters. PLoS ONE 6, e23157–e23158.

Paolicelli, R.C., Bolasco, G., Pagani, F., Maggi, L., Scianni, M., Panzanelli, P., Giustetto, M., Ferreira, T.A., Guiducci, E., Dumas, L., et al. (2011). Synaptic Pruning by Microglia Is Necessary for Normal Brain Development. Science 333, 1456–1458.

Paquet, D., Bhat, R., Sydow, A., Mandelkow, E.-M., Berg, S., Hellberg, S., Fälting, J., Distel, M., Köster, R.W., Schmid, B., et al. (2009). A zebrafish model of tauopathy allows in vivo imaging of neuronal cell death and drug evaluation. J. Clin. Invest. 119, 1382–1395.

Park, D., Han, C.Z., Elliott, M.R., Kinchen, J.M., Trampont, P.C., Das, S., Collins, S., Lysiak, J.J., Hoehn, K.L., and Ravichandran, K.S. (2011). Continued clearance of apoptotic cells critically depends on the phagocyte Ucp2 protein. Nature 477, 220–224.

Park, D., Tosello-Trampont, A.-C., Elliott, M.R., Lu, M., Haney, L.B., Ma, Z., Klibanov, A.L., Mandell, J.W., and Ravichandran, K.S. (2007a). BAI1 is an engulfment receptor for apoptotic cells upstream of the ELMO/Dock180/Rac module. Nature 450, 430–434.

Park, S.-Y., Jung, M.-Y., Kim, H.-J., Lee, S.-J., Kim, S.-Y., Lee, B.-H., Kwon, T.-H., Park, R.-W., and Kim, I.-S. (2007b). Rapid cell corpse clearance by stabilin-2, a membrane phosphatidylserine receptor. Cell Death and Differentiation 15, 192–201.

Parkhurst, C.N., Yang, G., Ninan, I., Savas, J.N., Yates, J.R., III, Lafaille, J.J., Hempstead, B.L., Littman, D.R., and Gan, W.-B. (2013). Microglia Promote Learning-Dependent Synapse Formation through Brain-Derived Neurotrophic Factor. Cell 155, 1596–1609.

Patton, E.E., and Zon, L.I. (2001). THE ART AND DESIGN OF GENETIC SCREENS: ZEBRAFISH. Nature 2, 956–966.

Peri, F., and Nüsslein-Volhard, C. (2008). Live Imaging of Neuronal Degradation by Microglia Reveals a Role for v0-ATPase a1 in Phagosomal Fusion In Vivo. Cell 133, 916–927.

Perry, V.H., Hume, D.A., and Gordon, S. (1985). IMMUNOHISTOCHEMICAL MACROPHAGES AND MICROGLIA IN THE ADULT AND DEVELOPING MOUSE BRAIN. Neuroscience 15, 313–326.

Peter, C., Waibel, M., Radu, C.G., Yang, L.V., Witte, O.N., Schulze-Osthoff, K., Wesselborg, S., and Lauber, K. (2008). Migration to Apoptotic "Find-me" Signals Is Mediated via the Phagocyte Receptor G2A. Thejournalofbiologicalchemistry 283, 5296–5305.

Plemel, R.L., Lobingier, B.T., Brett, C.L., Angers, C.G., Nickerson, D.P., Paulsel, A., Sprague, D., and Merz, A.J. (2011). Subunit organization and Rab interactions of Vps-C protein complexes that control endolysosomal membrane traffic. MBoC 22, 1353–1363.

Poon, I.K.H., Lucas, C.D., Rossi, A.G., and Ravichandran, K.S. (2014). Apoptotic cell clearance: basic biology and therapeutic potential. Nat Rev Immunol 14, 166–180.

Raff, M.C., Barres, B.A., Burne, J.F., Coles, H.S., Ishizaki, Y., and Jacobson, M.D. (1993). Programmed Cell Death and the Control of Cell Survival: Lessons from the Nervous System. Science 262, 695–700.

Ransohoff, R.M., and Khoury, J.E. (2016). Microglia in Health and Disease. Cold Spring Harb Perspect Biol 8, a020560.

Rathmell, J.C., and Thompson, C.B. (2002). Pathways of Apoptosis in Lymphocyte Review Development, Homeostasis, and Disease. Cell 109, S97–S107.

Ravichandran, K.S. (2010). Find-me and eat-me signals in apoptotic cell clearance: progress and conundrums. J Exp Med 207, 1807–1817.

Ravichandran, K.S. (2011). Beginnings of a Good Apoptotic Meal: The Find-Me and Eat-Me Signaling Pathways. Immunity 35, 445–455.

Ravichandran, K.S., and Lorenz, U. (2007). Engulfment of apoptotic cells: signals for a good meal. Nat Rev Immunol 7, 964–974.

Reddien, P.W., Cameron, S., and Horvitz, H.R. (2001). Phagocytosis promotes programmed cell death in C. elegans. Nature 412, 1–5.

Renehan, A.G., Booth, C., and Potten, C.S. (2001). What is apoptosis, and why is it important? Bmj 322, 1536–1538.

Renshaw, S.A., and Trede, N.S. (2011). A model 450 million years in the making: zebrafish and vertebrate immunity. Disease Models & Mechanisms 5, 38–47.

Rhodes, J., Hagen, A., Hsu, K., Deng, M., Liu, T.X., Look, A.T., and Kanki, J.P. (2005). Interplay of Pu.1 and Gata1 Determines Myelo-Erythroid Progenitor Cell Fate in Zebrafish. Developmental Cell 8, 97–108.

Roberts, R.L., Barbieri, M.A., Ullrich, J., and Stahl, P.D. (2000). Dynamics of rab5 activation in endocytosis and phagocytosis. Journal of Leukocyte Biology 68, 627–632.

Rodriguez-Manzanet, R., Sanjuan, M.A., Wu, H.Y., Quintana, F.J., Xiao, S., Anderson, A.C., Weiner, H.L., Green, D.R., and Kuchroo, V.K. (2010). T and B cell hyperactivity and autoimmunity associated with niche-specific defects in apoptotic body clearance in TIM-4-deficient mice. PNAS 107, 8706–8711.

Rosen, H., and Goetzl, E.J. (2005). Sphingosine 1-phosphate and its receptors: an autocrine and paracrine network. Nat Rev Immunol 5, 560–570.

Rossi, F.M. (2013). The role of slc7a7 in promoting brain colonization by microglia.

Rossi, F., Casano, A.M., Henke, K., Richter, K., and Peri, F. (2015). The SLC7A7 Transporter Identifies Microglial Precursors prior to Entry into the Brain. CellReports 11, 1–10.

Samie, M.A., and Xu, H. (2014). Lysosomal exocytosis and lipid storage disorders. J. Lipid Res. 55, 995–1009.

Sanagi, T., Yuasa, S., Nakamura, Y., Suzuki, E., Aoki, M., Warita, H., Itoyama, Y., Uchino, S., Kohsaka, S., and Ohsawa, K. (2010). Appearance of phagocytic microglia adjacent to motoneurons in spinal cord tissue from a presymptomatic transgenic rat model of amyotrophic lateral sclerosis. J. Neurosci. Res. 88, 2736–2746.

Sander, J.D., and Joung, J.K. (2014). CRISPR-Cas systems for editing, regulating and targeting genomes. Nat Biotechnol 32, 347–355.

Sander, J.D., Cade, L., Khayter, C., Reyon, D., Peterson, R.T., Joung, J.K., and Yeh, J.-R.J. (2011). Targeted gene disruption in somatic zebrafish cells using engineered TALENs. Nat Biotechnol 29, 697–698.

Schafer, D.P., Lehrman, E.K., Kautzman, A.G., Koyama, R., Mardinly, A.R., Yamasaki, R., Ransohoff, R.M., Greenberg, M.E., Barres, B.A., and Stevens, B. (2012). Microglia Sculpt Postnatal Neural Circuits in an Activity and Complement-Dependent Manner. Neuron 74, 691–705.

Schrijvers, D.M. (2005). Phagocytosis of Apoptotic Cells by Macrophages Is Impaired in Atherosclerosis. Arteriosclerosis, Thrombosis, and Vascular Biology 25, 1256–1261.

Segawa, K., and Nagata, S. (2015). An Apoptotic “Eat Me” Signal: Phosphatidylserine Exposure. Trends in Cell Biology 25, 639–650.

Serhan, C.N. (2014). Pro-resolving lipid mediators are leads for resolution physiology. Nature 510, 92–101.

Seye, C.I., Yu, N., Jain, R., Kong, Q., Minor, T., Newton, J., Erb, L., González, F.A., and Weisman, G.A. (2003). The P2Y2 nucleotide receptor mediates UTP-induced vascular cell adhesion molecule-1 expression in coronary artery endothelial cells. J. Biol. Chem. 278, 24960–24965.

Shen, K., Sidik, H., and Talbot, W.S. (2016). The Rag-Ragulator Complex Regulates Lysosome Function and Phagocytic Flux in Microglia. Cell Reports 14, 547–559.

Shui, W., Sheu, L., Liu, J., Smart, B., Petzold, C.J., Hsieh, T.-Y., Pitcher, A., Keasling, J.D., and Bertozzi, C.R. (2008). Membrane proteomics of phagosomes suggests a connection to autophagy. PNAS 105, 16952–16957.

Sieger, D., and Peri, F. (2012). Animal models for studying microglia: The first, the popular, and the new. Glia 61, 3–9.

Sieger, D., Moritz, C., Ziegenhals, T., Prykhozhij, S., and Peri, F. (2012). Long-Range Ca2+ Waves Transmit Brain-Damage Signals to Microglia. Developmental Cell 22, 1138–1148.

Sierra, A., Abiega, O., Shahraz, A., and Neumann, H. (2013). Janus-faced microglia: beneficial and detrimental consequences of microglial phagocytosis. Front. Cell. Neurosci. 7, 1–22.

Sierra, A., de Castro, F., del Río-Hortega, J., Rafael Iglesias-Rozas, J., Garrosa, M., and Kettenmann, H. (2016). The "Big-Bang" for modern glial biology: Translation and comments on Pío del Río-Hortega 1919 series of papers on microglia. Glia 64, 1801–1840.

Sierra, A., Encinas, J.M., Deudero, J.J.P., Chancey, J.H., Enikolopov, G., Overstreet-Wadiche, L.S., Tsirka, S.E., and Maletic-Savatic, M. (2010). Microglia Shape Adult Hippocampal Neurogenesis through Apoptosis-Coupled Phagocytosis. Cell Stem Cell 7, 483–495.

Sourjik, V., and Wingreen, N.S. (2012). Responding to chemical gradients: bacterial chemotaxis. Current Opinion in Cell Biology 24, 262–268.

Steven R Wiley, Schooley, K., Smolak, P.J., Din, W.S., Huang, C.-P., Nicholl, I.K., Sutherland, G.F., Smith, T.D., Rauch, C., Craig A Smith, et al. (1995). Identification and Characterization of a New Member of the TNF Family that Induces Apoptosis. Immunity 3, 673–682.

Stevens, B., Allen, N.J., Vazquez, L.E., Howell, G.R., Christopherson, K.S., Nouri, N., Micheva, K.D., Mehalow, A.K., Huberman, A.D., Stafford, B., et al. (2007). The Classical Complement Cascade Mediates CNS Synapse Elimination. Cell 131, 1164–1178.

Strader, C.D., Gaffney, T., Sugg, E.E., Candelore, M.R., Keys, R., Patchett, A.A., and Dixon, R.A. (1991). Allele-specific activation of genetically engineered receptors. J. Biol. Chem. 266, 5–8.

Streisinger, G., Walker, C., Dower, N., Knauber, D., and Singer, F. (1981). Production of clones of homozygous diploid zebra fish (Brachydanio rerio). Nature 291, 293–296.

Sulston, J.E., Schierenberg, E., White, J.G., and Thomson, J.N. (1983). The Embryonic Cell Lineage of the Nematode Caenorhabditis elegans. Developmental Biology 100, 64–119.

Swaney, K.F., Huang, C.-H., and Devreotes, P.N. (2010). Eukaryotic chemotaxis: a network of signaling pathways controls motility, directional sensing, and polarity. Annu Rev Biophys 39, 265–289.

Takahashi, Y., Miyata, M., Zheng, P., Imazato, T., Horwitz, A., and Smith, J.D. (2000). Identification of cAMP analogue inducible genes in RAW264 macrophages. Bba 1492, 385–394.

Tettamanti, G., Bassi, R., Viani, P., and Riboni, L. (2003). Salvage pathways in glycosphingolipid metabolism. Biochimie 85, 423–437.

Thomas, M.A., Kleist, A.B., and Volkman, B.F. (2018). Decoding the chemotactic signal. Journal of Leukocyte Biology 104, 359–374.

Tilly, J.L., Kowalski, K.I., Johnson, A.L., and Hsueh, A.J.W. (1991). Involvement of Apoptosis in Ovarian Follicular Atresia and Postovulatory Regression. Endocrinology 129, 2799–2801.

Toettcher, J.E., Voigt, C.A., Weiner, O.D., and Lim, W.A. (2010). The promise of optogenetics in cell biology: interrogating molecular circuits in space and time. Nat Meth 8, 35–38.

Tremblay, M.-E., Lowery, R.L., and Majewska, A.K. (2010). Microglial Interactions with Synapses Are Modulated by Visual Experience. PLoS Biol 8, e1000527–16.

Truman, L.A., Ford, C.A., Pasikowska, M., Pound, J.D., Wilkinson, S.J., Dumitriu, I.E., Melville, L., and Melrose, L.A. (2008). CX3CL1/fractalkine is released from apoptotic lymphocytes to stimulate macrophage chemotaxis. Blood 112, 5026–5036.

Tuteja, N. (2009). Signaling through G protein coupled receptors. Plant Signaling Behavior 4, 942–947.

Van der Kant, R., Zondervan, I., Janssen, L., and Neefjes, J. (2013). Cholesterol-binding molecules MLN64 and ORP1L mark distinct late endosomes with transporters ABCA3 and NPC1. The Journal of Lipid Research 54, 2153–2165.

Vieira, O.V., Bucci, C., Harrison, R.E., Trimble, W.S., Lanzetti, L., Gruenberg, J., Schreiber, A.D., Stahl, P.D., and Grinstein, S. (2003). Modulation of Rab5 and Rab7 Recruitment to Phagosomes by Phosphatidylinositol 3-Kinase. Mol. Cell. Biol. 23, 2501–2514.

Vieira, O.V., Botelho, R.J., and Grinstein, S. (2002). Phagosome maturation: aging gracefully. 366, 689–704.

Vieira, O.V., Botelho, R.J., Rameh, L., Brachmann, S.M., Matsuo, T., Davidson, H.W., Schreiber, A., Backer, J.M., Cantley, L.C., and Grinstein, S. (2001). Distinct roles of class I and class III phosphatidylinositol 3-kinases in phagosome formation and maturation. J Cell Biol 155, 19–26.

Wang, S., Tsun, Z.-Y., Wolfson, R.L., Shen, K., Wyant, G.A., Plovanich, M.E., Yuan, E.D., Jones, T.D., Chantranupong, L., Comb, W., et al. (2015). Lysosomal amino acid transporter SLC38A9 signals arginine sufficiency to mTORC1. Science 347, 188–194.

Wang, Y., Szretter, K.J., Vermi, W., Gilfillan, S., Rossini, C., Cella, M., Barrow, A.D., Diamond, M.S., and Colonna, M. (2012). IL-34 is a tissue-restricted ligand of CSF1R required for the development of Langerhans cells and microglia. Nat Immunol 13, 753–760.

Weavers, H., Evans, I.R., Martin, P., and Wood, W. (2016). Corpse Engulfment Generates a Molecular Memory that Primes the Macrophage Inflammatory Response. Cell 165, 1658–1671.

Weinhard, L., Bartolomei, G., Bolasco, G., Machado, P., Schieber, N.L., Neniskyte, U., Exiga, M., Vadisiute, A., Raggioli, A., Schertel, A., et al. (2018). Microglia remodel synapses by presynaptic trogocytosis and spine head filopodia induction. Nature Communications 9, 1–14.

Williams, J.A., and Holder, N. (2000). Cell turnover in neuromasts of zebrafish larvae. Hear. Res. 143, 171–181.

Willingham, S.B., Volkmer, J.-P., Gentles, A.J., Sahoo, D., Dalerba, P., Mitra, S.S., Wang, J., Contreras-Trujillo, H., Martin, R., Cohen, J.D., et al. (2012). The CD47-signal regulatory protein alpha (SIRPa) interaction is a therapeutic target for human solid tumors. PNAS 109, 6662–6667.

Worth, A., Thrasher, A.J., and Bobby Gaspar, H. (2006). Autoimmune lymphoproliferative syndrome: molecular basis of disease and clinical phenotype. Br J Haematol 133, 124–140.

Wu, Y.I., Frey, D., Lungu, O.I., Jaehrig, A., Schlichting, I., Kuhlman, B., and Hahn, K.M. (2009). A genetically encoded photoactivatable Rac controls the motility of living cells. Nature 461, 104–108.

Wu, Y.-C., Stanfield, G.M., and Horvitz, H.R. (2000). NUC-1, a Caenorhabditis elegans DNase II homolog, functions in an intermediate step of DNA degradation during apoptosis. Genes Development 14, 536–548.

Xu, J., Wang, T., Wu, Y., Jin, W., and Wen, Z. (2016). Microglia Colonization of Developing Zebrafish Midbrain Is Promoted by Apoptotic Neuron and Lysophosphatidylcholine. Developmental Cell 38, 214–222.

Yamashita, M. (2003). Apoptosis in zebrafish development. Comparative Biochemistry and Physiology Part B: Biochemistry and Molecular Biology 136, 731–742.

Yamashita, M., Mizusawa, N., Hojo, M., and Yabu, T. (2008). Extensive apoptosis and abnormal morphogenesis in pro-caspase-3 transgenic zebrafish during development. J. Exp. Biol. 211, 1874–1881.

Yeung, T., Ozdamar, B., Paroutis, P., and Grinstein, S. (2006). Lipid metabolism and dynamics during phagocytosis. Current Opinion in Cell Biology 18, 429–437.

Yoshida, H., Kawane, K., Koike, M., Mori, Y., Uchiyama, Y., and Nagata, S. (2005a). Phosphatidylserine-dependent engulfment by macrophages of nuclei from erythroid precursor cells. Nature 437, 754–758.

Yoshida, H., Okabe, Y., Kawane, K., Fukuyama, H., and Nagata, S. (2005b). Lethal anemia caused by interferon-beta produced in mouse embryos carrying undigested DNA. Nat Immunol 6, 49–56.

Yu, X., Lu, N., and Zhou, Z. (2008). Phagocytic Receptor CED-1 Initiates a Signaling Pathway for Degrading Engulfed Apoptotic Cells. PLoS Biol 6, 0581–0600.

Zemelman, B.V., Lee, G.A., Ng, M., and Miesenböck, G. (2002). Selective photostimulation of genetically chARGed neurons. Neuron 33, 15–22.

Zeng, J., Wang, G., Liu, X., Wang, C., Tian, H., Liu, A., Jin, H., Luo, X., and Chen, Y. (2014). P2Y13 Receptor-Mediated Rapid Increase in Intracellular Calcium Induced by ADP in Cultured Dorsal Spinal Cord Microglia. Neurochem Res 39, 2240–2250.

Zizzo, G., Hilliard, B.A., Monestier, M., and Cohen, P.L. (2012). Efficient clearance of early apoptotic cells by human macrophages requires M2c polarization and MerTK induction. J. Immunol. 189, 3508–3520.

Zlotnik, A., and Yoshie, O. (2000). Chemokines: A New Classification System and Their Role in Immunity. Immunity 12, 121–127.

ACKNOWLEDGMENTS

Three and a half years ago I started my PhD, and now I am writing my thesis as a brand-new person. This time has been priceless, and even disappointments have been turned into lessons, discoveries made and alternatives explored. A number of people helped me growing along this journey, not only as a scientist, but also as a person. For this I am deeply thankful to them.

First of all, I would like to thank my supervisor, Francesca, for giving me the opportunity to work in her lab and for her advice and encouragements along this path. I achieved a lot during my PhD, and all this would not have been possible without her, thanks. I would also like to thank previous and current members of the Peri lab for their support and for the nice atmosphere and fun times we had together. In particular, a big thanks to Shinya, for helping and teaching me at the beginning of my PhD. Thanks for the patience, the enthusiasm and for all the time spent after me and my project, I will always remember and acknowledge all this. Thanks Kerstin, for the careful proof reading of this thesis, and for always taking care of all of us. Thank you Ale, I learned a lot from you, and most importantly I got a good friend. A special thought to Jørgen, my colleague, friend and collaborator. We really had a great time, and also, you introduced me to the most important person of my life...! I will never forget the weekend-long microscopy, the deep conversations and the good fun together, thanks for everything! Thanks also to the Gilmour group, once the two groups "merged", we really established a nice little family. In particular, thanks to Jonas, for the genuine help in many occasions, and of course for all the pretty plots! And thanks to Elisa, a nice friend, colleague and most kind listener, you really are a great person. I am really thankful to Roland for the German translation of the abstract.

My dear friend Conny, where to put you? We met thanks to work, but we became so much more than just colleagues. Thanks for your constant support and encouragements and help in every single aspect of my life, once again: you are amazing!

Grazie alle mie amiche storiche: Carola, Chiara, Eli, Vale e ovviamente, Vera (29 anni dopo, sempre migliore amica oltre che sorella!). Ognuna di noi con la propria strada, ma ciò nonostante, comunque vicine. Siete speciali…

Un grazie di cuore alla mia famiglia. Mamma, papà, nonna, (ancora una volta) Vera e tu, piccola Lisa. Grazie per il vostro continuo supporto ed amore. Grazie per il sostegno in ogni mio passo e per aver reso tutto un po' più semplice. Siete lontani, ma vi sento sempre al mio fianco.

And last, but not least, thank you Millino. Thanks for your love, support and for being so patient, even in the toughest times. You always encouraged and believed in me. Once again, this is dedicated to you.